

1987

Aspects of the ecology of estuarine light with special reference to seagrasses of the Chesapeake Bay: measurements and models

Robin Francis Van Tine
College of William and Mary - Virginia Institute of Marine Science

Follow this and additional works at: <https://scholarworks.wm.edu/etd>



Part of the [Ecology and Evolutionary Biology Commons](#)

Recommended Citation

Van Tine, Robin Francis, "Aspects of the ecology of estuarine light with special reference to seagrasses of the Chesapeake Bay: measurements and models" (1987). *Dissertations, Theses, and Masters Projects*. Paper 1539616889.
<https://dx.doi.org/doi:10.25773/v5-vg2y-4656>

This Dissertation is brought to you for free and open access by the Theses, Dissertations, & Master Projects at W&M ScholarWorks. It has been accepted for inclusion in Dissertations, Theses, and Masters Projects by an authorized administrator of W&M ScholarWorks. For more information, please contact scholarworks@wm.edu.

INFORMATION TO USERS

The most advanced technology has been used to photograph and reproduce this manuscript from the microfilm master. UMI films the original text directly from the copy submitted. Thus, some dissertation copies are in typewriter face, while others may be from a computer printer.

In the unlikely event that the author did not send UMI a complete manuscript and there are missing pages, these will be noted. Also, if unauthorized copyrighted material had to be removed, a note will indicate the deletion.

Oversize materials (*e.g.*, maps, drawings, charts) are reproduced by sectioning the original, beginning at the upper left-hand corner and continuing from left to right in equal sections with small overlaps. Each oversize page is available as one exposure on a standard 35 mm slide or as a 17" x 23" black and white photographic print for an additional charge.

Photographs included in the original manuscript have been reproduced xerographically in this copy. 35 mm slides or 6" x 9" black and white photographic prints are available for any photographs or illustrations appearing in this copy for an additional charge. Contact UMI directly to order.



University Microfilms International, Inc. 300 N. Zeeb Road

Ann Arbor, MI 48106-1500, U.S.A. Tel: (313) 761-4000

Order Number 8724677

**Aspects of the ecology of estuarine light with special reference
to seagrasses of the Chesapeake Bay: Measurements and models**

van Tine, Robin Francis, Ph.D.

The College of William and Mary, 1987

Copyright © 1988 by van Tine, Robin Francis. All rights reserved.

U·M·I

300 N. Zeeb Rd
Ann Arbor, MI 48106

PLEASE NOTE:

In all cases this material has been filmed in the best possible way from the available copy. Problems encountered with this document have been identified here with a check mark ✓

- 1 Glossy photographs or pages
- 2 Colored illustrations, paper or print
- 3 Photographs with dark background ..
- 4 Illustrations are poor copy
- 5. Pages with black marks, not original copy ✓
- 6 Print shows through as there is text on both sides of page
- 7 Indistinct, broken or small print on several pages ✓
- 8. Print exceeds margin requirements
- 9. Tightly bound copy with print lost in spine
- 10. Computer printout pages with indistinct print
- 11 Page(s) lacking when material received, and not available from school or author
- 12 Page(s) seem to be missing in numbering only as text follows
- 13 Two pages numbered ____ Text follows.
- 14. Curling and wrinkled pages
- 15 Dissertation contains pages with print at a slant, filmed as received ✓
- 16 Other

University
Microfilms
International

ASPECTS OF THE ECOLOGY OF ESTUARINE LIGHT
with
SPECIAL REFERENCE TO SEAGRASSES OF THE CHESAPEAKE BAY:
MEASUREMENTS AND MODELS

A Dissertation
Presented to
The Faculty of the School of Marine Science
The College of William and Mary in Virginia

In Partial Fulfillment
Of the Requirements for the Degree of
Doctor of Philosophy

by
Robin F. van Tine
1987

APPROVAL SHEET


This dissertation is submitted in partial fulfillment of
the requirements for the degree of


Doctor of Philosophy


Robin F. van Tine

Approved, July 1987


Richard L. Wetzel
Committee Chairman/Advisor


Michael E. Bender


Evon P. Ruzicki


Robert J. Orth


Robert R. Christian
East Carolina University

©1988

ROBIN FRANCIS VAN TINE

All Rights Reserved

This work is dedicated to my Great Grandmother
Ada Adele Alexander
whose Spirit happily roams her beloved Berkshire Hills.
Her love of Mother Earth has been passed to me
through my mother Evelyn Sylvia.

TABLE OF CONTENTS

	<u>Page</u>
ACKNOWLEDGEMENTS	i
LIST OF TABLES	ii
LIST OF FIGURES	iii
ABSTRACT	vii
INTRODUCTION	
Purposes of Work	2
Light in the Estuarine Environment	3
Community Photosystem Response	17
MATERIALS and METHODS	
Spectral Irradiance Measurements	21
Study Sites	21
Calculation of Spectral Attenuation Coefficient	26
Relative Potential Photosynthetically Storable Radiation	28
RESULTS	
Mean Seasonal Spectral Attenuation in the lower Chesapeake Bay	29
Mean Monthly Spectral Attenuation in the lower Chesapeake Bay	39
Spectral Irradiance and Attenuation in Estero Pargo Creek	72
DISCUSSION	
Relative Potential Benthic Photosynthesis	78
Spectral Attenuation and Seagrass Occurrence	82
Wind, Gelbstoff and Spectral Attenuation in Estero Pargo Creek	87
COMMUNITY PHOTOSYSTEM RESPONSE MODEL	
Introduction	91
Physical Spectral Attenuation	94
Biological Absorption, Pigment Synthesis and Productivity	98
Computation	102
Model Output	102
Discussion of Model	109
Future Modifications of the Model	113

CONCLUSIONS 114
APPENDIX: Model Program Listings 117
LITERATURE CITED 132
VITA 140

ACKNOWLEDGEMENTS

Most of all I wish to express my gratitude to Dick Metzger for his unflagging personal and professional support and encouragement. Without his friendship, threats, and urgings this dissertation would never have been resurrected from its resting place amongst my son's old baby bottles and rattles - nor would it have survived the personal turmoil of a bitter divorce and child custody battle.

I also owe a debt of gratitude to my exceedingly patient committee members, Evon Ruzicki, Mike Bender, and Bob Orth who have given wise counsel over the many years and versions of this work and have consistently urged me to finish despite my repeated attempts to give it up.

Special thanks are due Bob Christian who stepped in at the last minute and spent considerable time and effort critically reviewing the manuscript.

Thanks also to Mike Kemp for serving on my original committee and participating in my comprehensive exam, to Denise Mosca, Sandra Sotsky, Rick Hoffman, and Laura Murray for assistance in the field and lab, and to the VIMS computer and library staff, and to Sue Presson for all the times she has re-filed my Candidacy forms.

Finally, thanks to my son Tristan for tolerating a grumpy, preoccupied Daddy for a long time!

ASPECTS OF THE ECOLOGY OF ESTUARINE LIGHT
with
SPECIAL REFERENCE TO SEAGRASSES OF THE CHESAPEAKE BAY:
MEASUREMENTS AND MODELS

LIST OF TABLES

<u>Table</u>		<u>Page</u>
I.	Approximate wavelength ranges of colors	8
II.	Mean seasonal shallow water spectral attenuation for vegetated and unvegetated sites in the lower Chesapeake Bay, 1981	31
III.	Daily mean spectral attenuation over a seagrass bed at the mouth of Estero Pargo Creek, Laguna de Terminos	75

LIST OF FIGURES

<u>Figure</u>	<u>Page</u>
1. Theoretical path of light from top of atmosphere to the benthic macrophytes	5
2. Downwelling spectral irradiance at the surface and at several depths above canopy of a <u>Zostera marina</u> bed off the Eastern Shore of the lower Chesapeake Bay	12
3. Comparison of historical spectral attenuation measurements reported for the Chesapeake Bay	16
4. Depth profiles of percentage of surface quanta for different water types	18
5. Locations of lower Chesapeake Bay sites	22
6. Location of Laguna de Terminos site	25
7. Mean seasonal spectral attenuation for shallow waters of the lower Chesapeake Bay	30
8. Mean Winter spectral attenuation at vegetated and unvegetated sites of the lower Chesapeake Bay	32
9. Mean Spring 1981 spectral attenuation at vegetated and unvegetated sites of the lower Chesapeake Bay	33
10. Mean Summer 1981 spectral attenuation at vegetated and unvegetated sites of the lower Chesapeake Bay	34
11. Mean Autumn 1981 spectral attenuation at vegetated and unvegetated sites of the lower Chesapeake Bay	35
12. Mean Spring 1981 violet-blue attenuation ± 1 s.d. at vegetated sites of the lower Chesapeake Bay	37
13. Mean Spring 1981 violet-blue attenuation ± 1 s.d. at unvegetated sites of the lower Chesapeake Bay	38

14.	Mean monthly violet-blue attenuation at vegetated sites of the lower Chesapeake Bay	40
15.	Mean monthly violet-blue attenuation at unvegetated sites of the lower Chesapeake Bay	41
16.	Mean monthly green-yellow attenuation at vegetated sites of the lower Chesapeake Bay	42
17.	Mean monthly green-yellow attenuation at unvegetated sites of the lower Chesapeake Bay	43
18.	Mean monthly orange-red attenuation at vegetated sites of the lower Chesapeake Bay	44
19.	Mean monthly orange-red attenuation at unvegetated sites of the lower Chesapeake Bay	45
20.	Mean monthly variability of attenuation of light of 441nm at unvegetated sites of the lower Chesapeake Bay	48
21.	Mean monthly variability of attenuation of light of 441nm at vegetated sites of the lower Chesapeake Bay	49
22.	Mean monthly variability of attenuation of light of 671nm at unvegetated sites of the lower Chesapeake Bay	50
23.	Mean monthly variability of attenuation of light of 671nm at vegetated sites of the lower Chesapeake Bay	51
24.	Mean May 1981 spectral attenuation at unvegetated and vegetated sites of the lower Chesapeake Bay	52
25.	Mean May 1981 spectral attenuation at individual sites of the lower Chesapeake Bay	54
26.	Mean seasonal spectral attenuation at Mumfort Is. site (York R.), Chesapeake Bay	57
27.	Mean seasonal spectral attenuation at Allen's Is. site (York R.), Chesapeake Bay	58
28.	Mean seasonal spectral attenuation at Guinea Marsh site (York R.), Chesapeake Bay	59
29.	Mean seasonal spectral attenuation at the mouth of the Severn R. (Mobjack Bay), Chesapeake Bay	60

30.	Mean seasonal spectral attenuation at Four Point Marsh (mouth of the Ware R., Mobjack Bay), Chesapeake Bay	61
31.	Mean seasonal spectral attenuation at Vaucluse Shores <u>Zostera marina</u> bed off the Eastern Shore of the lower Chesapeake Bay	62
32.	Mean seasonal spectral attenuation at the Deep Station at Vaucluse Shores off the Eastern Shore of the lower Chesapeake Bay	63
33.	Mean monthly attenuation of selected wavelengths off Mumfort Is., York R., Chesapeake Bay	65
34.	Mean monthly attenuation of selected wavelengths off Allen's Is., York R., Chesapeake Bay	66
35.	Mean monthly attenuation of selected wavelengths off Guinea Marsh, York R., Chesapeake Bay	67
36.	Mean monthly attenuation of selected wavelengths at the mouth of the Severn R., lower Chesapeake Bay	68
37.	Mean monthly attenuation of selected wavelengths at the Four Point Marsh site, York R., Chesapeake Bay	69
38.	Mean monthly attenuation of selected wavelengths in the <u>Zostera marina</u> bed off Vaucluse Shores, Chesapeake Bay	70
39.	Mean monthly attenuation of selected wavelengths at the Deep Station off Vaucluse Shores, Chesapeake Bay	71
40.	Downwelling spectral irradiance and spectral attenuation over a <u>Thalassia testudinum</u> bed off the mouth of Estero Pargo Creek, Laguna de Terminos	74
41.	Comparison of diffuse downwelling spectral attenuation at three sites in Estero Pargo Creek, Laguna de Terminos	76
42.	Relative potential PSR for vegetated and unvegetated sites of the lower Chesapeake Bay	79
43.	Conceptual model of critical feedback between biological and physical components of the seagrass ecosystem	85

44.	Schematic representation of spectral attenuation through an estuarine water column	88
45.	Conceptual diagram of community photosystem simulation model (4PIG17.5)	92
46.	Cycling receptor (Michaelis-Menten module) and production for a single photosystem	100
47.	Output of Standard Run of community photosystem simulation model (4PIG.17A).	103
48.	Output of community photosystem model with SS=0 and DOM=0	105
49.	Output of community photosystem model with Standard SS and 3xDOM	107
50.	Output of community photosystem model with Standard DOM and 3xSS	108
51.	Output of community photosystem model with 3xSS and 3xDOM	110
52.	Sequential blooms and crashes of specific photosystems in model run with constant maximum irradiance	111

ABSTRACT

The temporal spectral light environment of shallow areas of the lower Chesapeake Bay was characterized by cosine collection of downwelling diffuse irradiance at 12 wavelengths between 400 and 700 nm. An extensive monthly and site comparison of spectral attenuation coefficients is presented and compared with previous measurements of the light quality environment of the Chesapeake Bay and other estuaries and marine waters. Spectral irradiance and attenuation of light in a mangrove creek and *Thalassia testudinum* bed of Laguna de Terminos, Campeche, Mexico and their relationships to wind-driven suspension of particulate matter, and dissolved substances from the mangrove swamp is also discussed. A review of the physics of spectral attenuation in estuaries is included. Particular attention was given to the relationship between the occurrence of seagrasses (*Zostera marina* mainly) in the Chesapeake Bay and spectral attenuation. Potential losses of photosynthetically storable radiation (PSR) due to reduced light quality in non-vegetated areas is calculated. A theoretical homeostatic relationship between seagrass leaf baffling of the water column, light quality and critical bed size is presented. The logic and output of a digital ecosystem simulation model of theoretical estuarine photosystem responses to simulated varying underwater

light quality is presented. The model assumes that photosystems adapt to maximize power.

Conclusions include: a dramatic pattern of seasonal spectral attenuation in the lower Chesapeake Bay; seasonal differences in spectral attenuation between vegetated and unvegetated sites; 63% less violet light was able to pass through a meter of water at unvegetated sites in May than vegetated sites.

ASPECTS OF THE ECOLOGY OF ESTUARINE LIGHT
with
SPECIAL REFERENCE TO SEAGRASSES OF THE CHESAPEAKE BAY:
MEASUREMENTS AND MODELS

INTRODUCTION

Purpose of Work

The energetic basis of almost all life on Earth is light. For at least 3.5 billion years marine plants have been evolving exquisite mechanisms for the optimization of light capture and conversion of its elusive energy to their purposes. They were so successful that they forever changed the atmosphere and determined the course of evolution for all life to come. Descendants of these original producers are arguably still the most successful creatures on Earth today.

I have approached the problem of understanding the complex interactions of photons in the living matrix of estuarine waters from a systems ecology perspective. As I see it, primary production in the aquatic environment consists of an interactive set of pigment receptor systems that have coevolved in such a way as to maximize the capture of specific quanta of available light. Individual types of organisms evolve within ecosystems, all of whose parts must adapt to and with each other collectively and individually. Ecosystems survive whose members are best able to coadapt in such a way as to balance optimization of individual species needs with those of the larger system which supports the whole. The adaptations of the light capture mechanisms of planktonic and benthic aquatic macrophytes and microphytes are an example not so much of competition for light but of cooperation for maximum community light capture. The seasonally and spatially varying specific mixture of phytoplankton, benthic microalgae, macrophytes and epiphytic algae of a

particular environment constitutes that ecosystem's best current solution for the maximization of the seasonal and spatial distribution of pigment receptor systems necessary for the optimal conversion of seasonally and spatially varying mix of light energies available.

The work reported in this dissertation was undertaken for a number of purposes: (1) To gain an understanding of the physics of light in water; (2) To determine the feasibility of measuring spectral irradiance and spectral attenuation in shallow estuarine environments; (3) To describe the underwater light environment of the estuarine environment, especially the Lower Chesapeake Bay; (4) To determine if there was a relationship between the presence or absence of seagrasses in the Chesapeake Bay and spectral attenuation; (5) To identify those factors of the estuarine environment most related to spectral attenuation; (6) To investigate the theoretical relationship between light quality and potential estuarine primary productivity; (7) To conceptualize and simulate computer ecosystem models which describe the interactions between light and the estuarine environment with special reference to pigment systems. Included in this work is a brief summary of marine optical physics, a description of the light environments of several estuarine ecosystems - especially shallow regions of the lower Chesapeake Bay, and the results of a theoretical ecosystem simulation model.

Light in the Estuarine Environment

The study of the interaction of solar energy with the estuarine milieu

necessitates not only an understanding of the properties of light and water, but must also take into consideration the myriad living and non-living entities, both dissolved and suspended, which affect the propagation of light in aquatic environments.

The sun emits electromagnetic radiation in discrete packets of quanta (Q) of energy termed photons. The energy content (ϵ) of each quantum is directly proportional to the frequency (ν),

$$\epsilon = h\nu \quad (1.1)$$

and considering the speed of any wave form (δ), $c = \nu\delta$, we find:

$$\epsilon = \frac{hc}{\delta} \quad (1.2)$$

where h is Planck's universal constant, c is the speed of light in a vacuum and δ is the wavelength. Thus, quanta of shorter wavelengths contain more energy than do those of longer wavelengths.

The complete spectrum of downward irradiance for incoming solar radiation at the top of the atmosphere, at sea level, and at several water depths in the open ocean is illustrated in Figure 1a. Most of the energy reaching Earth's surface is contained within the shorter wavelengths (400-1000nm). Not surprisingly, this region includes the wavelengths of greatest biological importance, 400-700nm, the Photosynthetically Available Region of the spectrum termed PAR. There is almost no energy outside

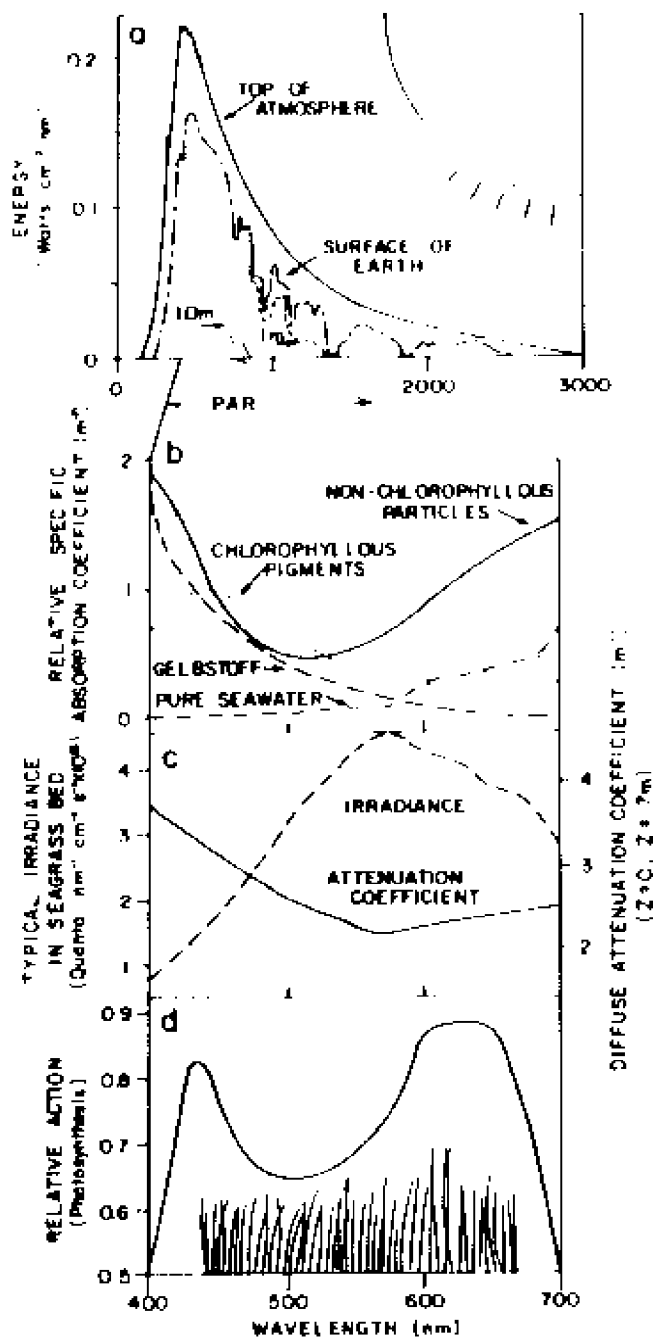


FIGURE 1. Theoretical path of light from top of atmosphere to the benthic macrophytes. (a) Spectral energy distribution of light from the top of the atmosphere, at the surface of Earth, and at two depths in the ocean on a clear day (Redrawn from Jerlov, 1976 and Gates, 1971), (b) Relative spectral absorption of various constituents of estuarine waters (Redrawn from Prieur and Sathyendranath, 1981), (c) Typical spectral irradiance and attenuation in a lower Chesapeake Bay seagrass bed (van Tine and Wetzel, 1983), (d) Mean quantum action spectrum for higher plants (after Inada, 1976).

the PAR at a depth of one meter in clear open ocean water. Most of the "missing" energy has been converted into heat via absorption. Only about 4-11% (depending on zenith angle) of incident irradiance between 300-700 nm is reflected from the surface of the water or backscattered out of the water column (Clark and Ewing, 1974). Slightly more may be backscattered from estuarine waters.

The properties and concepts of optical oceanography are usually divided into two mutually exclusive classes: (1) inherent, and (2) apparent properties. Inherent properties, such as absorption and scattering are independent of changes in insolation, whereas apparent properties, such as underwater irradiance, vary with changing solar and atmospheric conditions.

As light passes through the water column its energy content and spectral quality are changed by absorption and scattering due to the water itself, dissolved substances, and suspended particles. The combined effect of these processes is termed attenuation. The spectral distribution of the total attenuation coefficient (κ), measured with the beam transmissometer, generally shows high attenuation at both ends of the PAR. Since κ is an aggregated coefficient, it is necessary to consider the component parameters which cause the observed attenuation.

Scattering is the change in direction of light propagation caused by diffraction, refraction, and reflection due to particles, water molecules,

and dissolved substances. Backscattering results in the loss of energy from the aquatic environment. Forward and lateral scattering effectively increases the path-length of light thereby exposing it to additional absorption. The major particles in estuaries are clays and silts with small diameters which tend to scatter light of the shorter wavelengths of the visible light spectrum (blue end) more than the longer wavelengths (Williams, 1970). Therefore one would expect greater attenuation of blue light than red light in estuaries. (See Table I for the approximate perceived colors of wavelengths of light). Scattering is wavelength dependent, but in an irregular and complex manner (Jerlov, 1976).

Absorption is a thermodynamically irreversible process wherein photons are converted into thermal, kinetic or chemical energy -- as in photosynthesis. Absorption accounts for most of the observed attenuation of light in estuaries if one takes into account the additional absorption which occurs during the perambulations caused by the forward and lateral scattering induced by suspended silt and clay. Much of the attenuation of the energy contained in the long wavelengths (>600nm) is due to either the water molecules themselves, as shown by James and Birge (1938) for pure water, or to the water plus its dissolved salts (Clarke and James, 1939). There is little difference in attenuation between pure water and filtered seawater (Yentsch, 1960); the effect of sea salts themselves is insignificant, therefore estuarine salinity changes are of little direct importance in determining fluctuations in estuarine light attenuation (see Fig. 1b).

TABLE I
APPROXIMATE WAVELENGTH RANGE of VISIBLE LIGHT

Perceived Color	Nanometers
Ultraviolet	< 380
Violet	380-450
Blue	450-490
Green	490-560
Yellow	560-590
Orange	590-630
Red	630-760
Infrared	> 760

Natural water bodies, particularly estuaries, are not pure, but contain constantly varying amounts of particulate and dissolved substances (Burt, 1955; Kiefer and Austin, 1974; Riaux and Douville, 1980; Thompson et al., 1979). The energy contained in the lower and upper PAR, violet-blue and orange-red, respectively, is particularly susceptible to absorption by particulate matter. Burt (1958), using uncontaminated filtered seawater samples, was able to determine the attenuation due to dissolved substances. By subtracting this from the total attenuation coefficient of non-filtered seawater he was able to calculate the light attenuation due solely to particulate matter. The energy of blue and red wavelengths are selectively absorbed by particles, as shown in the example given by Prieur and Sathyendranath (1981) (see Fig. 1b).

The shorter wavelengths are also attenuated by DOM (Kirk, 1976; Zep & Schlothauer, 1981), or Gelbstoff, the name given to a complex mixture of organic compounds by Kalle (1966). Gelbstoff is formed from the decomposition of carbohydrates. Sources are both allochthonous and autochthonous. Flocculation of fine suspended and colloidal materials is also believed to participate in the formation of these organic complexes.

Chlorophyll pigments in the water column associated with phytoplankton and the breakdown products of plants also absorb most strongly in the blue and red. Thus, since estuaries are loaded with a myriad of autochthonous and allochthonous dissolved and suspended substances, the light energy reaching the benthic plants of an estuary is likely to be reduced in both

the red and especially the blue regions of the spectrum – exactly those portions to which green plants respond most efficiently photosynthetically. This is graphically depicted in Figure 1. Specific spectral attenuation patterns resulting from combinations of water column constituents are illustrated in Figure 1b. As these constituents change both temporally and spatially, the resultant spectral absorption patterns change. Pierce et al. (1981) have determined by step-wise multiple linear regression analysis that chlorophylls "a" and "c" and inorganic particles explain most of their observed variation in spectral attenuation in the Rhode River Estuary of the upper Chesapeake Bay. Prieur and Sathyendranath (1981) and Kirk (1983) have attempted to classify water bodies based on combinations of these factors.

The apparent optical properties of a body of water result from the measurement of natural light fields underwater, i.e. the measurement of in situ radiant flux. Irradiance (E), the flux of light reaching a defined area, is usually sampled with a flat circular opal glass or plastic diffuser called a 2π collector. The diffuser is designed so that light received from all angles is transmitted to the sensor according to Lambert's cosine law, i.e., the irradiance transmitted is proportional to the incident radiant intensity multiplied by the cosine of the angle of incidence. Jerlov (1976) reports that the ratio of cosine collection of downwelling irradiance (E_d) to equal hemispherical collection (E_0) is generally within the range .75 to .85. That is, more than 75% of the light actually downwelling on a perpendicular plane is registered by cosine

collection. Although hemispherical or spherical collection would be the preferable measurement to make for biological purposes, since that would more accurately measure what an organism in a three dimensional medium experiences, 2 π irradiance is the apparent property of water bodies most commonly made by biologists and ecologists. Although the numbers recorded from these devices are inaccurate in one sense, the majority of the literature contains comparative values (broad range integrated PAR irradiance) determined in this way. Irradiance can be expressed as either energy or quanta and measured in broad spectral ranges, such as PAR, or at discrete wavelengths, i.e., spectral irradiance. The measurements made in this study were downwelling 2 π spectral irradiance. A typical family of downwelling spectral irradiance curves by depth, in quanta, is presented in Figure 2 for the water column over a *Zostera marina* bed off the Eastern Shore of the Chesapeake Bay.

All plants, whether aquatic or terrestrial, differentially absorb the energy of specific ranges of light of different wavelengths via characteristic complements of photoreactive pigment molecules located within subcellular systems. The energy thus absorbed by quantum amounts is utilized, with varying spectral efficiency, to drive the reactions of photosynthesis - the synthesis of complex organic compounds from simple inorganic compounds using the photon energy of sunlight.

The light capture pigments of most phytoplankton are similar to those of higher plants. These pigment systems absorb strongly in the blue and

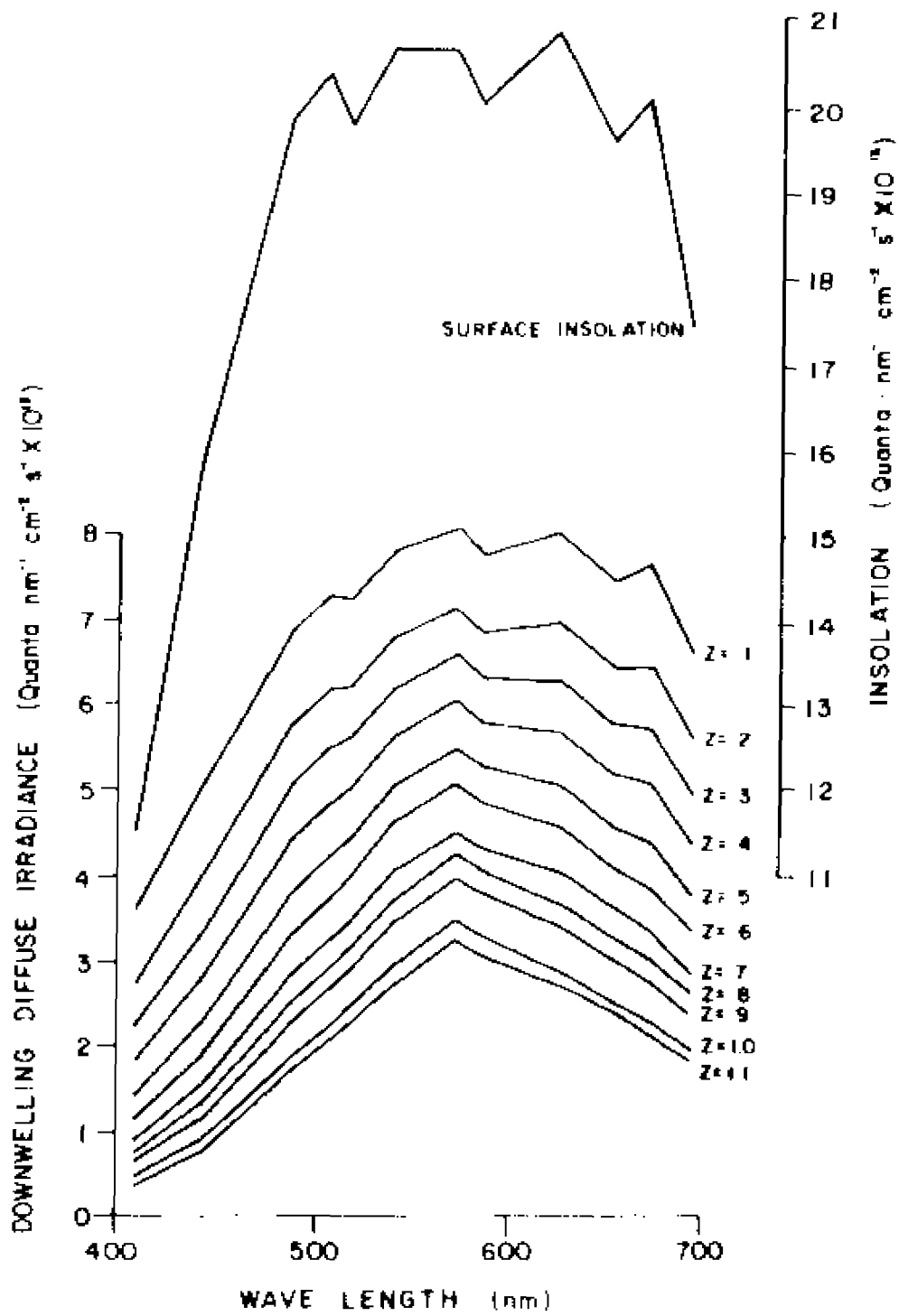


Figure 2. Downwelling spectral irradiance at the surface and at several depths above canopy of a Zostera marina bed off the Eastern Shore of the Lower Chesapeake Bay.

red regions of the spectrum. Green plants, both terrestrial and marine, photosynthesize most efficiently in the violet-blue (400-500nm) and orange-red (600-700nm) regions of the spectrum (Halldal, 1974). Inada (1976) summarized the action spectra literature for a diverse taxonomic group of terrestrial angiosperms and found quite a consistent pattern. The pattern for the common estuarine green alga Ulva is remarkably similar (cf. Levring, 1947, 1966; Haxo and Blinks, 1950; Halldal, 1974). All show the highest rates of photosynthesis in the above mentioned spectral regions. Of course this is no surprise. Green plants appear green because they absorb blue and red light and reflect green light!

Although I am unaware of any reported seagrass action spectra, it seems reasonable to assume that these plants are similar to their terrestrial taxonomic cousins and their marine ecological kin with similar pigment complexes, i.e., chlorophyll a, b and accessory pigments β -carotene and xanthophylls. The chlorophylls are solely responsible for the absorption of energy above 602 nm but that below 500 nm is due to both accessory pigments and chlorophylls a and b (Zscheile and Comar, 1941; Zscheile et al., 1942; Govindjee and Govindjee, 1975).

The diffuse downwelling (or vertical) attenuation coefficient (K_d) expresses the decay of irradiance as an exponential function of depth and is often referred to as the extinction coefficient with units of m^{-1} .

The reciprocal of the attenuation coefficient is termed attenuation length and is considered by some to be more intuitively understandable than the former.

If the depth interval over which the decay function (K_d) is calculated brackets the air-water interface it will include the effects of reflection. Therefore, K_d calculated between depths within the water column will measure the effects of the inherent properties of that layer of water on the propagation of light through the layer. Since this distinction is not always specified in the literature it is sometimes difficult to compare attenuation values. The well-defined spectral attenuation coefficient is a particularly useful parameter for comparing underwater irradiance between water bodies, seasons, and wavelengths and as such can be considered a "quasi-inherent" property of bodies of water (Baker and Smith, 1980). As K_d is inconsistent at different depths in water less than about 10 m deep, comparisons should be made between attenuation values calculated over the same depth intervals. A typical spectral distribution of both E_d and K is shown in Figure 1c for shallow Chesapeake Bay water over a seagrass meadow.

Since seagrasses exist in an environment characterized by drastic temporal and spatial fluctuations in absorption and scattering due to the water itself, dissolved inorganic and organic substances, and suspended particles, the resulting differential spectral attenuation causes light quality shifts which may have profound implications for fixed benthic

plants with their genetically determined finite range of usable light energies. This author (van Tine, 1977, 1981) found that the turbidity caused by effluent from a power plant eliminated a seagrass bed in the Gulf of Mexico.

The small amount of available Chesapeake Bay data on diffuse downwelling 2% irradiance attenuation indicates a severe attenuation of light energy in the photosynthetically important 400-500 nm (violet-blue) region of the spectrum. Attenuation in these short wavelengths is particularly marked in the turbidity maximum region of the Bay at the mouth of the Sassafras River and at the mouth of the Patuxent River during August (Champ et al., 1980). The mean Bay attenuation coefficients calculated by Champ et al. (1980) are about 1.0 m^{-1} higher than Jerlov's (1976) most turbid coastal water classification.

A comparison of attenuation coefficients reported for the Chesapeake Bay and its tributaries is presented in Figure 3 along with Jerlov's (1976) standard spectral attenuation curve representing his most turbid coastal water classification (specified Type 9). For the Chesapeake Bay, the earliest measurements of spectral attenuation were made by Hurlburt (1945) (Fig. 3a). His values fall in the lower range of more recent in situ measurements. Champ et al. (1980) conducted a light characterization survey of the Chesapeake Bay during August, 1977. Their mean values are shown in Fig. 3a. Specific site measurements made by them in and near the mouths of the Sassafras, Patuxent, Potomac and Chester Rivers appear in Fig. 3c. Their calculations in the turbidity maximum zone at the mouth of the Sassafras River are the highest reported for the Bay: there is

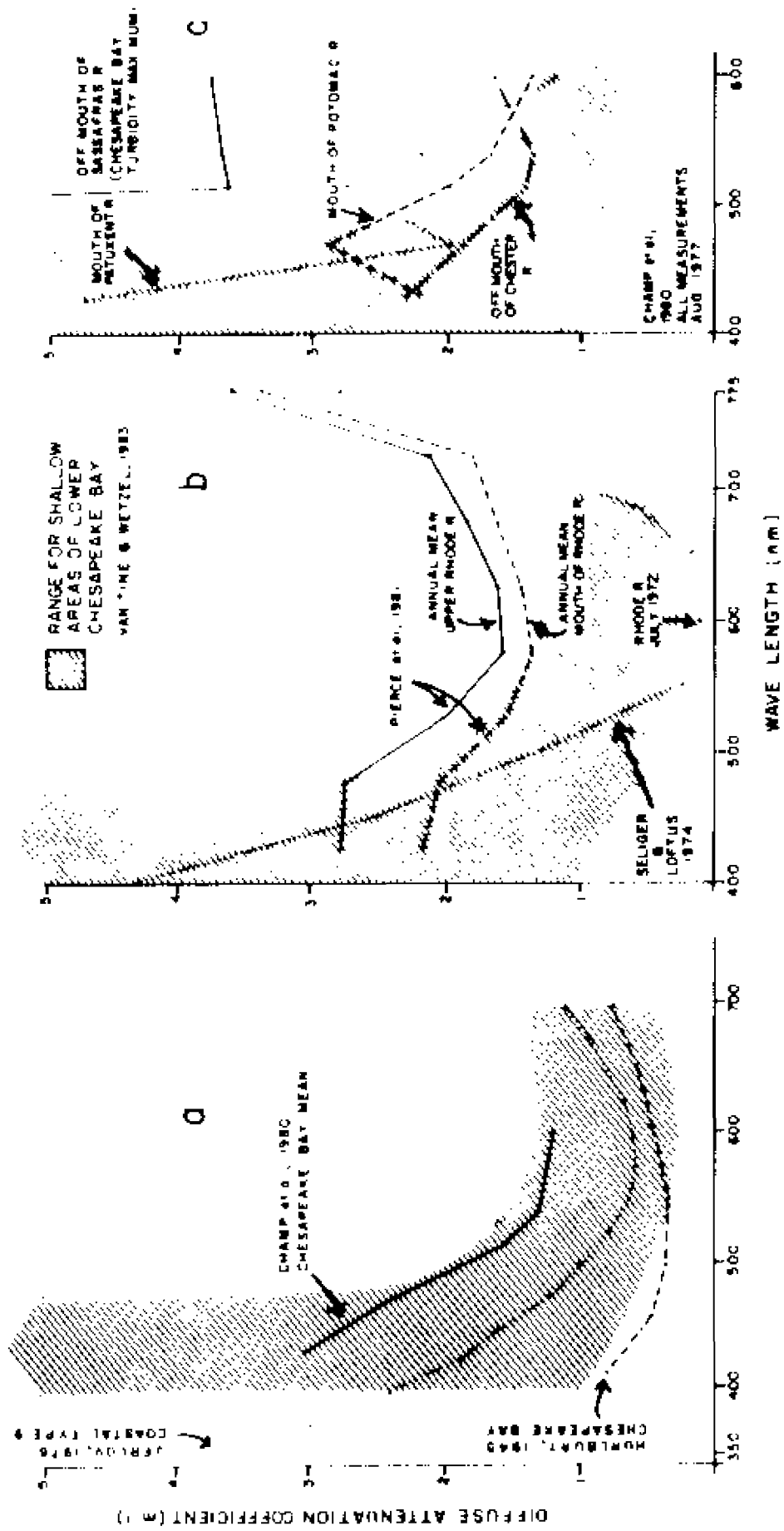


Figure 3. Comparison of diffuse downwelling spectral attenuation coefficients for Chesapeake Bay with Jerlov's most turbid coastal classification. (a) Plotted from tables in Jerlov, 1976; Huriburt, 1945; Champ et al., 1980 (b) Plotted from table in Pierce et al., 1981 and calculated from 4% irradiance curves in Seliger and Loftus, 1974 (c) Plotted from tables in Champ et al., 1980. Shaded area represents ranges of attenuation found by van Tine and Wetzel (1983) in shallow lower Bay waters.

essentially no available underwater light below 500 nm wavelength. Pierce et al. (1981) intensively monitored the Rhode River during 1980-1981. Their annual mean attenuation values for an upriver station and one at the mouth of the river are plotted in Fig. 3b. The upriver station was found to be consistently more turbid, presumably due to its proximity to autochthonous sources. Maximum penetration was at 575 nm and minima at 775 and 425nm. Attenuation coefficients derived from 4 π irradiance (spherical) measurements from the Rhode River (Seliger and Loftus, 1974) are also shown in the Figure.

Estuarine waters are naturally more turbid than coastal or oceanic waters as is shown in figure 4 which combines coastal and oceanic data from Jerlov (1976) and estuarine data from this study.

Community Photosystem Response to Variations in Estuarine Light Quality: A Theoretical Simulation Model

Instead of conceptualizing plant species that co-exist in an ecosystem as competitors for quanta, I have interpreted the ecosystem as an interactive and interdependent complex of complimentary and cooperative pigment systems which have co-evolved in such a way as to maximize the ecosystem's light capturing potential. From this perspective the bewildering variety of plants with diverse combinations of light absorbing pigment complexes perhaps becomes intelligible. If one considers the spatial, depth and seasonal distribution of photosystems it may be that

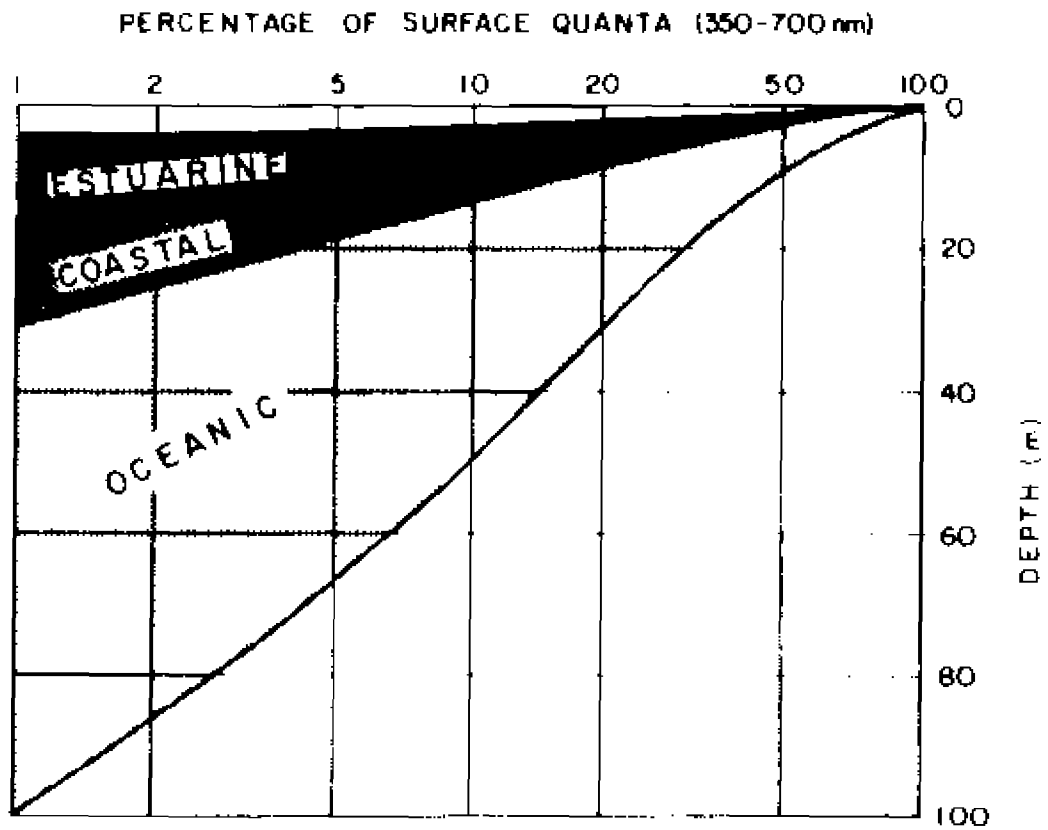


Figure 4. Depth profiles of percentage of surface quanta (350-700 nm) for different water types ranging from the clearest oceanic to coastal (After Jerlov, 1976) to estuarine (Lower Chesapeake Bay).

aquatic ecosystems that are successful have become expert at maximizing the total potential light energy seasonally available by distributing their specific absorption systems in space and time so that the particular combination of quanta available is harvested one way or another. It may matter little whether chlorophyll-green seagrasses or their epiphytic blue-green algae, or yellow-green phytoplankton or golden-brown benthic diatoms actually capture a specific photon - as long as it's captured and made available to the system in the form of fixed carbon!

In addition to this flexibility of community "chromatic cooperation", individual plants have an amazing plasticity with respect to their ability to adapt physiologically and morphologically to changing light quality conditions. (Björn, 1979; Smith, 1982; Humphrey, 1983; Bogard, 1975; Dring, 1981; Raghavendra & Das, 1977; Voskresenskaya, 1979; Spence, 1981; Corre, 1983; Stroos, 1981).

The model details the paths of "blue", "green", "yellow", and "red" quanta as they negotiate the hazards of navigation through an estuarine water column, meeting their eventual fate of absorption by either water molecules and dissolved salts, dissolved organic matter, non-pigmented suspended solids, or possible capture by "blue", "green", "yellow", or "red" plant antennae (see Fig. 45). The gross primary production of the system is considered a function of the total amount of activated pigments of all photosystems. Each specific pigment system is allowed to absorb all of the quanta surviving backscattering, attenuation by seawater,

particulate and DOM except for those quanta reflected by the pigment itself which then become available to the other pigment systems. Each part of the community light harvesting complex is allowed to grow in proportion to its quantity of excited pigment and the net productivity.

METHODS

Spectral Irradiance Measurements

Downwelling diffuse 2 θ spectral irradiance, E_d , was measured as quanta $\text{nm}^{-1} \cdot \text{cm}^{-2} \cdot \text{s}^{-1}$ at twelve biologically significant wavelengths (410, 441, 488, 507, 520, 540, 570, 589, 625, 656, 671 and 694 nm \pm 5 nm). The measurements were made using a Biospherical Labs model Mer-1000 multiwavelength spectroradiometer (Booth and Dustan, 1979), calibrated against U.S. Bureau of Standards lamps approximately every six months. Calibration curves changed less than 0.5% indicating an extremely stable system. Each measurement recorded was the mean of 250 scans made over an approximately 30 second interval in order to reduce variations in irradiance due to surface water wave crest refraction distortions, non-uniform distribution of suspended particulates and to integrate sky conditions.

Principal Sites

Measurements in the lower Chesapeake Bay were taken at six shallow sites (< 2 m depth) and at one relatively deep site in the lower Chesapeake Bay (Fig. 5). The shallow sites were chosen for their vegetational history - all but one having been vegetated by macrophytes in the recent past (Orth et al., 1979). Five of the sites were located on the western shore of the Lower Chesapeake Bay in the York River and Mobjack Bay. The remaining two

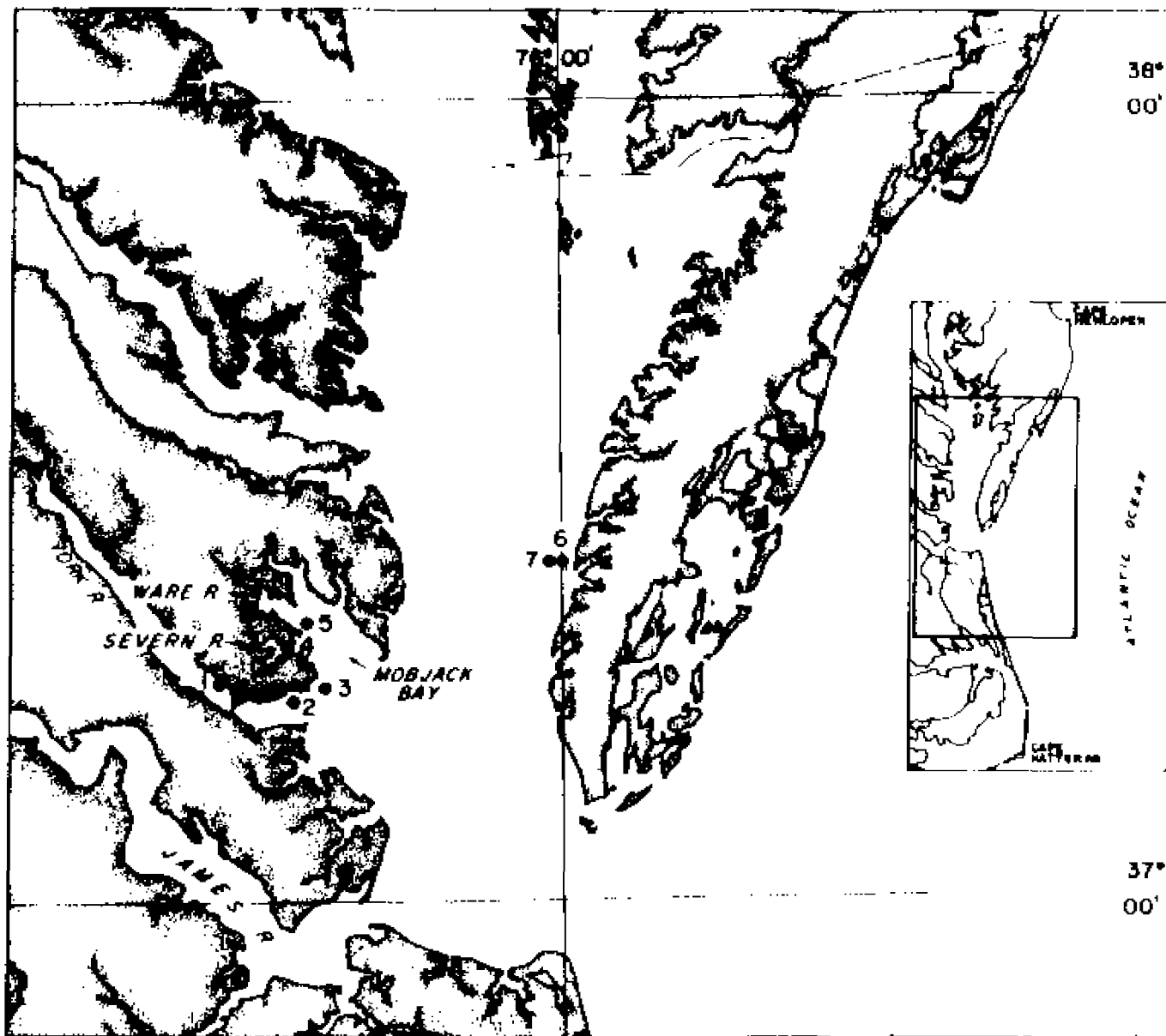


Figure 5. Locations of lower Chesapeake Bay sites. (1) Mumfort Is., York R. (unvegetated), (2) Allen's Is., York R. (transitional), (3) Guinea Marsh (vegetated), (4) Severn R. (unvegetated), (5) Four Point Marsh, Ware R. (vegetated), (6) Vancluse Shores (vegetated) (7) deep "Bay" Station 1 mi. west of site 6.

sites were across the Bay on the eastern shore of Virginia off Vaucluse Shores just north of the mouth of Hungar's Creek. The Mumfort Is. (York River) and Severn River (Mobjack Bay) sites were unvegetated during the study but had previously been part of seagrass beds. There were healthy seagrass beds (Zostera marina and Ruppia maritima) at the Guinea Marsh, Four Point Marsh (Mobjack Bay) and Vaucluse Shores sites during the course of the study. Measurements at the later site were made in corroboration with in situ productivity studies (Wetzel et al., 1982; Murray and Wetzel, 1982; Murray, 1983; Murray and Wetzel, 1987). The Allen's Island site (York River) represented a transitional vegetative state -- the natural population of macrophytes had disappeared yet Orth and colleagues (Orth et al., 1979) had successfully transplanted it. Furthermore, it appeared that a natural population may have been returning to this site (K. Moore, personal communication, 1981). The deep site on the Eastern Shore was located outside a sandbar and about 1 mile west of the Vaucluse Shores vegetated site. It was chosen as a reference station.

The western shore stations were monitored twice a month on paired dates approximately one week apart selected to coincide with the confluences of high tide with solar noon and low tide with solar noon. Measurements were made twice each day at each site. The eastern shore sites (Vaucluse Shores) were monitored at least every other month at times chosen to accommodate ongoing in situ productivity studies (Wetzel et al., 1982; Murray and Wetzel, 1982; Murray, 1983).

In order to facilitate an understanding of the possible trends in the spectral distribution of underwater light in the shallow Lower Chesapeake Bay, the data for the seven stations monitored has been summarized variously by month, season, site and vegetational state. All mention of attenuation coefficients, unless otherwise noted, refers to spectral $K_d(0.1,0.5)$, i.e., the diffuse downwelling spectral attenuation coefficient (m^{-1}) for the upper water column (between 0.1 and 0.5 m). This is a purposefully conservative measure of attenuation intended to characterize specific water bodies. The attenuation coefficient is not constant within water columns of less than 10 m in depth (Jerlov, 1976).

Laguna de Terminos, Campeche, Mexico

Light quality measurements were made at three sites: at the mouth of Estero Pargo Creek over a Thalassia testudinum bed, at a site approximately 1km up the Creek just off the U.N.A.M. Centro de Ciencias del Mar y Limnologia dock, and at an intermediate midstream site (see fig. 6). Measurements at the Thalassia site were made periodically throughout the daylight hours over a three day period coinciding with other studies described in van Tine and Wetzel, 1982. The water depth ranged from 0.75 to 1.1 m at the mouth of the creek.

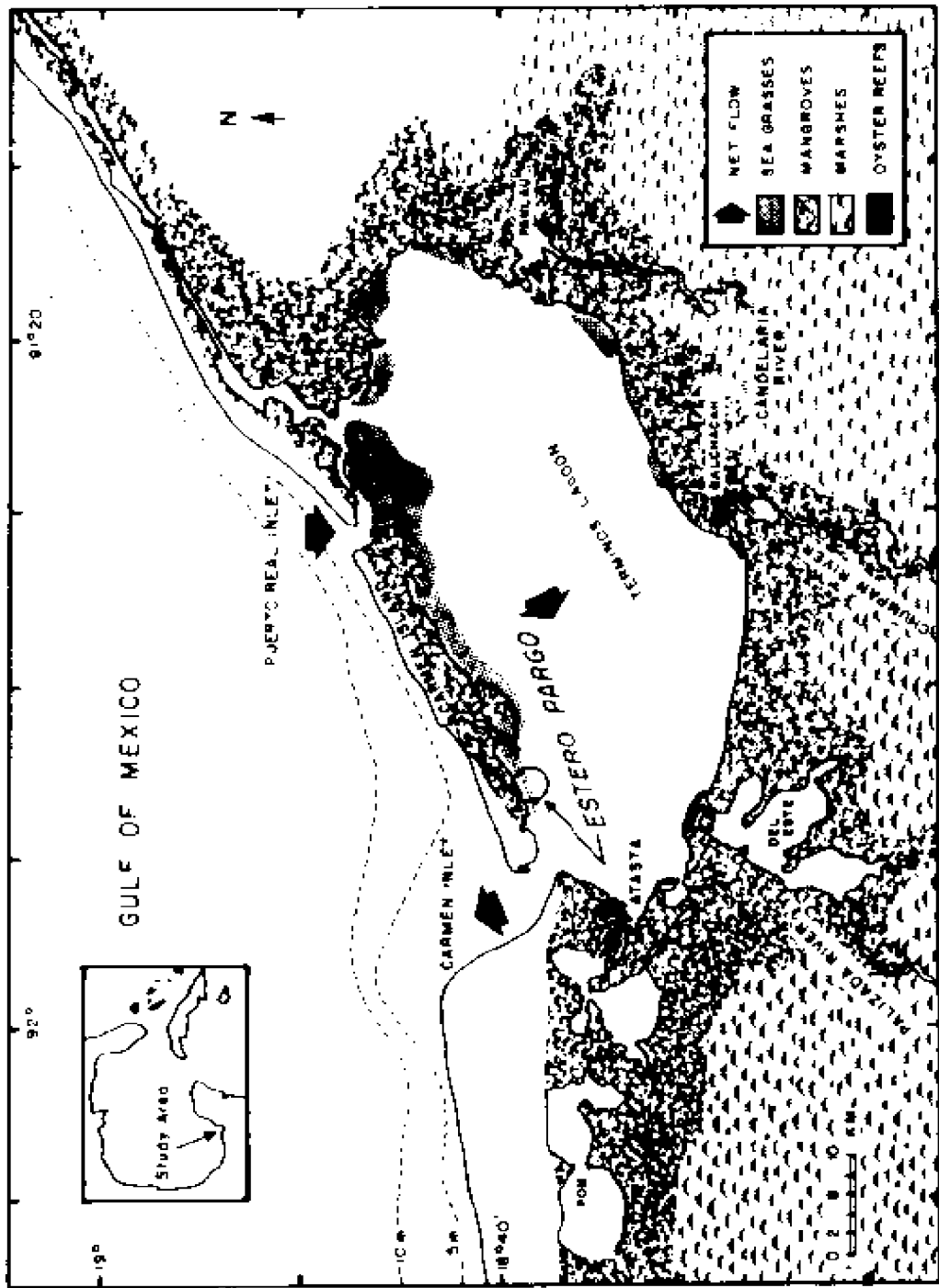


Figure 6. Location of Laguna de Terminos site.

Calculation of Spectral Attenuation Coefficient

The diffuse spectral attenuation coefficient, k_d , for downwelling 2 μ irradiance was chosen as the most suitable parameter for the characterization and comparison of the underwater light environments at each site due to its quasi-inherent nature. It has been found to be relatively insensitive to changes in solar zenith angle except for very large angles (Baker and Smith, 1980).

The diffuse downwelling attenuation coefficient was calculated for each wavelength measured between depths of interest as:

$$k_d(z_1, z_2) = \frac{-\ln[E_d(z_2)/E_d(z_1)]}{(z_2 - z_1)} \quad (2.1)$$

where k_d has units of reciprocal length (m^{-1}), and z_n is the depth at which the downwelling irradiance $E_d(z)$, is measured. The attenuation coefficient is usually considered a value representing the assumed exponential decay of light with depth. Irradiance at depth z_2 can be estimated for a body of water with known k_d from:

$$E_d(z_1) = E_d(z_2) \exp[-k_d(z_2 - z_1)] \quad (2.2)$$

The attenuation coefficients extensively evaluated for the seagrass portion of this work (stations 1-7 in the York R., Mobjack Bay and at Vaucluse Shores) were calculated between depths of 0.1 and 0.5 m as an estimator of water column attenuation not associated with air-water or water-substrate

interface phenomena. Hence, these values are a function of the inherent optical properties of the water bodies concerned. Since k_d is not a constant for water bodies less than 10 m deep, all comparisons between sites and seasons were made for the same depth interval, i.e., 0.1 to 0.5 m. All such calculations were based on irradiance measures taken at these depths between 1000 and 1400 hours E.S.T. Variations in k_d due to sun zenith angle differences at this time of day are less than 5% in the extreme (Baker and Smith, 1979).

Mean monthly attenuation coefficients reported for the lower Chesapeake Bay stations include all measurements made during that month. Mean seasonal values were calculated over seasons defined as: Winter - January through March; Spring - April through June; Summer - July through September; and Autumn - October through December.

It should be emphasized that attenuation coefficients are log transforms of numbers. Comparisons of the various attenuation coefficient means reported in this work therefore are actually comparisons between very large numbers of quanta with large differences. For example, if there are 100×10^{13} quanta $\text{nm}^{-2} \cdot \text{cm}^{-2} \cdot \text{s}^{-1}$ at the surface and 1×10^{13} quanta $\text{nm}^{-2} \cdot \text{cm}^{-2} \cdot \text{s}^{-1}$ left 1 meter below, the attenuation coefficient representing this difference of 99×10^{13} quanta $\text{nm}^{-2} \cdot \text{cm}^{-2} \cdot \text{s}^{-1}$ would be only 4.6 m^{-1} . If the irradiance at 1.0 meter were 2×10^{13} quanta $\text{nm}^{-2} \cdot \text{cm}^{-2} \cdot \text{s}^{-1}$ instead of 1×10^{13} quanta $\text{nm}^{-2} \cdot \text{cm}^{-2} \cdot \text{s}^{-1}$, then the attenuation coefficient

would be 3.9 m^{-1} , a difference of only 0.7 m^{-1} representing a real difference of $10,000,000,000,000 \text{ quanta nm}^{-2}\text{-cm}^{-2}\text{-s}^{-1}$.

Relative Potential Photosynthetically Storable Radiation

The relative potential photosynthetically storable radiation, PSR, was calculated as the product of the irradiance distribution and the theoretical photosynthetic action spectrum. The PSR is defined by Morel (1978) and Smith (1979) as that portion of absorbed energy actually transferred into stored chemical energy in the form of organic matter through photosynthesis. The relative potential PSR thus expresses the relative potential efficiency of photosynthesis given a specific irradiance distribution and a specific absorption complex (set of pigments).

RESULTS

Mean Seasonal Spectral Attenuation

The mean seasonal spectral attenuation for all stations in the lower Chesapeake Bay seagrass study is presented in Fig. 7. A comparison of the distribution of the mean seasonal spectral attenuation coefficients (Figs. 8 through 11 and Table II) reveals a seasonal pattern and some significant differences between vegetated and unvegetated sites. The season of least attenuation (greatest water clarity) was winter and of greatest attenuation was summer. Spring and Autumn were intermediate. There was no obvious difference in mean spectral attenuation between the average vegetated and unvegetated sites during the seasons of maximum and minimum attenuation, summer and winter respectively. Winter values calculated for seagrass beds ranged from a low of 0.371 m^{-1} at 570 nm to a high of 1.14 m^{-1} at 410 nm while corresponding values for unvegetated sites were 0.283 and 1.04. The highest winter mean attenuation of red light was calculated as 0.834 m^{-1} for the vegetated sites and 0.679 m^{-1} for the unvegetated sites, both at 694 nm, the longest wavelength measured.

The summer values were the highest mean seasonal coefficients calculated, ranging from 3.07 m^{-1} at 410 nm to 1.08^{-1} at 570 nm for vegetated sites and 3.08 m^{-1} to 1.00 m^{-1} for the same wavelengths of light at unvegetated sites. For example, if 1.0 unit of irradiance were

Mean Seasonal Spectral Attenuation

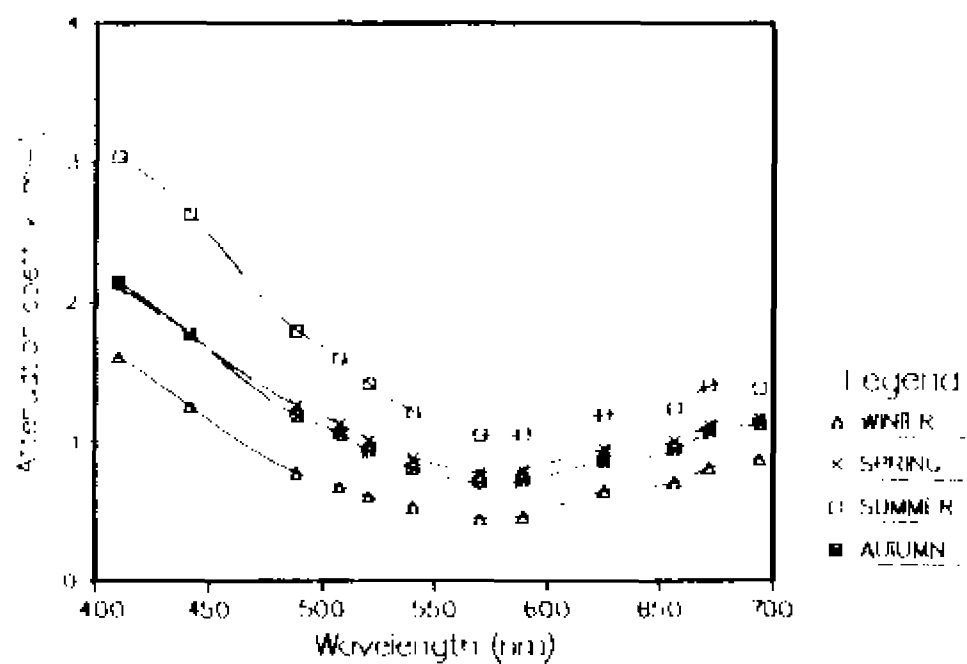


Figure 7. Mean seasonal spectral attenuation for shallow waters of the lower Chesapeake Bay.

TABLE II
MEAN SEASONAL SHALLOW WATER SPECTRAL ATTENUATION (m^{-1})
Vegetated and Unvegetated Stations of the Lower Chesapeake Bay, 1981
(Depth Interval 0.1 - 0.5 m)

Wave- length (nm)	WINTER		SPRING		SUMMER		AUTUMN	
	Veg	Unveg	Veg	Unveg	Veg	Unveg	Veg	Unveg
VIOLET								
410	1.14	1.04	1.91	2.48	3.07	3.00	2.21	2.04
441	0.892	0.868	1.62	2.04	2.70	2.62	1.85	1.64
BLUE								
488	0.566	0.503	1.14	1.45	1.79	1.70	1.28	1.054
GREEN								
507	0.510	0.435	1.02	1.20	1.00	1.58	1.15	0.918
520	0.460	0.397	0.919	1.14	1.41	1.40	1.03	0.802
540	0.404	0.364	0.813	0.973	1.22	1.19	0.887	0.674
YELLOW								
570	0.371	0.283	0.711	0.841	1.00	1.00	0.787	0.581
589	0.407	0.317	0.735	0.858	1.09	1.01	0.798	0.599
ORANGE								
625	0.563	0.497	0.907	0.907	1.24	1.15	0.935	0.754
RED								
656	0.644	0.522	0.956	1.05	1.20	1.21	1.01	0.842
671	0.731	0.623	1.06	1.10	1.41	1.30	1.14	0.961
694	0.834	0.679	1.11	1.22	1.43	1.34	1.19	1.02

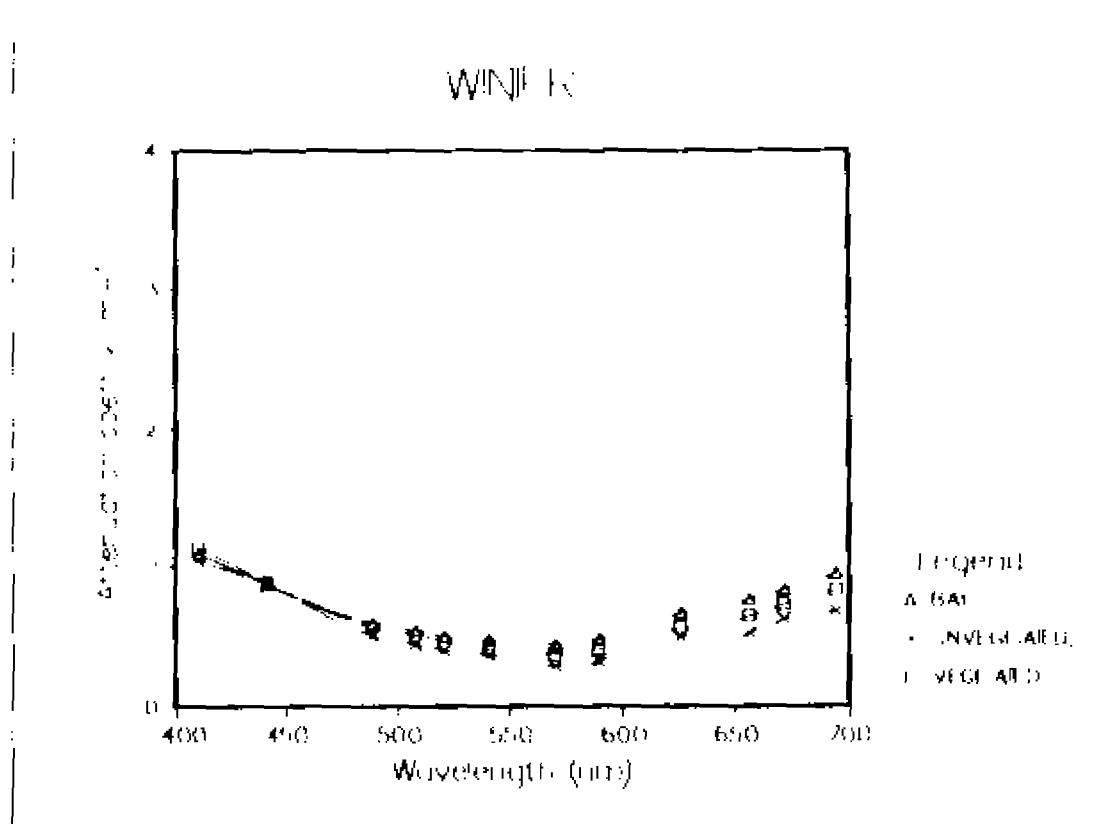


Figure 8. Mean Winter spectral attenuation at vegetated and unvegetated sites of the lower Chesapeake Bay.

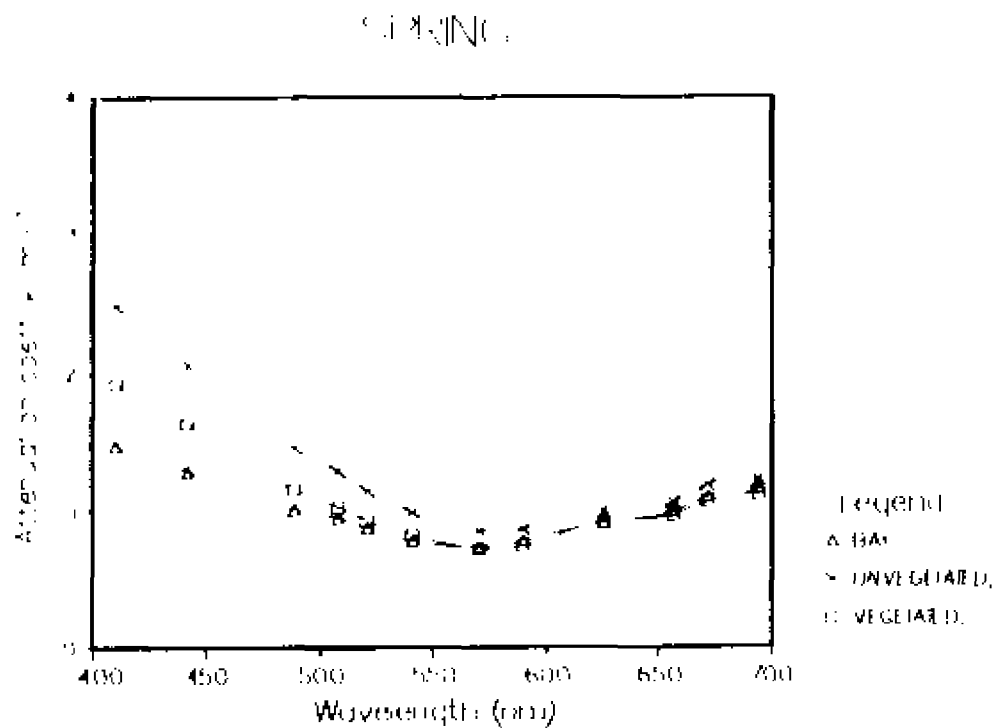


Figure 9. Mean Spring 1981 spectral attenuation at vegetated and unvegetated sites of the lower Chesapeake Bay.

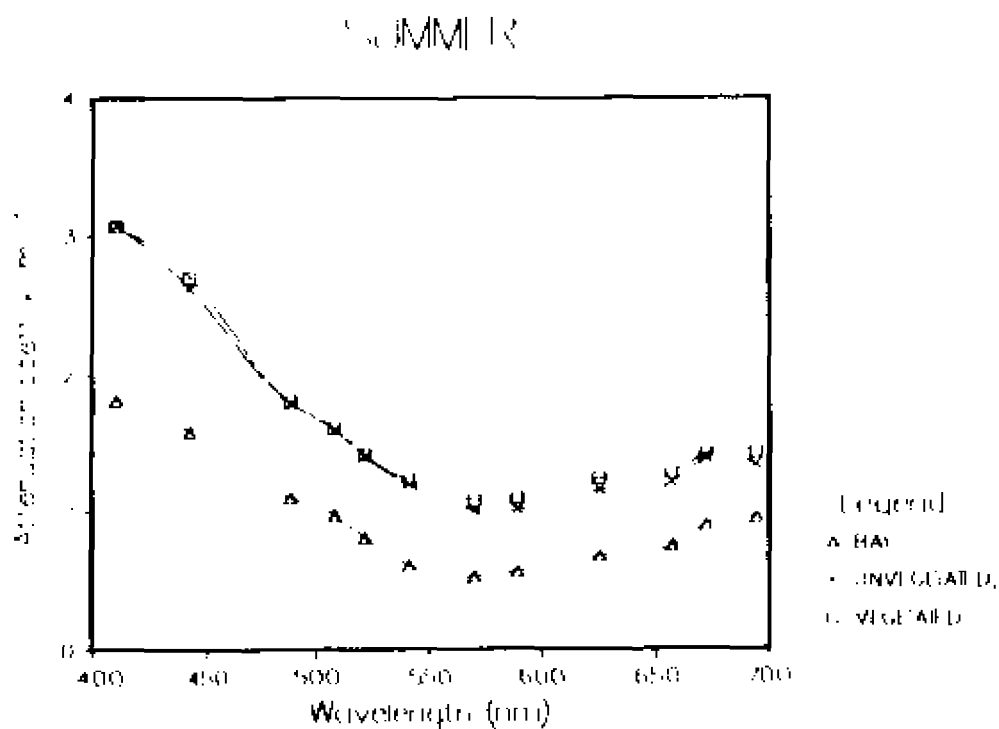


Figure 10. Mean Summer 1981 spectral attenuation at vegetated and unvegetated sites of the lower Chesapeake Bay.

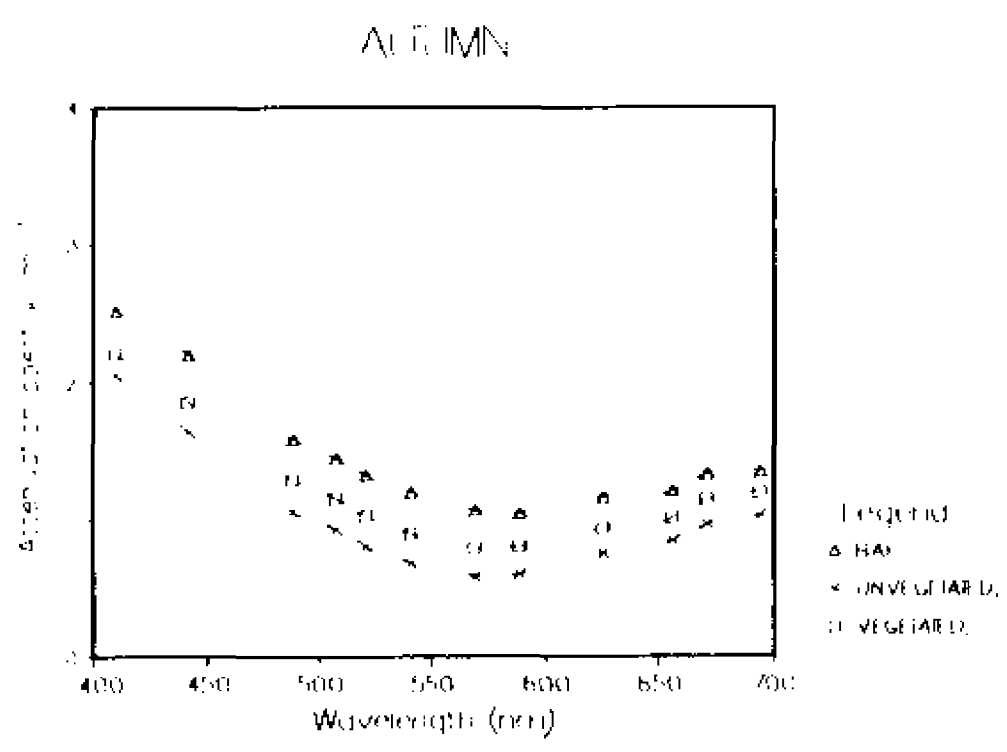


Figure 11. Mean Autumn 1981 spectral attenuation at vegetated and unvegetated sites of the lower Chesapeake Bay.

attenuated over a distance of 1.0 m at a rate of 3.0 m^{-1} only 0.05 units of irradiance would remain. Over a path of 2.0 m of water the unit would be reduced to about 0.0025. The mean seasonal coefficients for vegetated and unvegetated sites were almost identical but there was a large difference between the mean deep-water (bay site) coefficients and the shallow water coefficients possibly due to lesser resuspension of particulates at the deep site.

The mean autumnal values were similar to the spring mean coefficients for the vegetated sites, and ranged from 0.787 m^{-1} at 570 nm to 2.21 m^{-1} at 410 nm and the unvegetated mean from 0.581 m^{-1} to 2.04 m^{-1} at the same wavelengths.

A large difference between the mean spectral attenuation coefficients for vegetated and unvegetated sites was found for spring (Fig. 9). The mean spring violet-blue (<500 nm) unvegetated spectral k_d was found to be more than one standard deviation higher than the mean attenuation of violet-blue light in the water column at the vegetated sites (cf. Figs. 12, 13). Both shallow water vegetated and unvegetated mean attenuation values were higher than those for the deep water reference site (bay station). Mean spring vegetated spectral k_d ranged from 0.711 m^{-1} at 570 nm to 1.91 m^{-1} at 410 nm. Corresponding values for the unvegetated sites were 0.841 m^{-1} and 2.48 m^{-1} , respectively. Violet light of 410 nm was reduced 85% per meter at the average vegetated site and over 92% per meter at the average unvegetated site during spring. There was little or

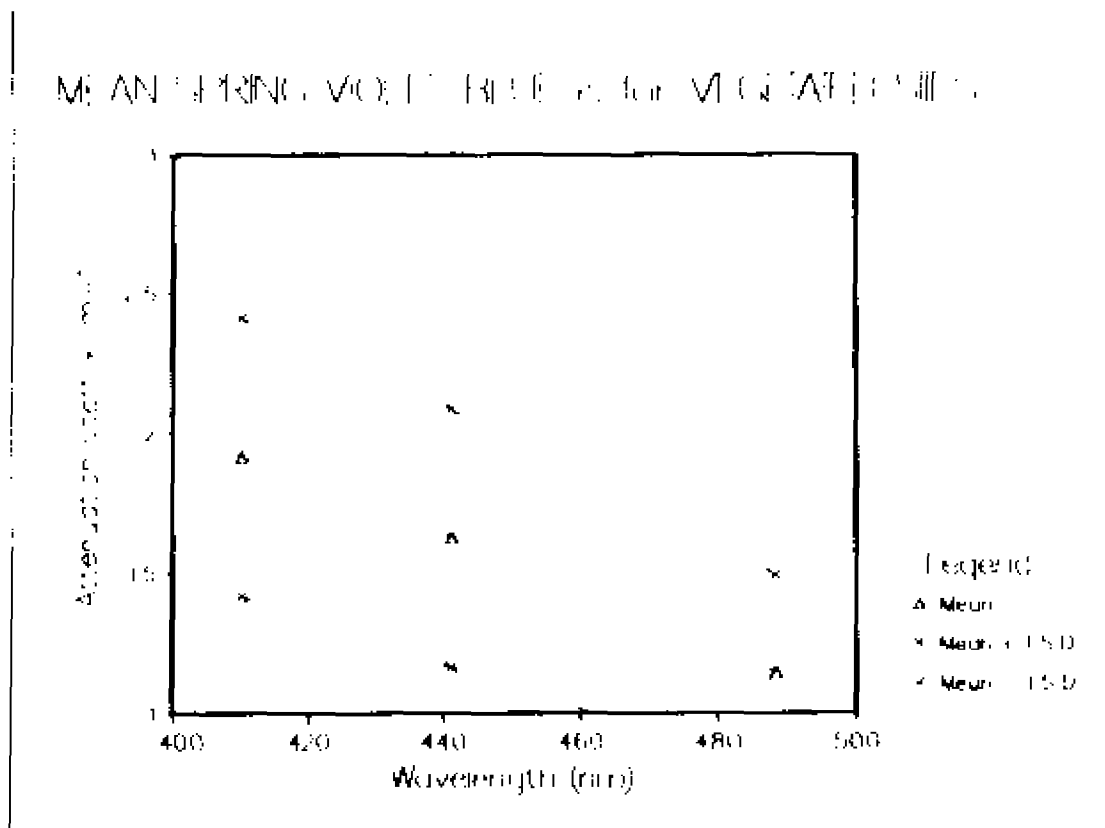


Figure 12. Mean Spring 1981 violet-blue attenuation \pm 1 s.d. at vegetated sites of the lower Chesapeake Bay.

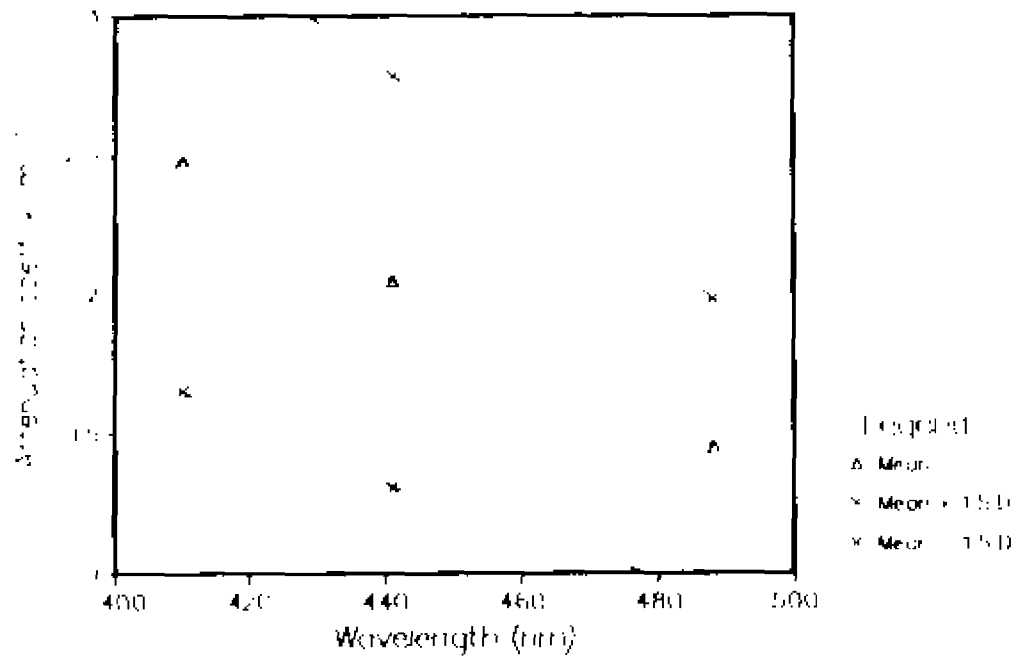
MEAN SPRING 1981 VIOLET-BLUE ATTENUATION \pm 1 S.D. AT UNVEGETATED SITES

Figure 13. Mean Spring 1981 violet-blue attenuation \pm 1 s.d. at unvegetated sites of the lower Chesapeake Bay.

no mean difference for wavelengths greater than 550 nm (yellow, orange, red). The deep water station ranged from about 1 to 1.5 m^{-1} during spring.

Mean Monthly Spectral Attenuation

Comparison of the monthly mean spectral attenuation for vegetated sites (Figs. 14, 16, 18) with that for unvegetated sites (Figs. 15, 17, 19) shows that the most obvious difference to be found, as discussed above, is the higher attenuation of shorter wavelengths at the unvegetated sites during the spring of the year. Unvegetated sites are characterized by elevated attenuation over the entire measured spectrum from May through October, whereas vegetated sites do not show consistently elevated attenuation coefficients over the same time period. Attenuation of the violet and blue wavelengths (400-500 nm) at the vegetated sites increases gradually, reaching its maximum during September with minor peaks occurring during April and July. The attenuation coefficient for the remainder of the PAR spectrum (500-700 nm) also exhibits these minor peaks but there is no increase towards the September maximum.

There does, however, appear to be a strong seasonal pattern to the attenuation coefficient at both vegetated and unvegetated sites, differing mainly in the timing of commencement of high values. For example, the mean-monthly violet-blue attenuation values for unvegetated sites (Fig. 15) reveals that attenuation of light of 410 and 441 nm exceeded 2 m^{-1} starting during May of 1981 and lasted into October of that year. However,

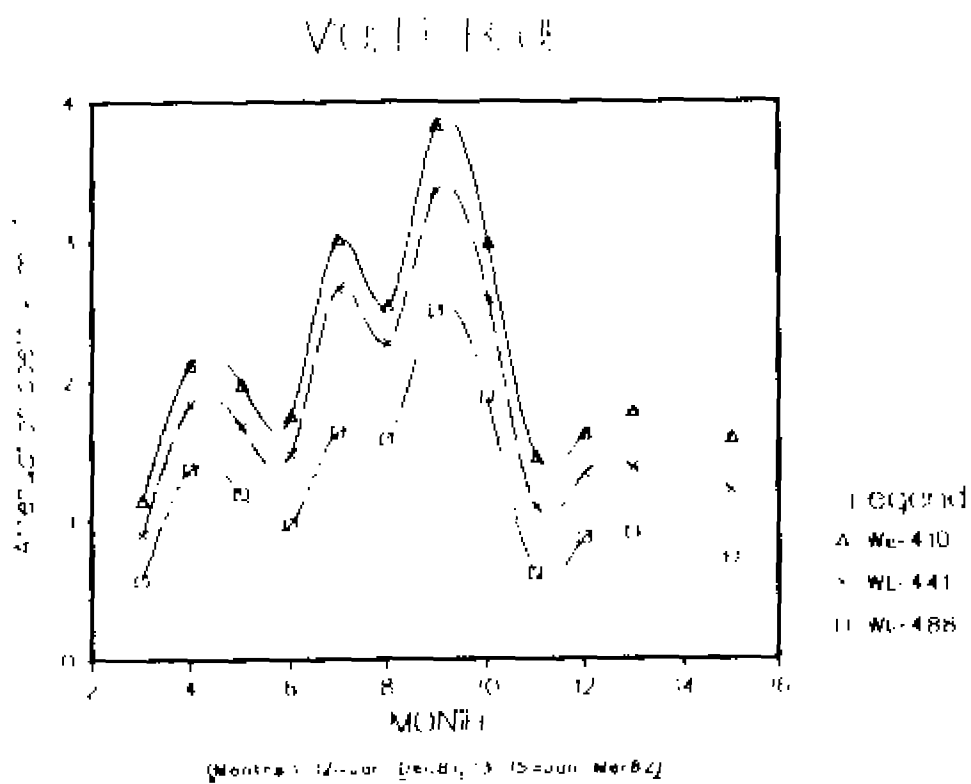


Figure 14. Mean monthly violet-blue attenuation at vegetated sites of the lower Chesapeake Bay.

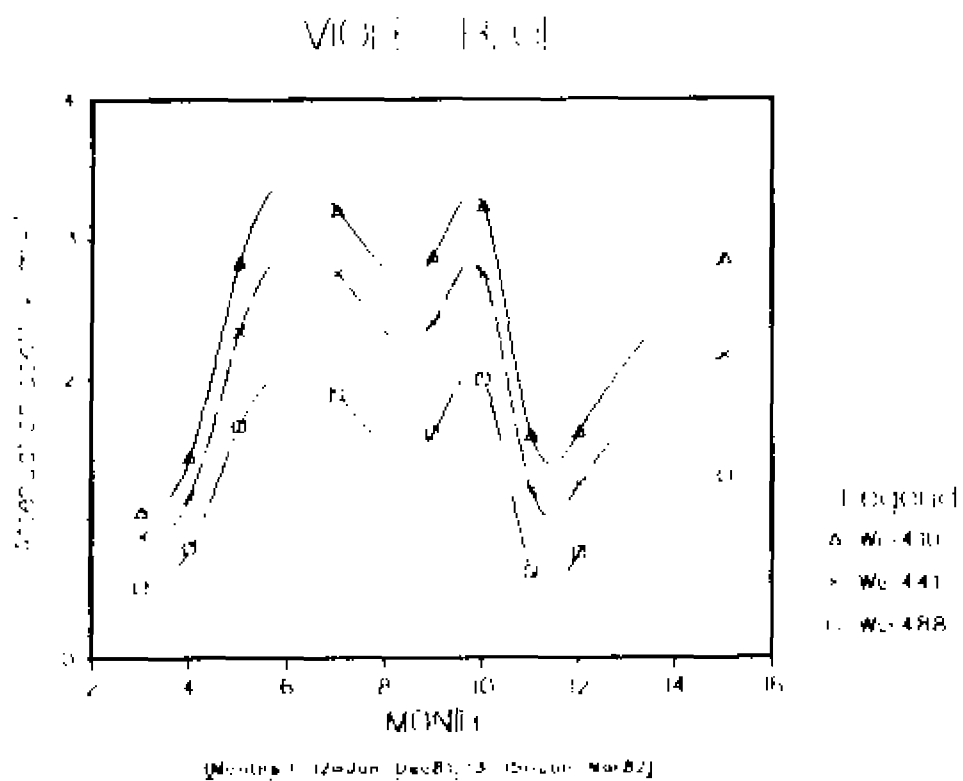


Figure 15. Mean monthly violet-blue attenuation at unvegetated sites of the lower Chesapeake Bay.

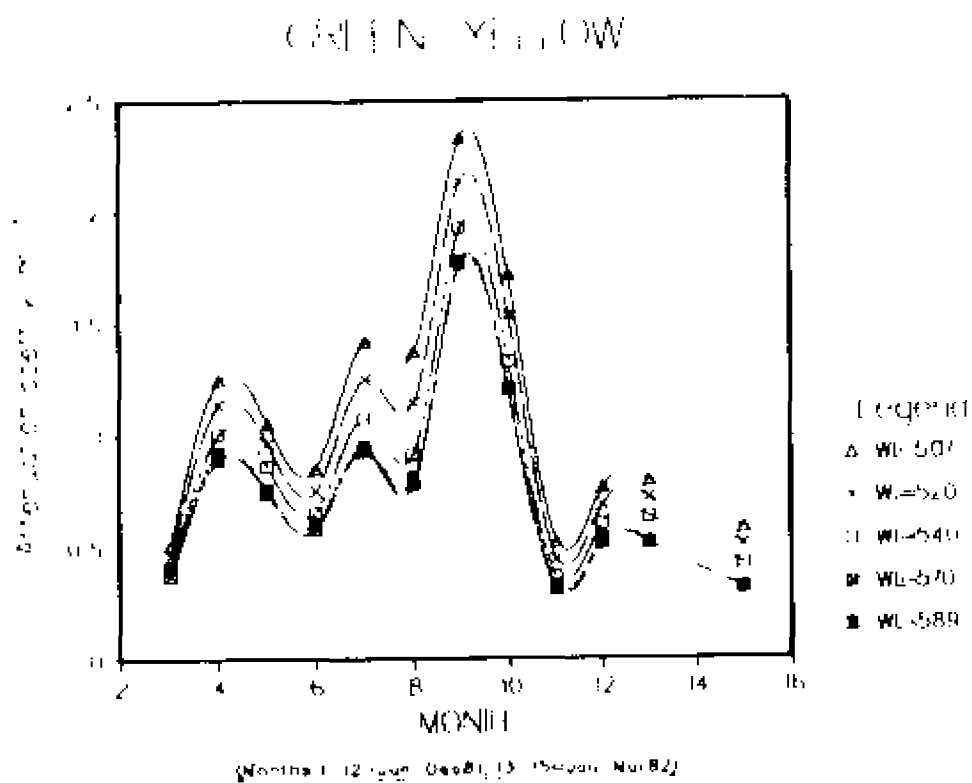


Figure 16. Mean monthly green-yellow attenuation at vegetated sites of the lower Chesapeake Bay.

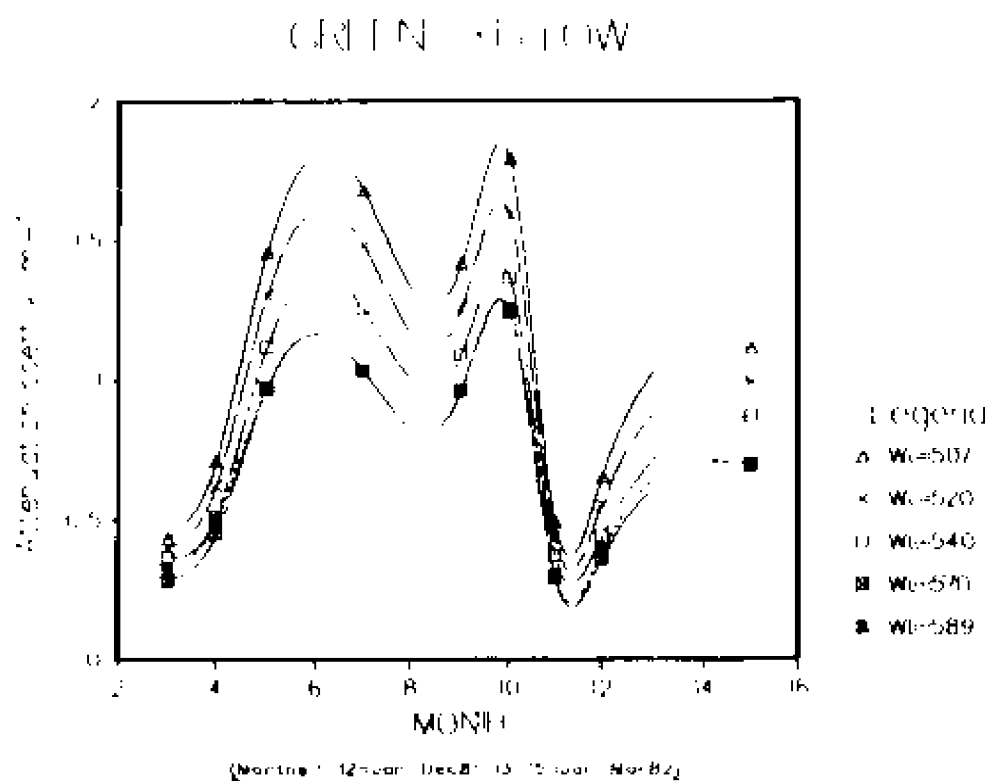


Figure 17. Mean monthly green-yellow attenuation at unvegetated sites of the lower Chesapeake Bay.

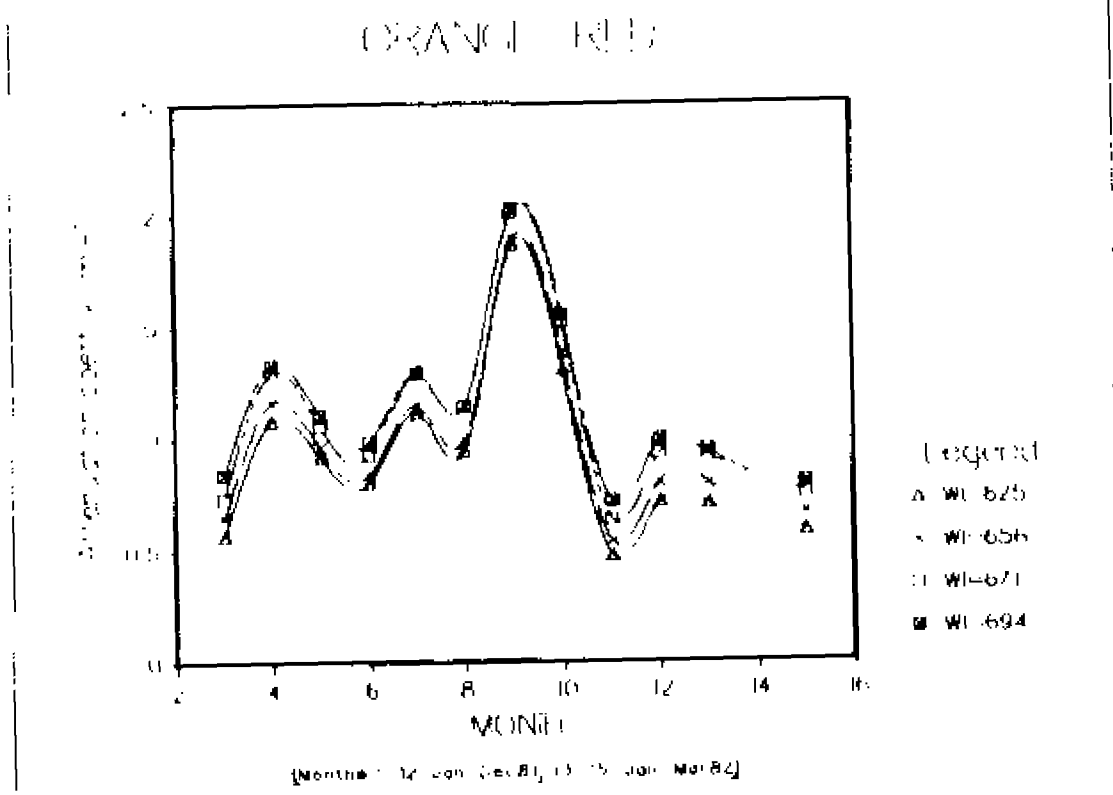


Figure 18. Mean monthly orange-red attenuation at vegetated sites of the lower Chesapeake Bay.

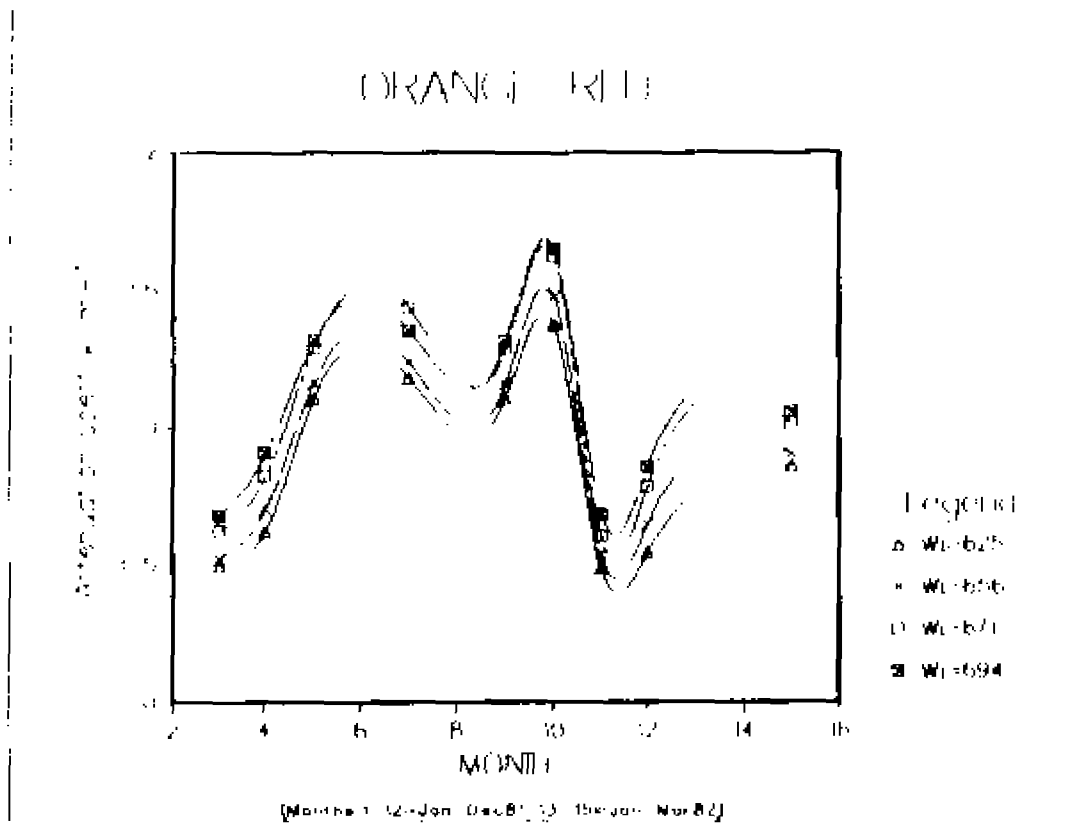


Figure 19. Mean monthly orange-red attenuation at unvegetated sites of the lower Chesapeake Bay.

similarly high attenuation of the same wavelengths of light at the vegetated sites did not occur until July. During 1982, the high attenuation values at the unvegetated sites started even earlier in the year (i.e. March), whereas, short wavelength (410-441 nm) attenuation at the vegetated sites during January and March of 1982 were only about half as high. This timing difference in light quality could effect biological events such as flowering and germination processes (Spence, 1981). The onset of high attenuation, especially of short wavelengths, appears to differ from year to year, as can be seen by comparing the March 1982 values (month 15 on the Figures) with the March and May 1981 values (Figs. 14, 15). The correspondences at each type of site between the March 1982 short wavelength attenuation coefficients and those for the preceding May (month 5) are quite striking. The relationship between the vegetated and unvegetated sites for the March 1982 attenuation coefficients is also analogous to their relationship in May, 1981. That is, for the vegetated sites the mean values of coefficients for the attenuation of violet light (at 410, 441 nm) for May 1981 and for March 1982 were both between about 1.5 and 2.0 m^{-1} whereas those for the unvegetated sites were between about 2 and 3 m^{-1} for both months.

For the unvegetated sites the year 1981 was divided into two distinct light environments with little transition, while in the vegetated sites there was a shorter high attenuation period with a more gradual transition from low to high values. This gradual transition may be important in allowing the plants to acclimate.

The variability of the monthly mean attenuation for vegetated and unvegetated sites is shown for wavelengths of 441 nm and 671 nm in Figures 20, 21, 22, and 23. These wavelengths are near the photosynthetic action peaks for marine green plants (Halldal, 1974). The variation in violet attenuation (441 nm) is consistently greater during the high turbidity season (May through October, 1981) for unvegetated sites than it is for vegetated sites (cf. Figs. 20, 21). A comparison of the variability of red light attenuation between vegetated and unvegetated sites reveals much less difference. Constancy of light quality may be of consequence to benthic plants.

May 1981 seems to have been not only a pivotal month for the relative light environment in the unvegetated sites of the Lower Bay, but is also the month with the highest observed net seagrass community productivity (Murray and Wetzel, 1982; Murray, 1983; Murray and Wetzel, in press). The mean irradiance values calculated for vegetated and unvegetated sites during May are shown in Fig. 24. The unvegetated mean is much higher at all wavelengths. There is a difference of more than 1.0 m^{-1} at 410 nm, and a difference of about 1.0 at 441 nm. The difference decreases to about 0.5 at 520 nm. Below 540 nm there is a constant difference of less than 0.4 m^{-1} . A 1.0 m^{-1} difference in attenuation represents a relative irradiance reduction of 63% over just 1 meter! That is, during May approximately 63% less violet light was able to pass through a meter of water at the "average" unvegetated site than at the "average" vegetated site. Over a two meter path the reduction would be 88%.

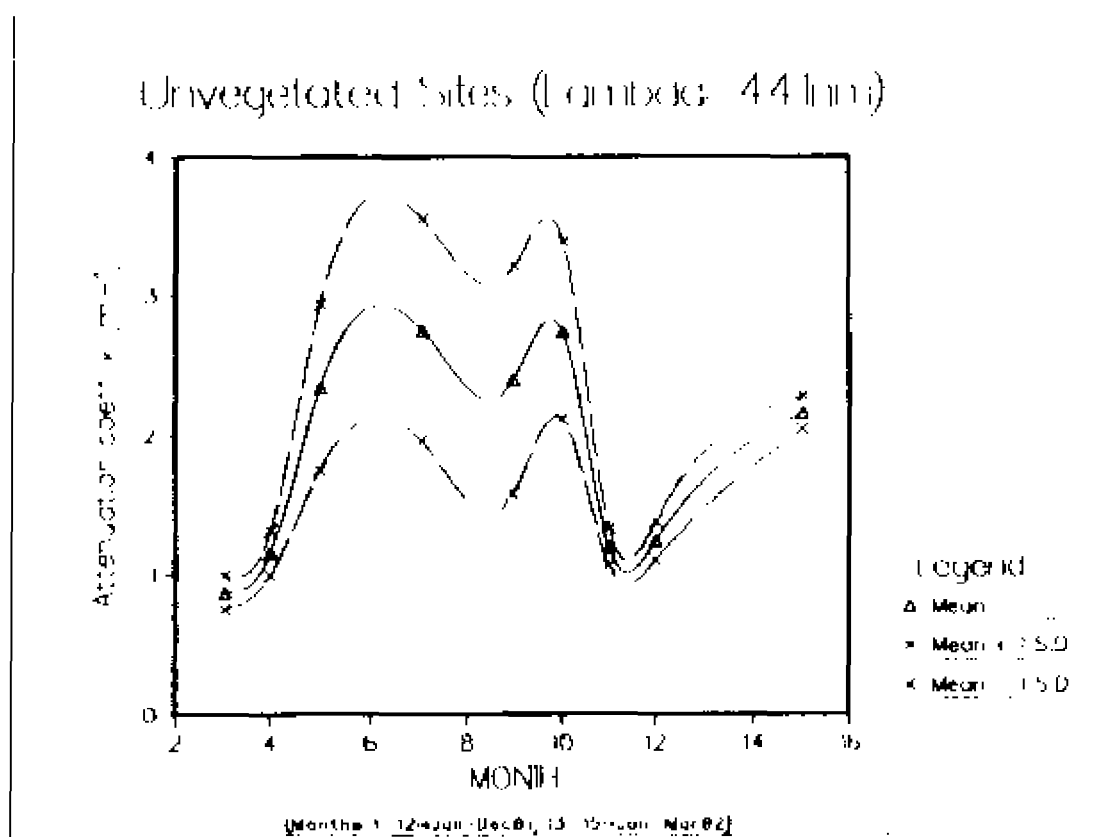


Figure 20. Mean monthly variability of attenuation of light of 441nm at unvegetated sites of the lower Chesapeake Bay.

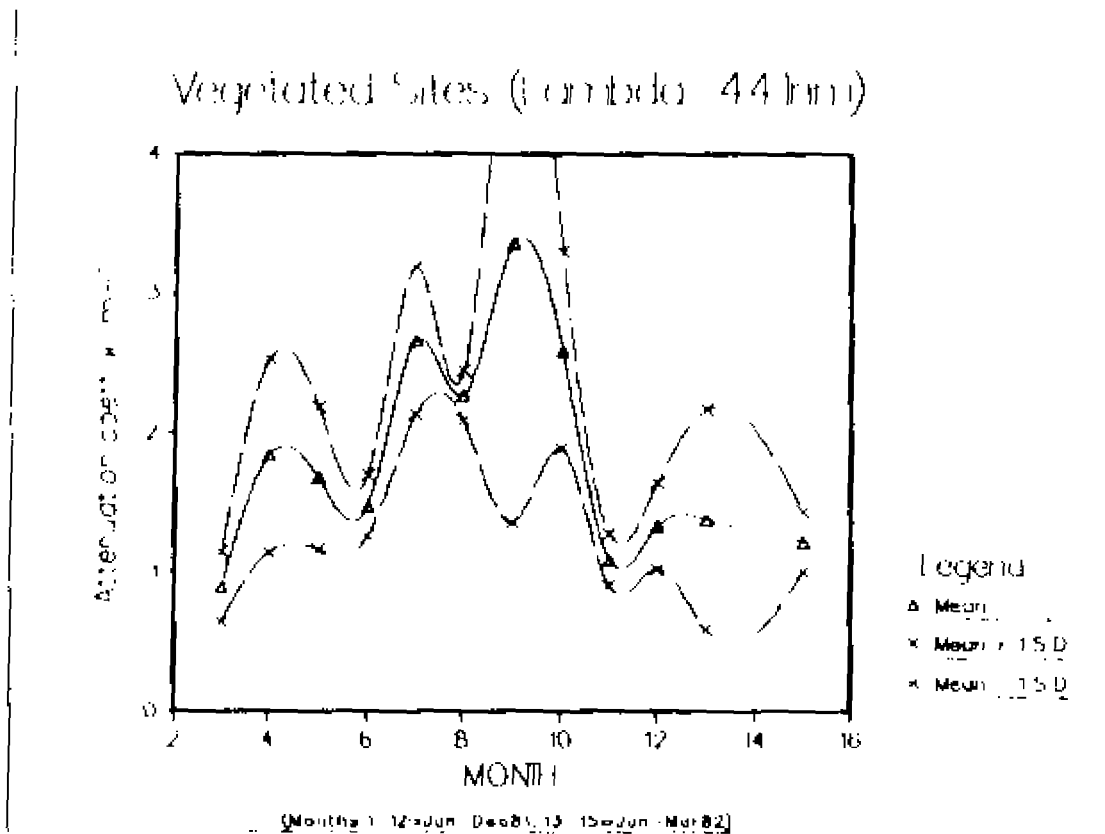


Figure 21. Mean monthly variability of attenuation of light of 441nm at vegetated sites of the lower Chesapeake Bay.

unvegetated sites, (average: 671nm)

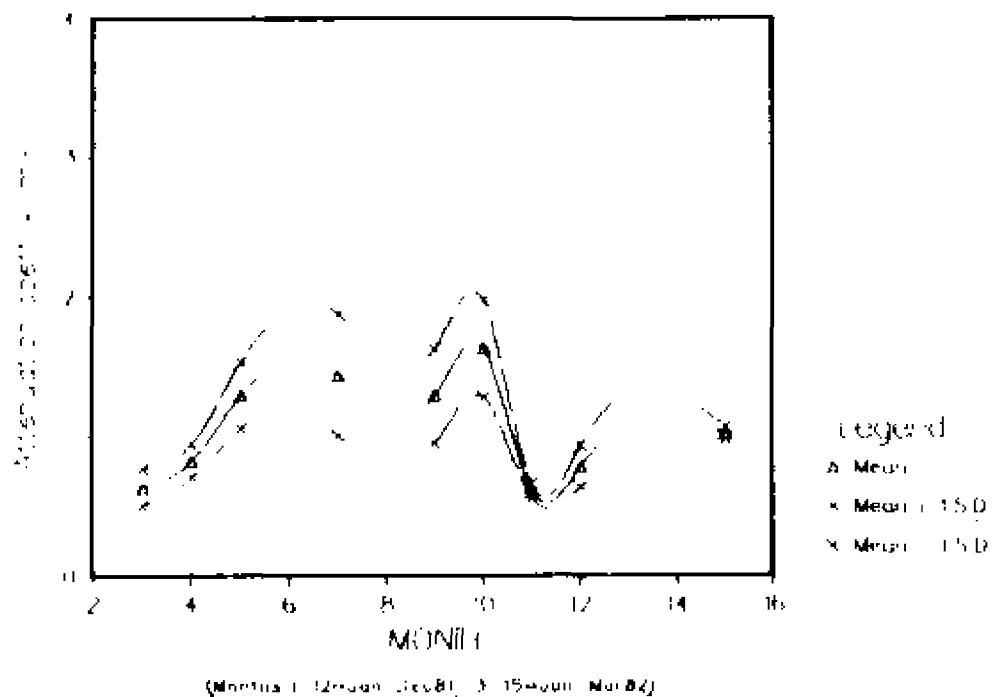


Figure 22. Mean monthly variability of attenuation of light of 671nm at unvegetated sites of the lower Chesapeake Bay.

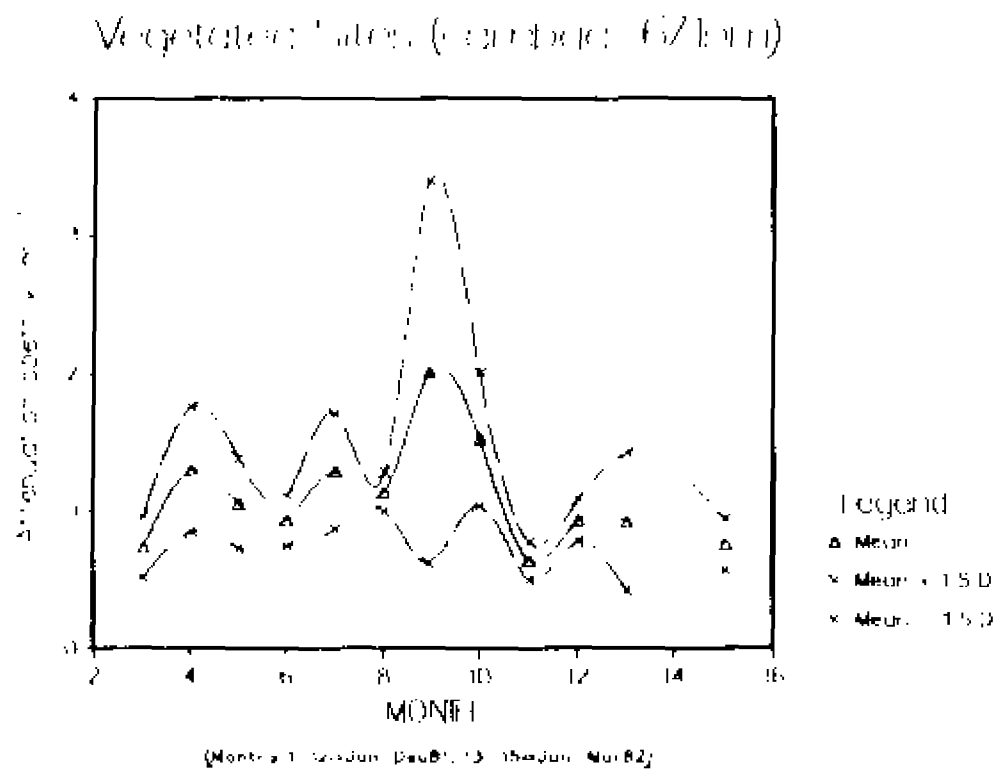


Figure 23. Mean monthly variability of attenuation of light of 671nm at vegetated sites of the lower Chesapeake Bay.

Mean May Spectral Attenuation by Vegetation

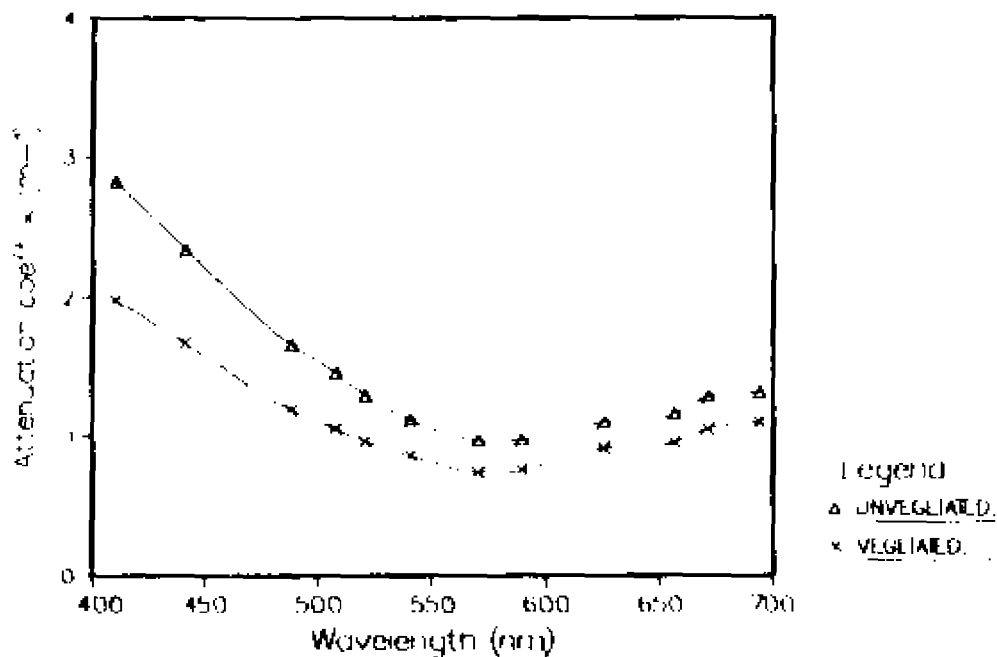


Figure 24. Mean May 1981 spectral attenuation at unvegetated and vegetated sites of the lower Chesapeake Bay.

A comparison of the mean spectral attenuation for May for each site is presented in Fig. 25. The two unvegetated sites (Mumfort Is. in the York River and the site in the mouth of the Severn River) had the highest attenuation at all wavelengths. The Severn R. site was especially high below 500 nm. The mean k_d for the violet wavelengths (410, 441 nm) was between 3.5 and 4.0 m^{-1} for this site. A hundred quanta would be reduced to just 2 or 3 quanta in just one meter of water with an attenuation coefficient between 3.5 and 4.0! A reduction of greater than 99% would result from the passage of light through two meters of water with a k_d value greater than 3.5 m^{-1} . That is, there was essentially no violet light below the surface of the water at the Severn R. site during the May sampling period. Blue light (488 nm) was also greatly attenuated at this site, reduced about 98% per meter. Mean attenuation at the Mumfort Is. site ranged from a high of about 3.0 m^{-1} at 410 nm to about 1.5 at 507 nm and no higher than that for the remainder of the spectrum. The red region of the spectrum was even more attenuated at the Mumfort Is. site than in the Severn.

All mean spectral attenuation coefficients for May at the vegetated sites - Guinea Marsh, Four Point Marsh and Vaucluse - were found to be below about 2 m^{-1} except those for violet light at Four Point Marsh. However, the attenuation of yellow, orange and red light at the Four Point Marsh site was extremely low - less than 0.5 m^{-1} . This is a reduction of about 40% per meter. This site and the unvegetated Severn R. site are located very close to each other. Both are in Mobjack Bay and have very similar patterns of spectral attenuation but of differing magnitudes. The

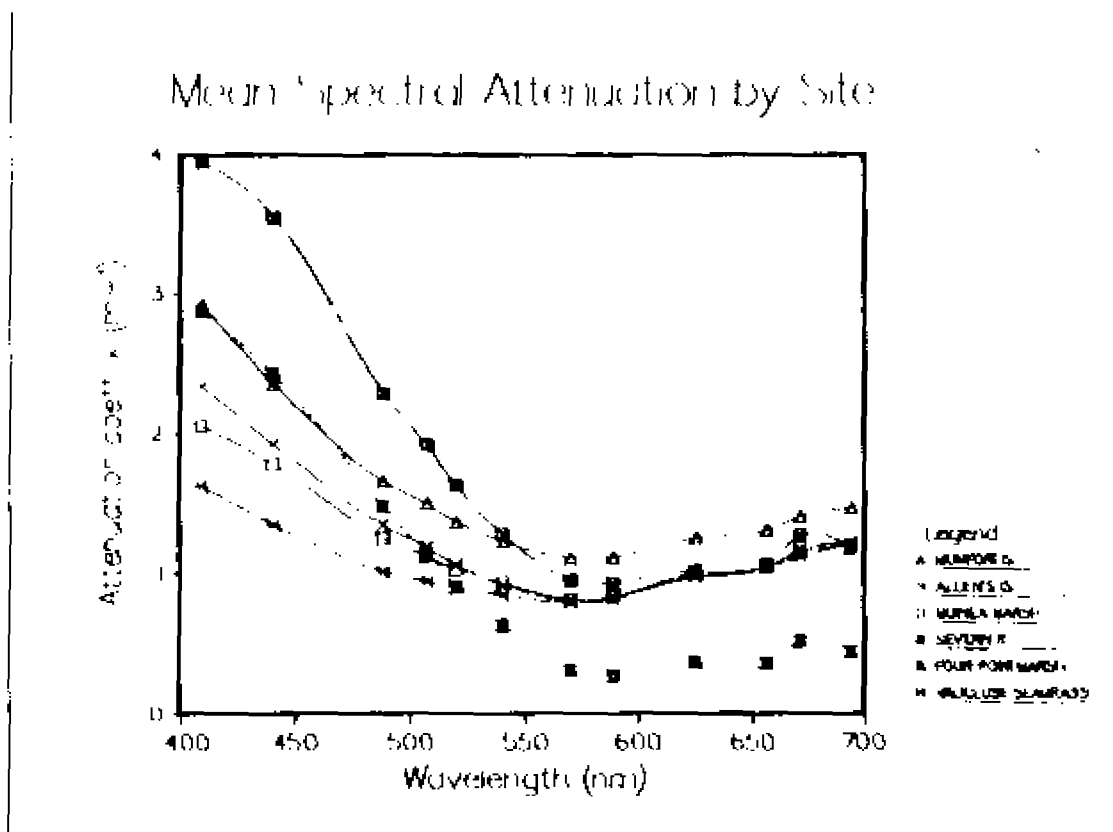


Figure 25. Mean May 1981 spectral attenuation at individual sites of the lower Chesapeake Bay.

mean value for the unvegetated Severn R. site is about 1 m^{-1} consistently higher than that of the vegetated Four Point Marsh site during May. Violet attenuation at the Guinea Marsh and Vaucluse Shore vegetated sites was between 1 and 1.5 m^{-1} . The Vaucluse site had the lowest violet-blue mean attenuation during May while the Four Point Marsh site had the lowest yellow to red attenuation; lower than even the mean winter values at all other sites. With the exception of the violet light at Four Point Marsh the mean May attenuation for all vegetated sites at all wavelengths was less than about 2 m^{-1} . Thus, the extremely low May attenuation of the longer wavelengths at Four Point Marsh may have compensated for the high attenuation of the short wavelengths in terms of total light energy available for photosynthesis.

The spectral attenuation at the Allen's Is. site was intermediate to that of the vegetated and unvegetated sites. This is interesting because this site is also intermediate with respect to its benthic vegetation. Seagrasses here were considerably reduced in the 1970's with vegetation persisting in only the shallowest areas. In the last few years, however, seagrasses have been slowly returning at this site via natural recolonization as well as from transplant experiments (Orth et al., 1985, 1986). Since this site appeared to be in a transitional vegetational state, its irradiance measurements and calculated attenuation values have been included in neither the "vegetated" nor the "unvegetated" means reported herein, but have been treated separately.

A comparison of the mean seasonal spectral irradiance attenuation values calculated for the individual sites (Figs. 26 - 32) reveals both differences between vegetated (Vaucluse, Guinea, Four Point) and unvegetated (Mumfort, Severn) sites and reveals individual site idiosyncracies.

Mean seasonal spectral attenuation values were at or below 2 m^{-1} for all seasons except summer at the western shore vegetated sites (Figs. 28, 30). As noted previously, attenuation at the red end of the spectrum was particularly low at Four Point Marsh (Fig. 30). Autumn, winter and spring values appear quite similar at this site. Winter and spring mean values were also less than 2.0 m^{-1} at the Vaucluse Shore vegetated site (Fig. 31) on the other side of the Chesapeake Bay, but autumn was the most turbid season for this site and also for the deep site on the eastern shore (Bay, Fig. 32). None of the western shore sites showed this pattern. The light environment, not surprisingly, appears to be quite different in the different masses of water on opposite sides of the Bay. With the exception of fall, the mean seasonal attenuation at the deep site (Fig. 32) was consistently lower than the corresponding values at any other site. Note the relative color shift from blue to red between spring and summer at this site (the intersection of the two seasonal curves). This shift also occurs in modified form at the Vaucluse Shore seagrass site (Fig. 31). Here, though, the penetration of red light is not increased.

The western shore unvegetated sites (Mumfort, Severn, Figs. 26, 29) both had mean spring violet attenuation values between about 2 m^{-1} and

Mean Seasonal Spectral Attenuation

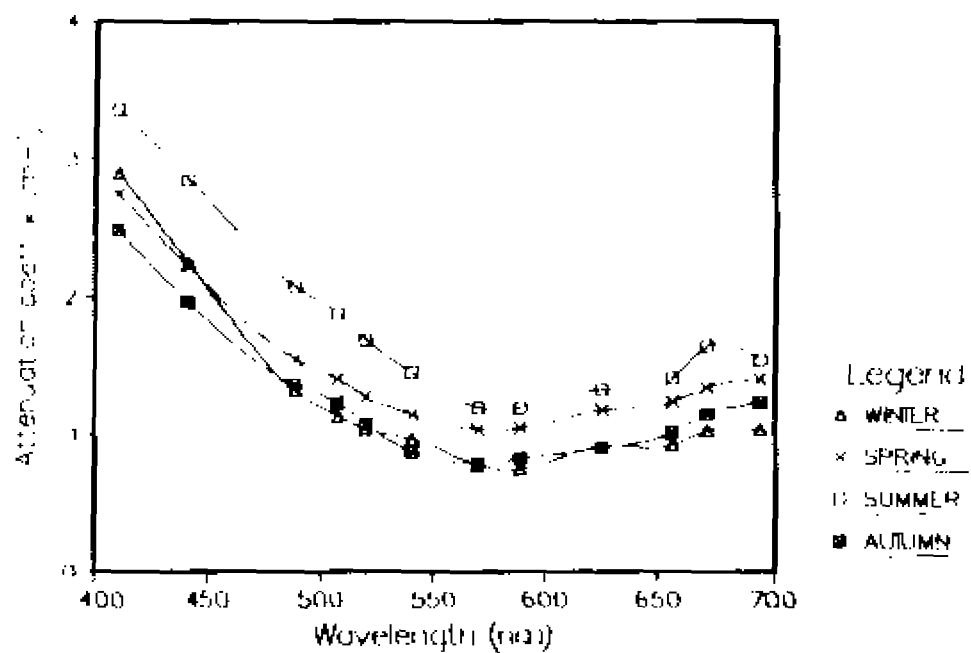


Figure 26. Mean seasonal spectral attenuation at Mumfort Is. site (York R.), Chesapeake Bay.

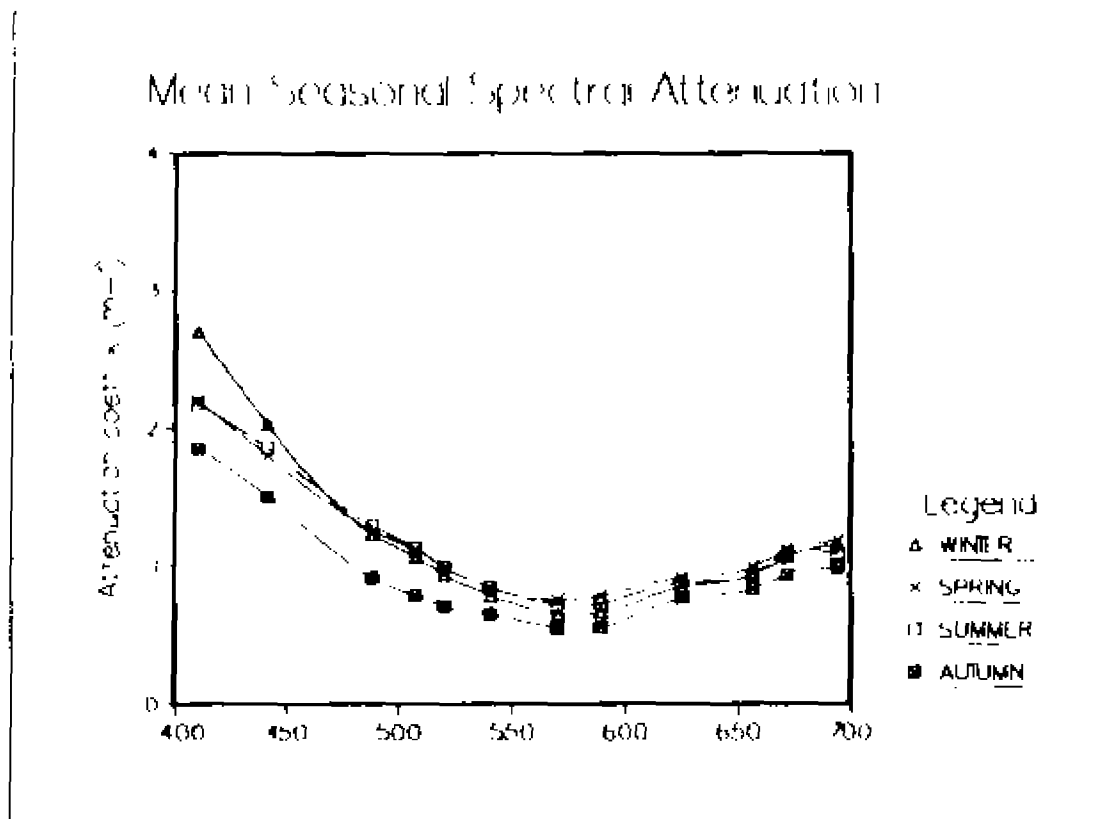


Figure 27. Mean seasonal spectral attenuation at Allen's Is. site (York R.), Chesapeake Bay.

Mean Seasonal Spectral Attenuation

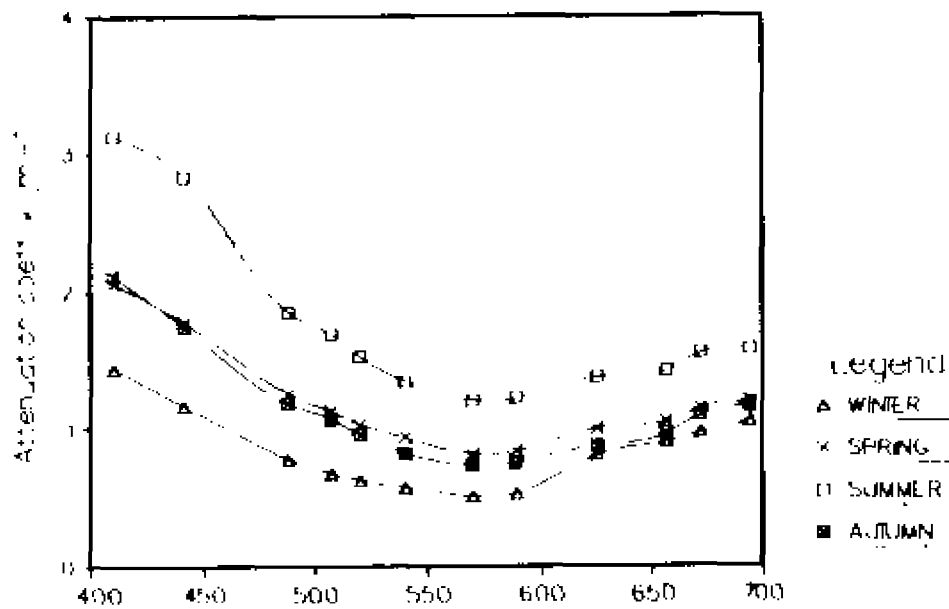


Figure 28. Mean seasonal spectral attenuation at Guinea Marsh site (York R.), Chesapeake Bay.

Mean Seasonal Spectral Attenuation

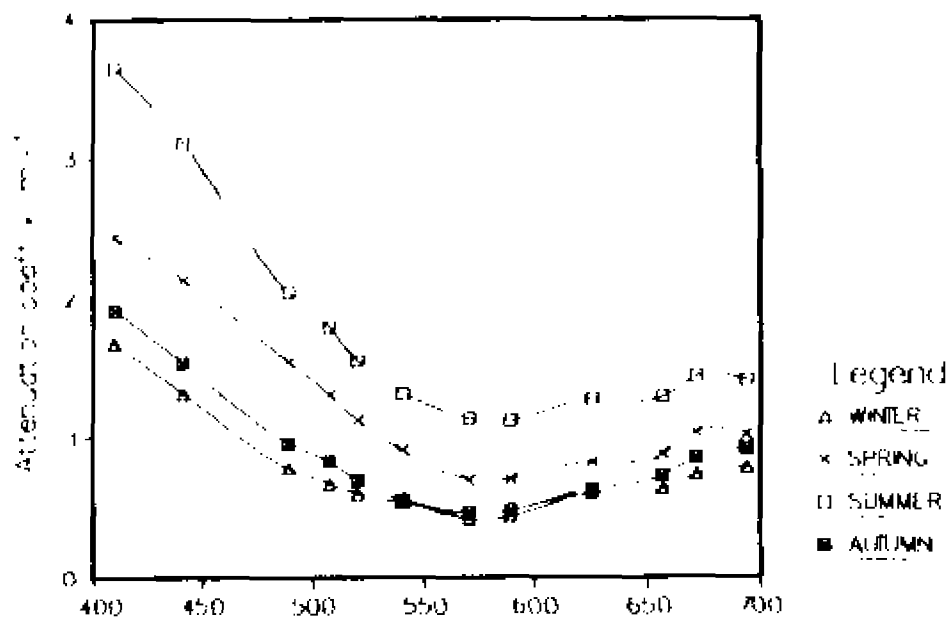


Figure 29. Mean seasonal spectral attenuation at the mouth of the Severn R. (Mobjack Bay), Chesapeake Bay.

Mean Seasonal Spectral Attenuation

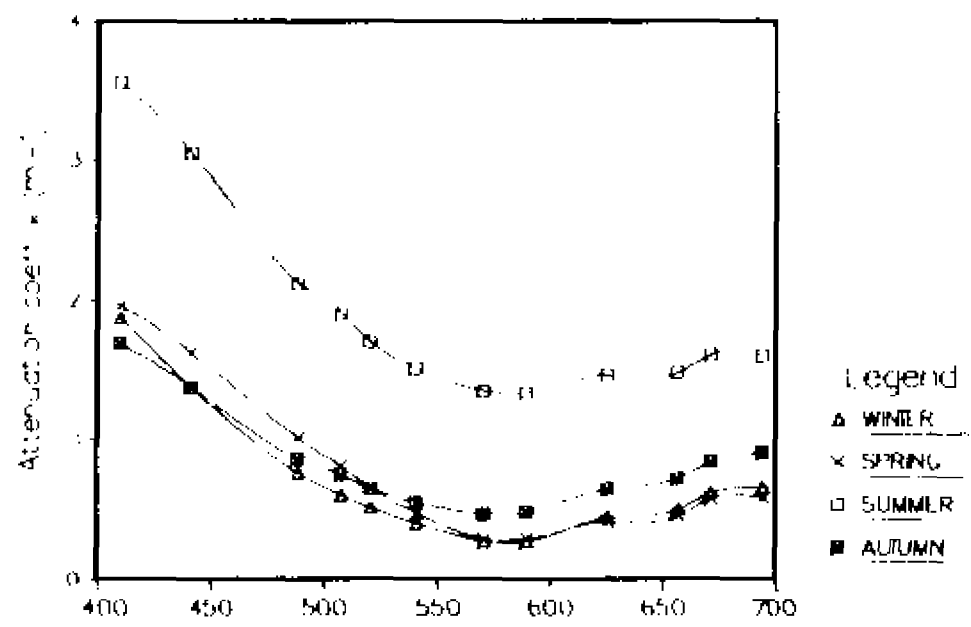


Figure 30. Mean seasonal spectral attenuation at Four Point Marsh (mouth of the Ware R., Mobjack Bay), Chesapeake Bay.

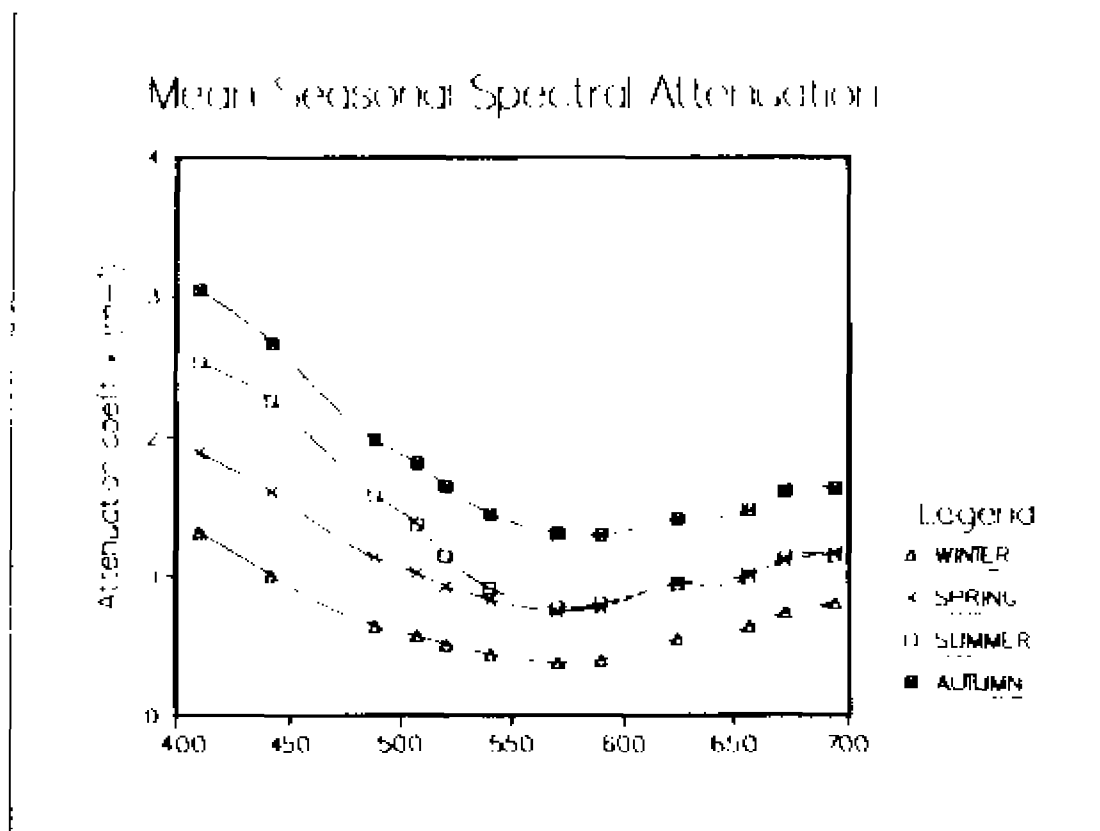


Figure 31. Mean seasonal spectral attenuation at Vaucluse Shores *Zostera marina* bed off the Eastern Shore of the lower Chesapeake Bay.

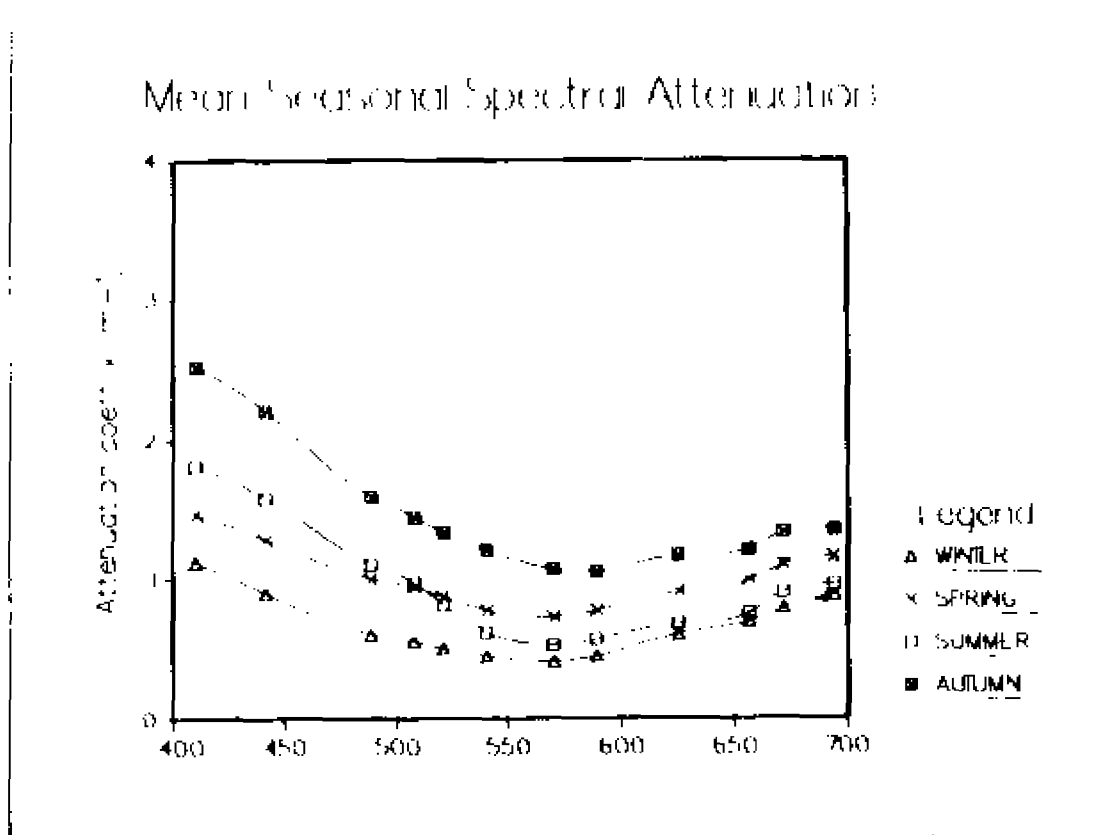


Figure 32. Mean seasonal spectral attenuation at the Deep Station at Vaucluse Shores off the Eastern Shore of the lower Chesapeake Bay.

3 m^{-1} , much higher than the corresponding values at any vegetated site. Each of the seasonal mean attenuation curves for Mumfort Is. (Fig. 26) are high compared to the other sites. The autumn and winter mean spectral attenuation coefficients for the Severn R. site are, however, similar to the corresponding curves for vegetated sites.

The Allen's Is. site (Fig. 27) is once again difficult to classify. Its mean spring spectral attention curve is intermediate - summer low, winter high and fall about average.

The mean monthly water column attenuation curves for selected wavelengths at individual sites are presented in Figs. 33 through 39. The wavelengths presented in these figures (410, 441, 488, 576, 671, and 694 nm) were selected not only for their biological relevance with respect to photosynthetic action spectra and in vivo pigment absorption peaks, but to outline the extremes and means of the full set of twelve wavelengths measured with more clarity and less confusion than would be possible using the complete set measured.

A seasonal pattern of turbidity at all sites is most obvious. As previously mentioned, the high turbidity at the unvegetated sites (Figs. 33, 36) clearly starts in May and continues through October, during 1981. This is especially obvious for the shorter wavelengths. The onset of high turbidity appears earlier in 1982, during March, with violet attenuation approaching or exceeding 3.0 m^{-1} at the unvegetated sites. At Guinea Marsh (vegetated, Fig. 35) the violet attenuation increased gradually from

Mean Monthly Attenuation by Wavelength

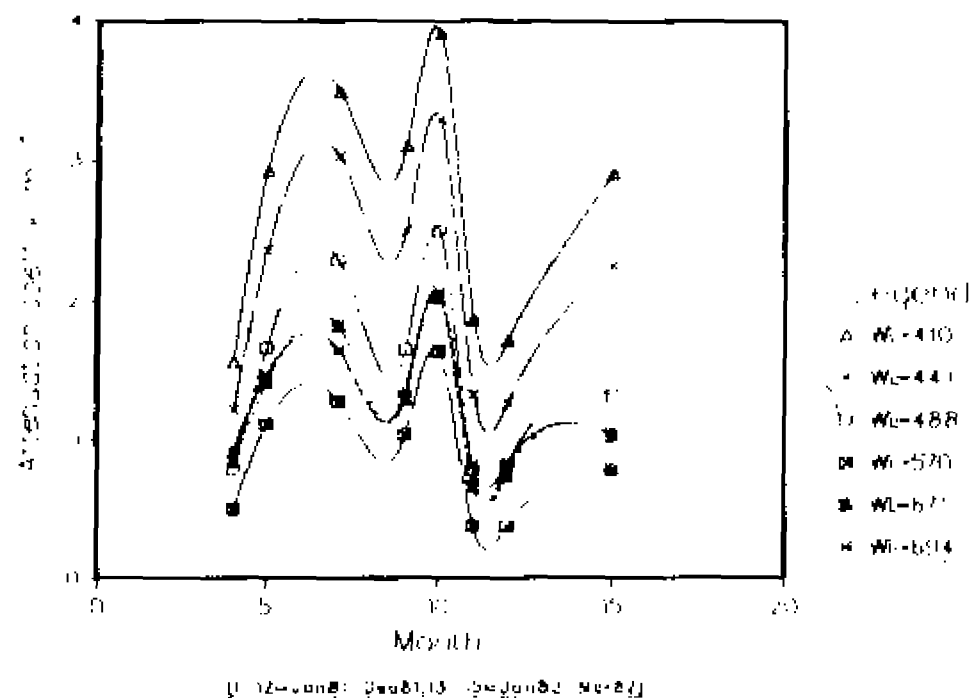


Figure 33. Mean monthly attenuation of selected wavelengths off Mumfort Is., York R., Chesapeake Bay.

Mean Monthly Attenuation by Wavelength

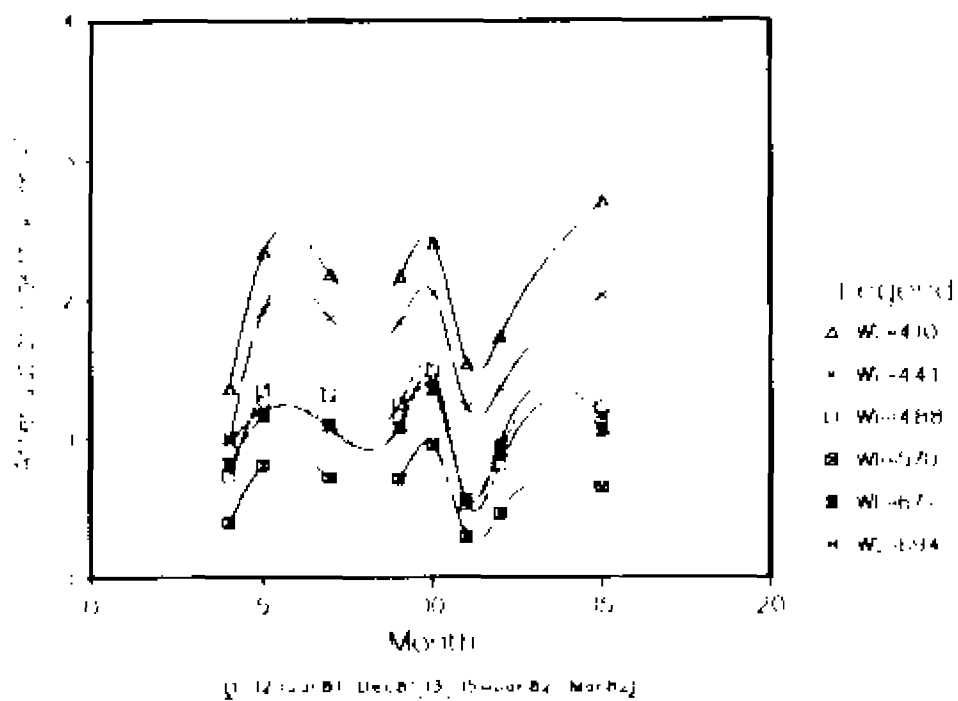


Figure 34. Mean monthly attenuation of selected wavelengths off Allen's Is., York R., Chesapeake Bay.

Mean Monthly Attenuation by Wavelength

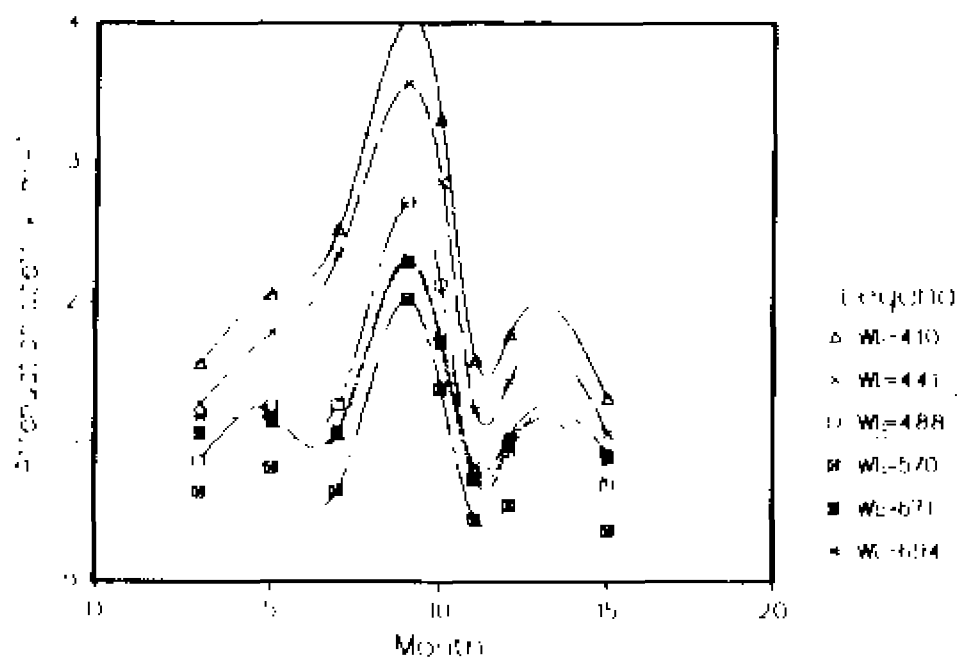
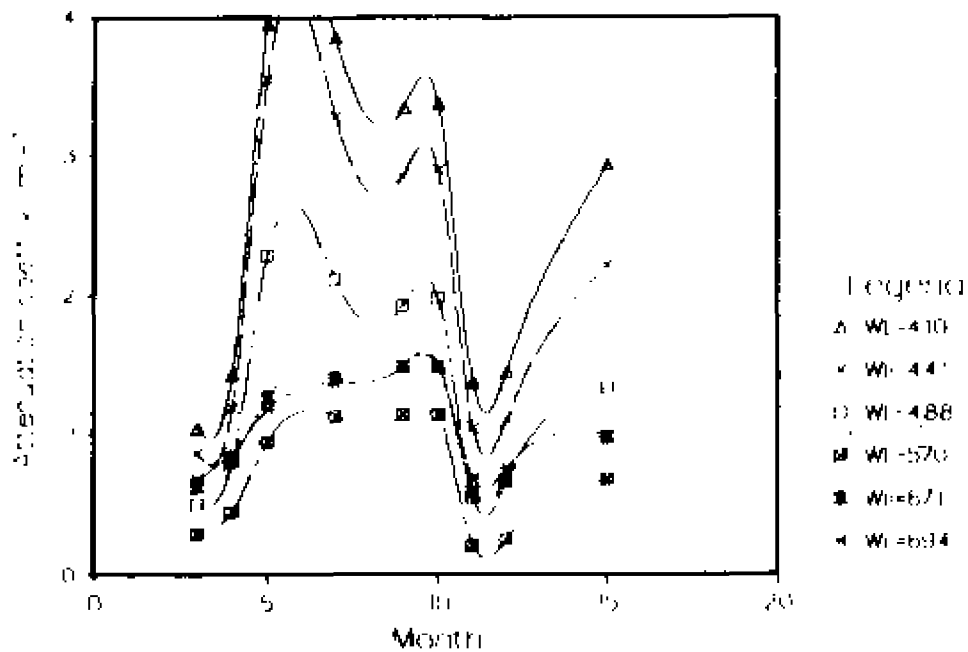


Figure 35. Mean monthly attenuation of selected wavelengths off Guinea Marsh, York R., Chesapeake Bay.

Mean Monthly Attenuation by Wavelength



U.S. 12-04081 (06-21-3) (0-000R, Not R2)

Figure 36. Mean monthly attenuation of selected wavelengths at the mouth of the Severn R., lower Chesapeake Bay.

Mean Monthly Attenuation by Wavelength

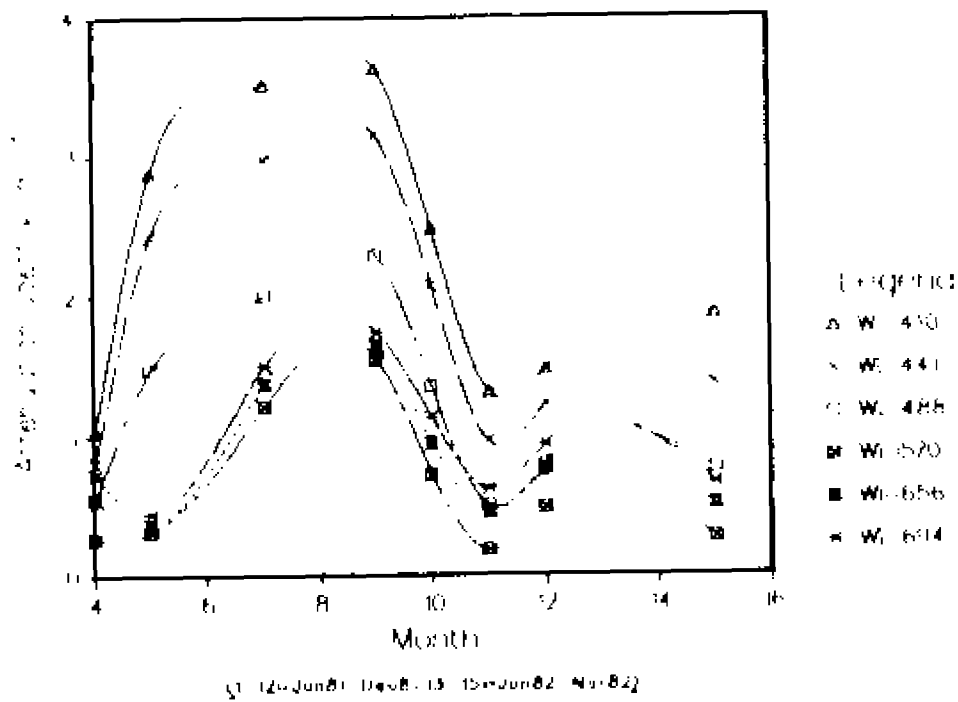


Figure 37. Mean monthly attenuation of selected wavelengths at the Four Point Marsh site, York R., Chesapeake Bay.

Mean Monthly Attenuation by Wavelength

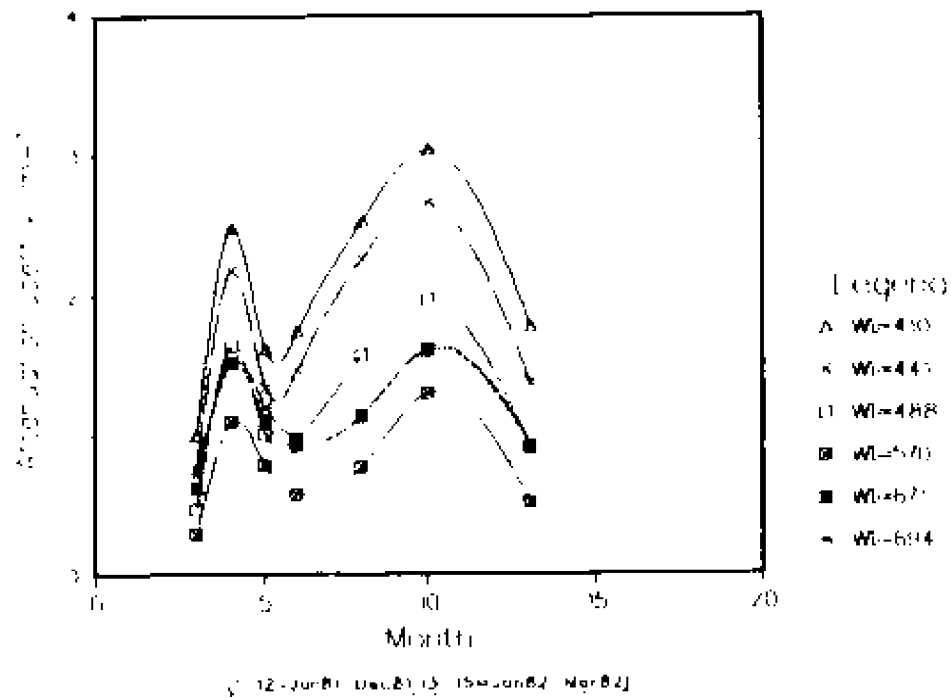


Figure 38. Mean monthly attenuation of selected wavelengths in the Zostera marina bed off Vaucluse Shores, Chesapeake Bay.

Mean Monthly Attenuation by Wavelength

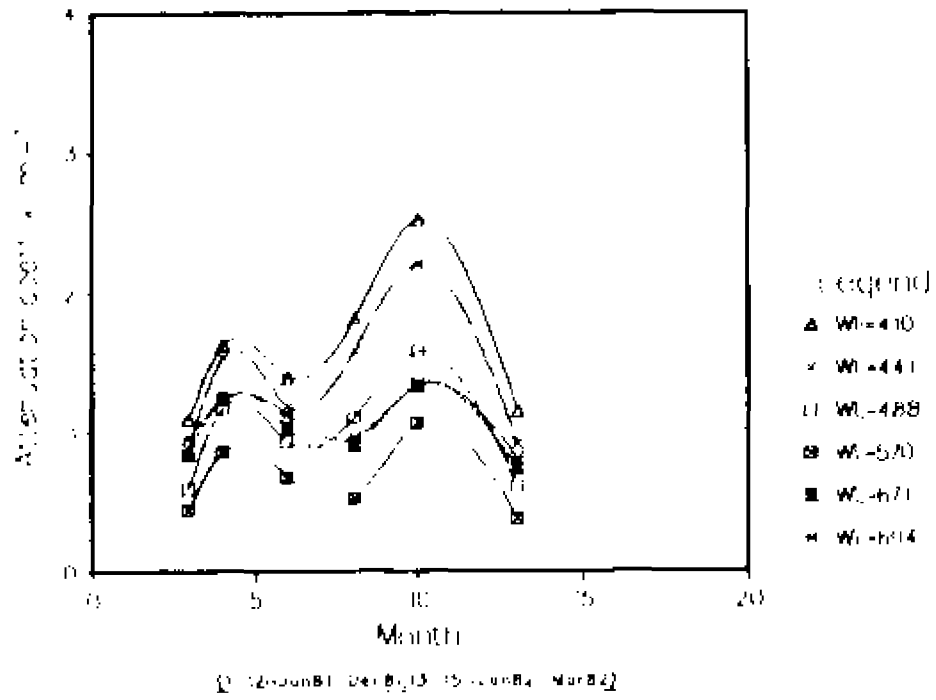


Figure 39. Mean monthly attenuation of selected wavelengths at the Deep Station off Vaucluse Shores, Chesapeake Bay.

a low of about 1.5 m^{-1} in March of 1981 to a peak of between 3.5 and 4.1 m^{-1} during September, declining dramatically to winter levels in November. As of March 1982, no increase was evident. The attenuation of longer wavelengths at Guinea Marsh peaked sharply in September and declined during October to reach otherwise constantly low values during November. A similar pattern of attenuation for the longer wavelengths of light was found at the other western shore vegetated site, Four Point Marsh (Fig. 37). However, May 1981 values were extraordinarily low (0.5 m^{-1}) for the red end of the PAR at this site. Simultaneously, the violet-blue attenuation during May was higher than the other vegetated sites. The Allen's Is. site (Fig. 34) shows much less monthly variation than any other western shore site.

The Vaucluse Shore vegetated site (Fig. 38) reached its maximum short wave attenuation during October, but also peaked in April. The minima occurred during March, May and June 1981 and January 1982. The long wave attenuation followed the same pattern but with much less magnitude. March, May and June, 1981 were also the months of maximum net productivity for the benthic *Zostera* community at this site (Murray & Wetzel, 1982; Murray, 1983). The same pattern of attenuation, but with less extreme oscillation is apparent at the deep water reference station (Fig. 39) adjacent to the Vaucluse site.

Spectral Irradiance & Attenuation in Estero Pargo Creek

The downwelling spectral irradiance for noon and 1300 hours, both at the surface (incident irradiance) and at a depth of just less than a meter

(benthic irradiance) are presented in Figure 40 along with the corresponding attenuation coefficients for a clear sky at the Thalassia site. The noon measurement (Fig. 40A) was made during a 10-15 knot southwest wind, whereas the measurements made at 1300 hours (Fig. 40B) were made after the wind had ceased. There is a sharp attenuation of blue and violet light below about 500 nm, while the lowest attenuation occurs in the yellow region between 550 and 600 nm. As indicated, although little appreciable difference exists between the two insolation curves, there is a considerable increase in attenuation, across the spectrum, between the windy noon and the calm (1300 hours) values (see shaded area of Fig. 40). Noontime PAR insolation was about 23×10^{16} quanta \cdot cm $^{-2}$ \cdot s $^{-1}$, while benthic PAR irradiance ranged from 3×10^{16} to 6×10^{16} quanta \cdot cm $^{-2}$ \cdot s $^{-1}$.

Mean daily spectral attenuation coefficients are shown in Table III for three days at the Thalassia site off the mouth of the creek. Attenuation per meter of the shortest wavelengths ranged from a mean daily low of 3.64 to a high of 5.27 -- the highest value measured at the site. The mid-band yellow light (570-590 nm) was least attenuated, ranging from 1.40 m $^{-1}$ to 2.10 m $^{-1}$. The grand weekly mean attenuation coefficients represent the average of 4000 scans. Climatic conditions ranged from windy and cloudy to clear and calm, covering the time period 1115 to 1730 hours C.S.T. Depths ranged from 0.76 to 1.1 m. The grand mean (Fig.

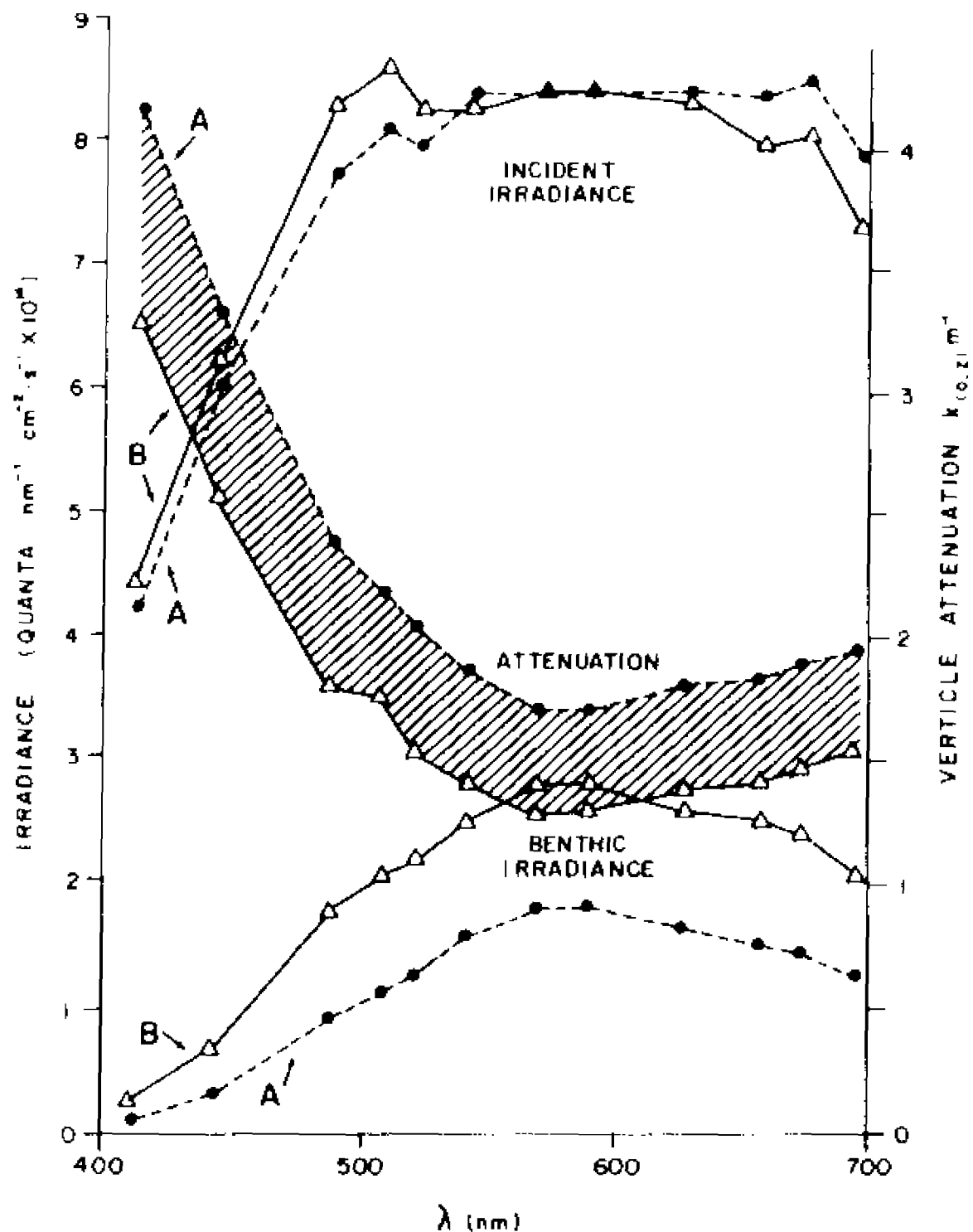


Figure 40. Downwelling spectral irradiance and spectral attenuation coefficients over a *Thalassia testudinum* bed off the mouth of Estero Pargo Creek on a clear day. (A) 1200 C.S.T., 10-15 knot SW wind, $z = .88 \text{m}$, (B) 1300 C.S.T., Calm, $z = .85 \text{m}$. Shaded area represents difference in attenuation which may be due to wind driven resuspension.

TABLE III
DAILY MEAN SPECTRAL ATTENUATION COEFFICIENTS (m^{-1})
Seagrass bed at mouth of Estero Pargo Creek, 1981

Color	(nm)	Feb. 6	Feb. 8	Feb. 10	Mean
Violet	410	3.64	3.48	5.27	4.13
	441	3.02	2.77	4.26	3.35
Blue	488	2.22	1.92	2.99	2.38
Green	507	2.05	1.76	2.74	2.18
	520	1.90	1.66	2.55	2.04
	540	1.75	1.54	2.34	1.87
Yellow	570	1.63	1.40	2.10	1.71
	589	1.66	1.40	2.00	1.71
Orange	625	1.86	1.52	2.26	1.88
Red	656	1.94	1.53	2.25	1.91
	671	2.06	1.58	2.34	1.99
	694	2.11	1.65	2.40	2.05
PAR	400-700	2.01	1.74	2.54	2.10

41-1, curve "C") should characterize the spectral attenuation at this site during the "El Norte" season since the measurement period was between two such weather events.

Comparison of spectral attenuation coefficients along a 1 km upstream transect (Fig. 41-1) reveals a dramatic decrease of violet and blue light (400-500 nm). Attenuation of underwater light in Estero Pargo Creek was higher at all wavelengths upstream (Fig. 41-1A) than at the mouth (Fig. 41-1C), the difference asymptotically increasing to almost 3.0 m^{-1} at the violet end of the spectrum and approaching zero in the red region (650-700 nm). Midstream attenuation (Fig. 41-1B) was intermediate between these extremes.

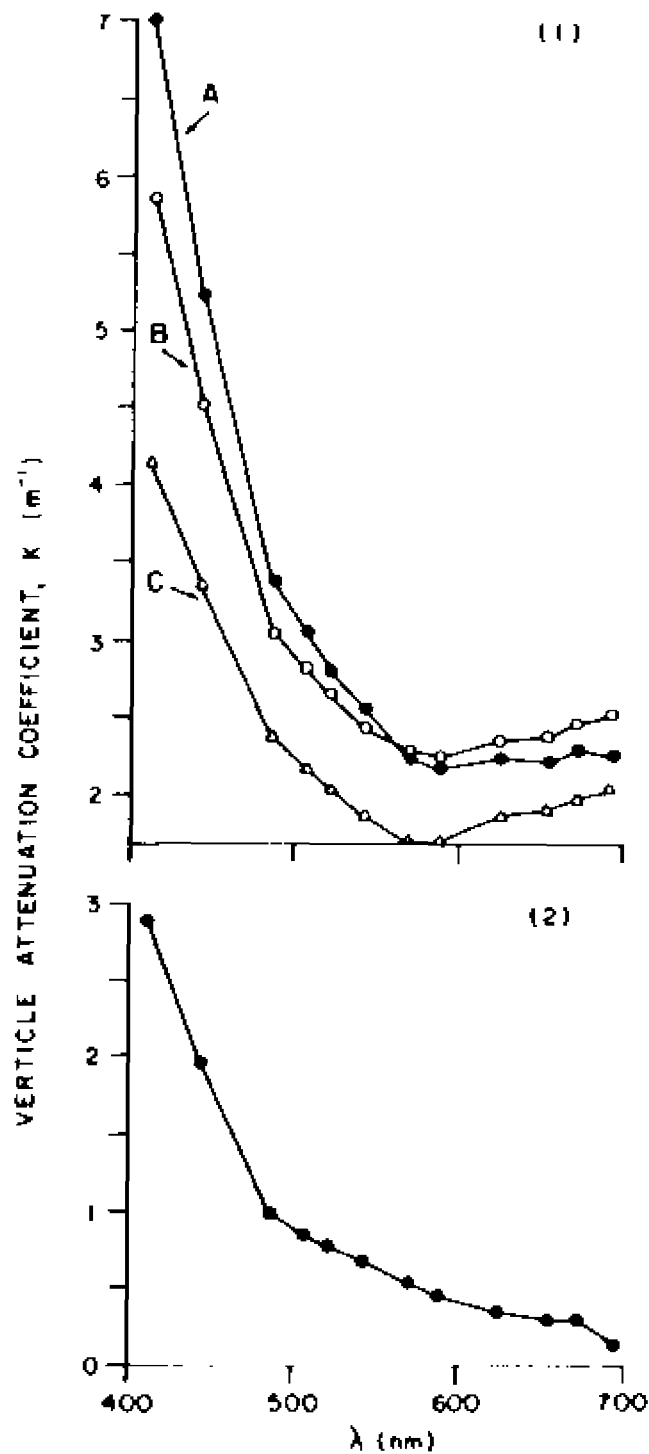


Figure 41. (1) Comparison of diffuse downwelling spectral attenuation coefficients at three sites in Estero Pargo Creek. (A) Upstream off the U.N.A.M. dock (B) midstream, (C) off the mouth in a *Thalassia* bed. Data for curves A and B represent the mean of 250 scans. Curve C represents the mean of 4000 scans taken during 3 days. (2) The difference in downwelling spectral attenuation coefficient between the upstream site and the mouth of Estero Pargo Creek. The curve represents the arithmetic difference between curves A and C.

DISCUSSION

Relative Potential Benthic Photosynthesis

Potential benthic production is determined both by the light available for photosynthesis at the bottom of the water column and by the inherent photosynthetic response of the plants present. Limiting this discussion to green plants and using published photosynthetic action spectra, mean seasonal attenuation coefficients and incident irradiance measurements from this study, the relative potential photosynthetically storable radiation, PSR (Morel, 1978; Smith, 1979), can be calculated. The results of these calculations for spring are presented in Figure 42. Spring was chosen for this example not only because it is the season with the greatest difference in attenuation between vegetated and unvegetated sites, but because it is the season of highest net seagrass community productivity, period of highest growth, and the time of greatest leaf turnover (Murray & Wetzel, 1982; Wetzel et al., 1982; Murray, 1983; Murray and Wetzel, 1987).

The total attenuation to a depth of 1.0 m, $k_{(0,1.0)}$, plotted in Figure 42 was estimated as a weighted average between the water column attenuation $k_{(.1,.5)}$ (depth interval 0.1 to 0.5 m), and the

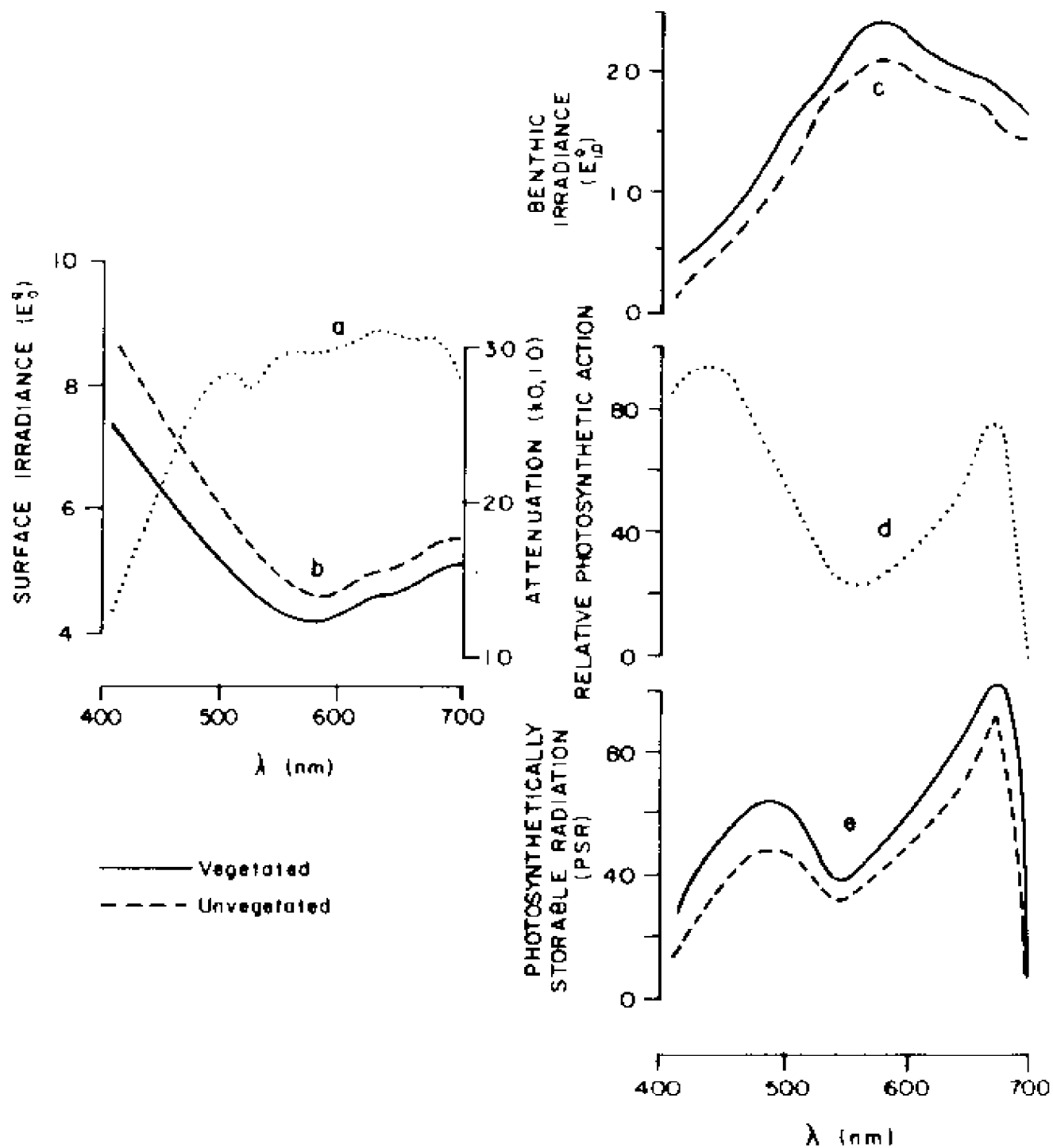


Figure 42. Relative potential spring PSR for vegetated and unvegetated sites. Solid lines represent vegetated areas, dashed lines represent unvegetated. (a) Mean spring surface irradiance at noon on a clear day, (b) total attenuation, (c) benthic irradiance at 1.0 m, (d) relative photosynthetic action spectrum, (e) relative potential photosynthetically storable radiation (PSR).

air-water interface attenuation $k_{(0,.1)}$, (depth interval 0 to 0.1 m):

$$k_{(0,1.0)} = \frac{(9)k_{(.1,.5)} + (1)k_{(0,.1)}}{(10)} \quad (4.1)$$

where $k_{(.1,.5)}$ is a conservative estimator of $k_{(.1,1.0)}$ since water column, substrate interactions are not considered. The air-water interface attenuation coefficient $k_{(0,.1)}$ was calculated as the seasonal mean for calm sunny days at 1200 - 0030 hours E.S.T.

The mean incident spectral irradiance during clear spring days at noon is plotted as curve "a" in figure 42. The quantum distribution decreases rapidly below about 500 nm. The estimated total attenuation coefficient for both vegetated and unvegetated sites are labelled "b" in the same figure. These represent the spring spectral attenuation from just above the water's surface to a depth of 1.0 m on calm, clear days around noon. The attenuation of light at all wavelengths is higher at the unvegetated sites than is the attenuation at vegetated sites during spring: especially for wavelengths of light less than 500 nm. This difference increases from 0.23 m^{-1} at 507 nm to 0.51 m^{-1} at 410 nm. There is a difference between vegetated and unvegetated sites of about 0.1 m^{-1} from 570 to 700 nm. Additionally, attenuation across the PAR spectrum at unvegetated sites begins earlier in the year and increases at a more rapid rate than at the vegetated sites.

The resulting estimated benthic irradiances for both vegetated and unvegetated sites are labelled "c" on Figure 42. (Note that the scale of the vertical axis of "c" is only a fifth that of the vertical axis of "a"). A comparison of curves "a" and "c" reveals the dramatic decrease in irradiance over just a meter of water. The benthic irradiance at the average spring unvegetated site ranges from $0.21 \text{ quanta} \cdot \text{cm}^{-2} \cdot \text{s}^{-1} \cdot 10^{13}$ at 410 nm to $2.13 \text{ quanta} \cdot \text{cm}^{-2} \cdot \text{s}^{-1} \cdot 10^{13}$ at 570 nm. The corresponding irradiance for vegetated sites is $0.349 \text{ quanta} \cdot \text{cm}^{-2} \cdot \text{s}^{-1} \cdot 10^{13}$ and $2.37 \text{ quanta} \cdot \text{cm}^{-2} \cdot \text{s}^{-1} \cdot 10^{13}$, respectively.

The relative photosynthetic action spectrum for *Ulva lactuca*, a typical shallow water estuarine green alga is plotted as curve "d" after Haxo and Blinks (1950) and Halldall (1974). The photosynthetic pigment complex of green algae is very similar to that of seagrasses. Quanta of 400-500 nm and 650-680 nm are used most efficiently by this green plant.

The potential PSR for the average spring vegetated and unvegetated site is presented as curve "e" in Figure 42. This is simply the normalized (0-100) product of curves "c" and "d". The resulting potential PSR curve is a function therefore of incident radiation, total attenuation and the inherent spectral efficiency of "typical green marine plant" photosynthesis. This PSR spectral distribution includes two peaks: one broadly centered about 490 nm in the blue end of the spectrum and the other extending from about 590 to 690 nm. The blue peak has been shifted from

about 440 nm in the action spectrum to about 490 nm in the PSR due to the combined effects of the high attenuation of violet and the low original violet insolation. Much of the difference between the mean vegetated and mean unvegetated PSR curves lies within the blue peak. The unvegetated blue peak is quite insubstantial whereas the vegetated peak is from 12 to 16 relative units higher. In a marginal light environment this difference in potential storable radiant energy may be quite important. In the red peak region, the difference between the two curves is much less pronounced, being only 5 to 8 relative units in the 590 to 670 nm region of the spectrum.

Using ^{14}C , Wetzel and Penhale (1983) calculated a theoretical P_{max} of $2.084 \text{ mgC}\cdot\text{g}^{-1}\cdot\text{h}^{-1}$ for individual leaves of Zostera marina removed from the same Vauckee Shores site studied in this work. They also reported a community apparent gross O_2 productivity of $464 \text{ mgO}_2\cdot\text{m}^{-2}\cdot\text{h}^{-1}$ in the same seagrass bed. The difference in PSR discussed above could result in reductions of about $0.2 \text{ mgC}\cdot\text{g}^{-1}\cdot\text{h}^{-1}$ for leaves or about $46 \text{ mgO}_2\cdot\text{m}^{-2}\cdot\text{h}^{-1}$ for the entire benthic community.

Spectral Attenuation and Seagrass Occurrence

In the lower Chesapeake Bay the light available to benthic plants may not include great quantities of energy at those wavelengths which can be most efficiently used by these plants. The greatest loss of potential energy appears to be in those regions of the spectrum most significant for

photosynthesis. Whether the reduced levels of light of critical wavelengths is causally related to the absence of seagrasses and the direction of that causality is difficult to assess. But, there does appear to be a correlation between the high attenuation of certain photosynthetically significant wavelengths and the lack of seagrasses. Consideration of the direction of the causality may be analogous to asking - Which came first the chicken or the egg? - and just as insignificant. That is, does the baffling effect of seagrasses cause the settling of enough fine suspended material to reduce scattering and absorption to the point that enough quanta of appropriate wavelengths reaches the benthos enabling the seagrasses to continue growth? Or, does a water body with relatively little suspended material provide a light environment suitable for seagrasses to survive, grow and thus baffle the water and maintain water clarity so light of sufficient quality and quantity can continue to reach the benthos and support seagrasses which baffle the water - etc.?

The answer is yes - to both! Ecosystems are comprised of dynamically interconnected biological and physical components which interact materially and energetically. The morphogenesis of an ecosystem from simple pioneer beginnings to mature dynamically stable stages involves a continual reciprocal induction process between its physical and biological parts. This is achieved through sensitive feedback mechanisms. A mature ecosystem is a homeostatic entity capable of internal adjustment to a range of external conditions - within limits, and it may be those

limits that are the critical aspect of the success or failure or disappearance or reappearance of seagrasses in the Chesapeake Bay.

Let's define the benthic seagrass community and its overlying water column an ecosystem. The water clarity is affected by the baffling effect of the plants (Ginsburg and Lowenstam, 1958; Scoffin, 1970; Wanless, 1981; Boynton & Heck, 1982) and the plants are certainly affected by the water clarity. A minimal water clarity is necessary for a seedling of seagrass to successfully colonize a suitable barren substrate and to grow vegetatively to some minimal size (cf. Boynton & Heck's "critical bed size", 1982) necessary to provide the baffling which will in turn induce settling and trapping of enough fine particles to clear the water column and maintain a tolerable light environment for continued growth. Seeds of many angiosperms need specific wavelengths of light energy before germination will occur (Vázquez-Yanes, 1980; Stoutjesdijk, 1972). If, during the early seedling stage, water clarity is insufficient then the ecosystem will not succeed to the self regulatory, homeostatic stage and a seagrass community will not be established.

A model of a seagrass ecosystem including the water column is shown in Figure 43 as an aid to the conceptualization of the sensitive feedback relationship between the seagrass community and water clarity. Of particular interest is the relationship between critical bed size and sedimentary baffling and attenuation.

Due to the dynamic nature of the littoral zone and coastline, normal variations in physical and biological parameters (Burt, 1955; Klefer and

Austin, 1974; Kranck, 1980; Scott, 1978) may often exceed an established seagrass community's ability to adjust and survive on a local scale. Rapid recolonization - both vegetatively and sexually (via seeds) - would be expected if water clarity permits. But, if - due to nutrient enrichment and subsequent plankton blooms, or particulate runoff, or due to a combination - the light environment becomes unsuitable for the re-establishment of a new seagrass community, then the net seagrass ecosystem size may diminish despite survival of established beds not affected by normal local perturbations. That is, since there must be thresholds below which the critical feedback between biological and physical parameters of the system cannot be established (critical bed size and a minimal light environment); replacement of seagrass communities lost due to normal processes may be impossible during periods of reduced water quality and altered light quality.

There is a dramatic difference between the Spring attenuation at vegetated vs. unvegetated sites. Peak attenuation at all wavelengths doesn't occur until late Summer at the vegetated sites (Figs. 14, 16, 18) whereas the onset of high attenuation at unvegetated sites starts during Spring. The May, June, and July peak attenuations found at unvegetated stations (Figs. 15, 17, 19) may be due to the baffling effect on the water column by seagrasses during spring runoff conditions.

The historical pattern of increasing nutrient enrichment of the Chesapeake Bay from agricultural runoff, municipal waste water effluent

and urban non-point sources and their presumed contribution to excess planktonic productivity (Heinle et al., 1988) coupled with increased particulate loads associated with the escalating urban, suburban and economic development of the Chesapeake Bay's watershed may have altered the water clarity enough to account for the decline in submerged aquatic vegetation via the mechanism discussed above. The spectral irradiance measurements and spectral attenuation calculations reported in this study indicate a scarcity of benthic light in shallow areas of the lower Chesapeake Bay, especially in those wavelengths most efficiently used by green plants for photosynthesis.

Wind, Gelbstoff and Spectral Attenuation in Estero Pargo Creek

A schematic representation of spectral energy flow through the marine environment is presented as Figure 44. The relative proportions of the various constituents of seawater determine the ultimate light quality and quantity available to power benthic photosynthesis. The typical noon clear sky quanta distributions for both incident and benthic irradiance measured at Estero Pargo are indicated graphically in the conceptual diagram. Typical marine specific absorption curves for dissolved organic matter, non-green particulate matter, chlorophyll, and pure seawater are shown interacting with the underwater quanta. Rain and wind (Los Nortes) cause runoff with increased dissolved organics and resuspension of particulate matter and benthic chlorophyll bearing microalgae, thus increasing particle scattering, absorption and consequently total attenuation. The specific

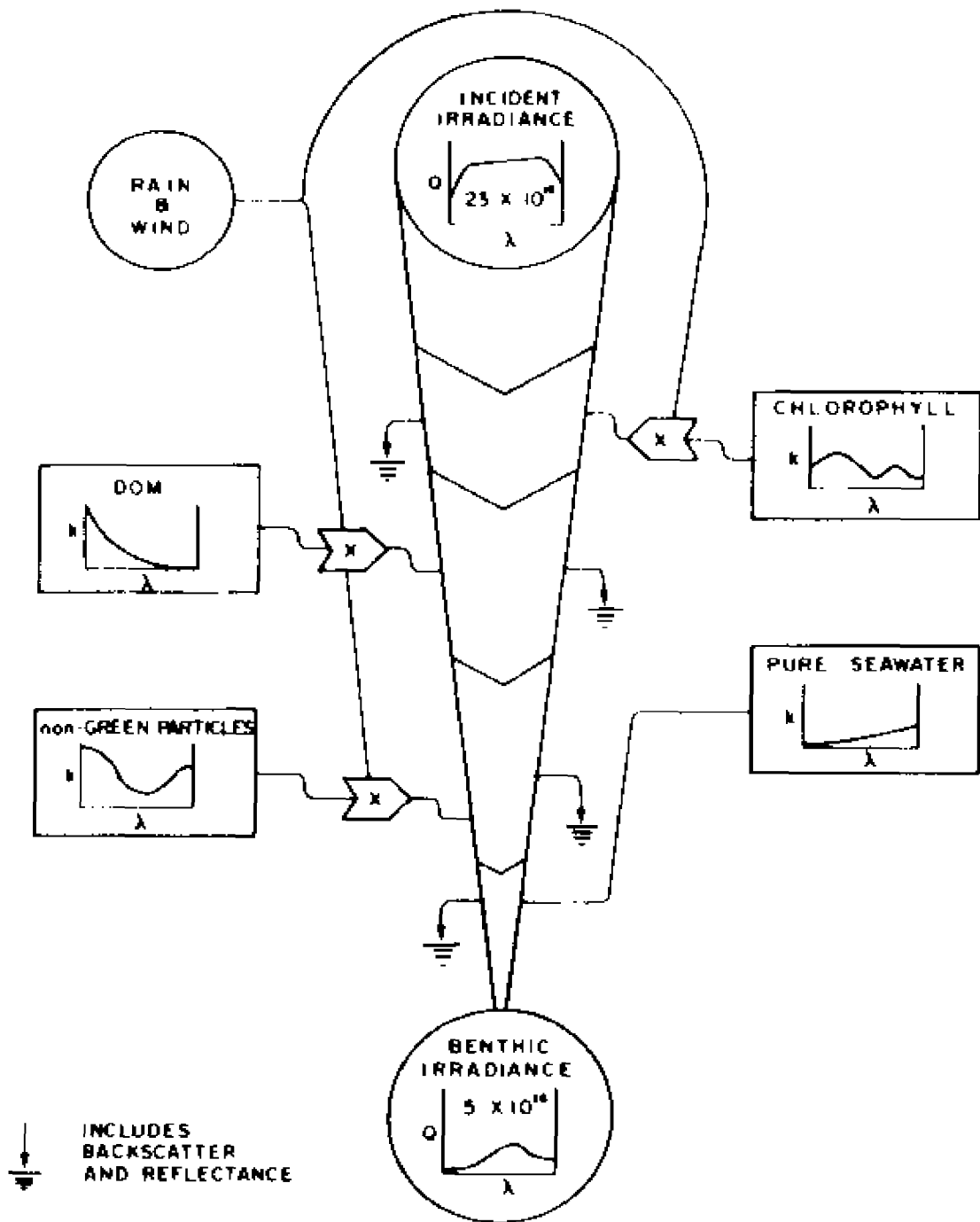


Figure 44. Schematic representation of spectral attenuation through an estuarine water column. Q = quanta \cdot nm $^{-1}$ \cdot cm $^{-2}$ \cdot s $^{-1}$; λ = wavelength, 400-700 nm; k = specific absorption coefficients, m $^{-1}$; numbers for irradiance are PAR integrals, quanta \cdot PAR \cdot cm $^{-2}$ \cdot s $^{-1}$. Energy circuit language after Odum 1972; specific absorption curves redrawn from Prieur and Sathyendranath, 1981).

spectral energy characteristics of the water column and the forcing functions impinging on the system.

In Estero Pargo Creek the dominating influence seems to be from dissolved organics. If the spectral attenuation coefficients for the mouth of the creek are subtracted from those at the upstream site (Curve A - Curve B, Fig. 41-1), the resultant curve, Figure 41-2, may represent the attenuation due solely to the constituents of the water column present upstream but not downstream. If this curve (Fig. 41-2) is compared with the specific absorption curves in Figure 44 and Fig. 1b, (Introduction) it can be seen that it matches the shape of the dissolved organic matter curve quite closely. The extreme attenuation of the short wavelengths decreases downstream as the diluting effect of the waters from the lagoon become more apparent. The creek waters no doubt affect the light environment in the grassbed at its mouth, contributing to the high violet-blue attenuation.

An example of the effects of resuspension caused by wind can be seen in Figure 48. The shaded area of the figure represents the decreased attenuation corresponding to a decrease in wind from 10-15 knots to calm during a one hour interval. Both sets of measurements were taken during a clear sky. Notice that although the incident irradiances at the mid-spectral region (550-625 nm) are almost identical, the attenuation coefficients and benthic irradiances differ significantly. This is probably due to resuspension of particulate matter and benthic microalgae.

At the Estero Pargo study site, an area of seagrasses that are probably light-stressed (Metzel et al., 1982), there is a significant attenuation ($2-4 \text{ m}^{-1}$) of the photosynthetically important short wavelengths, 400-500 nm. Incident noon PAR irradiance was about $23 \times 10^{16} \text{ quanta} \cdot \text{cm}^{-2} \cdot \text{s}^{-1}$ and benthic irradiance ($z=1 \text{ m}$) was between 3 and $6 \times 10^{16} \text{ quanta} \cdot \text{cm}^{-2} \cdot \text{s}^{-1}$. In the upstream mangrove swamp channel (Estero Pargo Creek) there is extreme blue-violet attenuation which is probably due to dissolved organics originating from mangrove litter decomposition.

At the Thalassia study site, wind events of even relatively mild magnitude (10-15 knots), affected both light quality and quantity reaching the plant canopy. Since the greatest attenuations occurred in a spectral region (400-525 nm) which is extremely important for absorption by chlorophylls and accessory pigments in higher plants, the observed benthic irradiance distribution has significant implications for seagrass community productivity.

COMMUNITY PHOTOSYSTEM RESPONSE MODEL

Introduction

I have conceptualized and simulated a model which traces "blue", "green", "yellow", and "red" quanta as they propagate through an estuarine water column, and are eventually absorbed by either water molecules and dissolved salts, dissolved organic matter, non-pigmented suspended solids, or captured by "blue", "green", "yellow", or "red" plant antennae (see Fig. 45). The spectrum has been arbitrarily divided into four regions as a simple approximation of reality. Of course quanta of each wavelength are different and plants attempt to capture most of these. Correspondingly, I've grouped plant photosystems into four categories.

The conceptual diagram presented as Figure 45 uses the symbols of the widely used "Energy Circuit Language" (also termed "Visual Systems Mathematics") of H.T. Odum (1960, 1967, 1971a, 1975a, 1975b, 1963). In this language each symbol has implicit physical and biological meaning and an associated mathematical structure based on well known biological, chemical and physical relationships. Use of this symbolic language frees the creator of a conceptual model to work out all the interrelationships of a system without concern for the mathematical intricacies

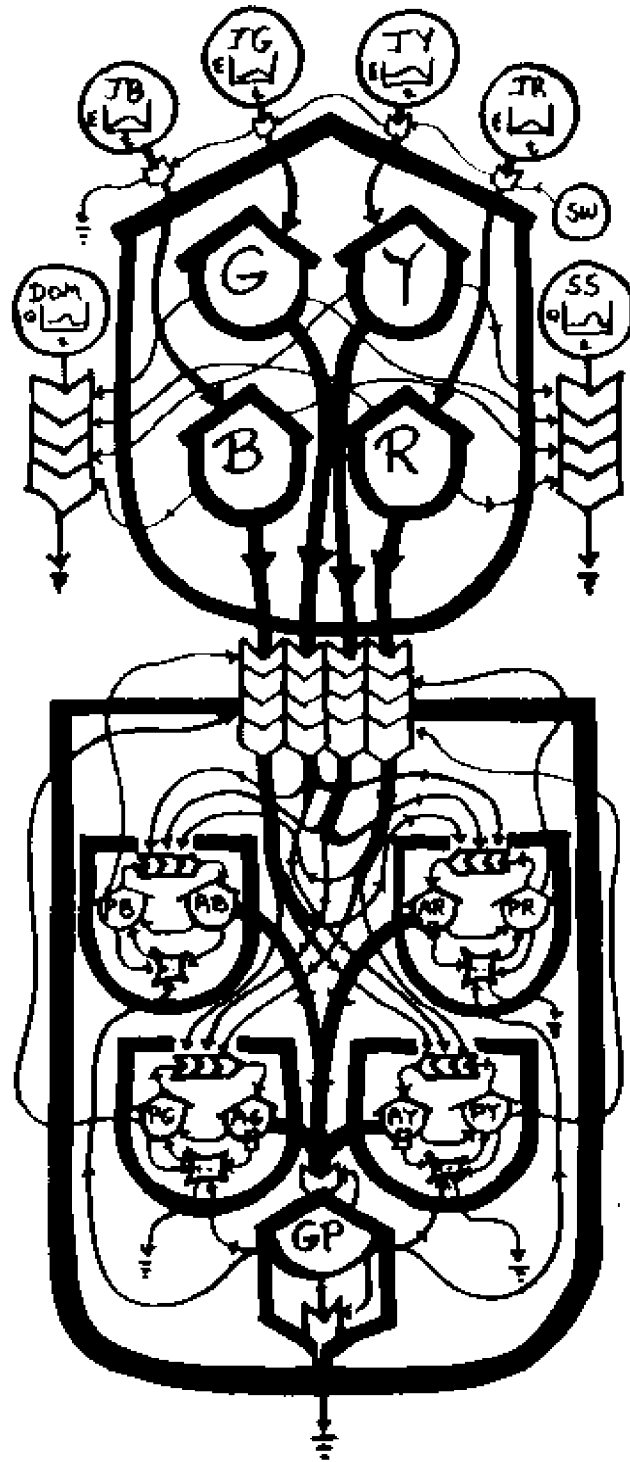


Figure 45. Conceptual diagram of community photosynthesis simulation model (4PIG17.5).

during the conceptualization. After the model is conceptualized, the author may then translate the diagram into a series of simultaneous differential equations for mathematical analysis or into a set of difference equations that can be digitally evaluated via iterative procedures in a computer language. Appendix I lists one of the Basic 4.0 programs developed to simulate the conceptual model of an estuarine community photosystem (4PIG17.5) illustrated in Figure 45. Lines 7627 - 8006 show the equations of state for the non-biological attenuation of light and lines 8100 - 8930 describe the biological difference equations used to simulate absorption, photosynthesis and pigment synthesis.

The model is forced by seasonally varying functions simulating the relative spectral proportions of energy incident on the water column. Albedo (reflection and backscatter out of water) are then subtracted. Seasonally varying functions for suspended solids and DOM, based on runoff maxima and estimated peak in situ decomposition, respectively, interact with each arriving spectral group of quanta and specifically attenuate them. The relative attenuation is based on literature values, especially those of Prieur and Sathyendranath (1981). These specifically attenuated quanta become unavailable to the pigmented plant photosystems and are eliminated from further iterations via heat sinks.

The pigment systems - blue, green, yellow, and red - are modelled as cycling receptors (Odum, 1983) which alternate between activated (excited) and basal states. The gross primary production (GP) of the system is

considered a function of the total amount of activated pigments of all photosystems. Each specific pigment system is allowed to absorb all of the quanta surviving seawater, particulate and DOM attenuation except for those quanta reflected by the pigment. For example, green pigments absorb blue, yellow and red quanta but reflect green quanta. Each pigment system is allowed to grow in proportion to the quantity of excited pigment and the net productivity. Thus, pigment synthesis is stimulated by absorption - a positive feedback, similar to the approach of French & Fork, 1961.

The model includes two major sections: (1) Spectral attenuation of light by non-biological processes, (2) Biological absorption, reflection and consequent photosynthetic production via wavelength specific pigment systems.

Physical Attenuation

The PAR spectrum was arbitrarily divided into four broad spectral bands termed "Blue" (400-490nm), "Green" (490-560nm), "Yellow" (560-630nm), and "Red" (630-700nm). Forcing functions JB, JG, JY, and JR, respectively were derived to drive the model and to represent downwelling incident spectral irradiance within the above wavelength bands. The relative number of quanta in each of these spectral regions of the PAR used in model versions through 4PIG.17A was estimated from field measurements of the downwelling spectral irradiance distribution just above the water at the Vaucluse Shores study site during noon in April (see "surface insolation", Fig. 2). The relative values thus derived were $B = 0.147$ (Blue),

G = 0.301 (Green), Y = 0.288 (Yellow), and R = 0.265 (Red). Estimates of relative irradiance for model versions 4PIG.17.5 and beyond were based on an average spectral distribution calculated from data of Tyler and Smith (1970 as plotted by Kirk, 1983, p. 29). The average spectral distribution was based on irradiance measurements made by Tyler and Smith at two latitudes: 42°56'N and 25°45'N around noon during summer. These relative percentages were used to derive the individual daily time varying functions (JB, JG, JY, JR) for each band by applying them to a sinusoidal function for maximum daily total PAR incident irradiance described by Krewer and Nixon (1978) for their Narragansett Bay model:

$$PAR_{max} = 677.5 - 371.5 \cos [2\pi(t+10)/365],$$

where t is the day of the year ($t=1$ at January 1). Their daily maximum radiation function accounted not only for sun angle changes but also for daily photoperiod length. It fit the predicted clear sky PAR irradiance maximums calculated for the solstices and equinoxes. Applying the relative wavelength band percentages calculated above to this equation and arbitrarily dividing by two to approximate air-water interface attenuation due to reflection and backscatter yielded:

$$JB = 49.8 - 27.3 \cos [2\pi(t+10)/365]$$

$$JG = 102 - 55.7 \cos [2\pi(t+10)/365]$$

$$JY = 97.6 - 53.5 \cos [2\pi(t+10)/365]$$

$$JR = 90 - 49.2 \cos [2\pi(t+10)/365],$$

where t is the number of the day of the year. Subsequent functions derived using the data of Smith and Tyler (1970) for versions 4PIGI7.5 and beyond were:

$$JB = 88.1 - 48.3 \cos[2\pi(t+10)/365]$$

$$JG = 84.7 - 46.5 \cos[2\pi(t+10)/365]$$

$$JY = 94.9 - 52.0 \cos[2\pi(t+10)/365]$$

$$JR = 71.1 - 39.0 \cos[2\pi(t+10)/365]$$

Specific spectral attenuation coefficients for absorption and scattering due to the water molecules and their dissolved ions were estimated based on spectral attenuation distribution curves calculated by Prieur and Sathyendranath (1981), Clark and James (1939), and Yentsch (1968). The coefficients thus derived were $k_b = 0.03$ (Blue), $k_g = 0.05$ (Green), $k_y = 0.25$ (Yellow), and $k_r = 0.4$ (Red), representing the relatively large attenuation of the long wavelength quanta by water molecules and dissolved ions.

Specific attenuation within these four wavelength bands due to absorption and scattering by particles (SS) and dissolved organic matter (DOM) involved the use of time varying truncated sinusoidal functions to describe nominal suspended solid loads and the nominal quantity of DOM. These cosine functions were based on those derived by Kremer and Nixon (1978) to fit data of Hess and White (1974) which described the seasonal pattern of river flow into Narragansett Bay. The function resulted in a

sinusoidal increase to a maximum followed by a sinusoidal decrease to a minimum which is sustained until the next seasonal increase begins. The functions were devised so as to allow manipulation of the maximum and the timing of the commencement of the increase. Suspended solid concentrations in estuaries are largely a function of runoff and river flow. The output of the equation thus derived for suspended solids seemed to fit observations made for the Chesapeake Bay and its tributaries (Smullen, et al., 1982) reasonably well:

$$SS = S2 + S2 \cos[2\pi(t - S1)/365],$$

where S1 determines the timing of the onset of the increase and S2 its magnitude. A similar function was used for DOM concentrations:

$$JDOM = G2 + G2 \cos[2\pi(t - G1)/365].$$

Specific spectral attenuation coefficients for suspended solids (i.e., non-chlorophyllous particulate matter) were derived from the curves presented by Prieur and Sathyendranath (1981: see Fig. 1b, this dissertation) resulting in relative values of 1.0 for blue attenuation (cc), 0.5 for green (cd), 0.75 for yellow (ce) and 1.25 for red (cf) specific relative non-chlorophyllous particulate attenuation — normalized for blue light.

Specific relative attenuation coefficients for DOM absorption and scattering were also derived from Prieur and Sathyendranath (1981). These estimates resulted in relative coefficient values of 1.0 for blue (c8), 0.2 for green (c9), 0.05 for yellow (ca) and 0.01 for red (cb) specific attenuation due to dissolved organic material. This simulates the relatively large attenuation of quanta of short wavelength by Gelbstoff. Both particulate and DOM attenuation are mathematically handled as exponential decay based on the coefficients discussed above.

Biological Absorption, Pigment Synthesis and Productivity

The quanta surviving the above reflection, backscattering, non-chlorophyllous particulate absorption, and DOM absorption are now made available to the four pigment systems arbitrarily defined by their colors (blue, green, yellow, and red). PB, PG, PY and PR designate the quantity of unexcited blue, green, yellow and red pigments, respectively, while AB, AG, AY and AR represent the quantity of activated pigment. PB is conceptualized as being able to receive and use wavelengths of all colors except that of its namesake, blue. Likewise, PG absorbs Blue, Yellow and Red, while PY absorbs all except Yellow and PR absorbs all specified quanta except those defined as Red. The quanta of light of improper wavelength which impinge upon a pigment system are reflected and returned to the pool of stored light of that color, thus becoming available to the other pigment systems which may be able to absorb them. Since each pigment system can absorb three colors - any two of which can be absorbed by another photosystem - a specific absorption coefficient has been devised for each

pigment receptor system to allow it to absorb light of a specific color in proportion to both the number of quanta of that color available and to the relative abundance of that particular pigment system during the iteration.

The amount of light "stored" underwater (B, G, Y, R) and available to the pigment receptor systems is calculated anew at the beginning of each iteration by starting with the forced irradiance functions (JB, JG, JY, and JR) and attenuating them via the above coefficients and attenuation functions. These quanta are then allowed to be absorbed by the pigments resulting from the previous iteration. During that previous iteration, the pigments may have increased due to pigment synthesis or decreased due to catabolism -- both dependent upon the rate of absorption of light for that specific pigment, and the overall growth or decline of the entire primary production of the ecosystem. That is, specific pigment synthesis or catabolism is controlled by the rate of increase or decrease of activated pigment between two iterations and by the overall growth or decline of gross productivity.

A single pigment photosystem and its interconnections with the general productivity module are diagrammed as Figure 46. This example uses the Blue photosystem with its inactive PB pigments and active AB pigments. G, Y, and R represent the number of quanta of Green, Yellow and Red light actually impinging upon this photosystem. The amount of activated pigment (AB) is dependent upon the number of quanta, above, which interact with the Blue pigments present (PB). The light energy thus trapped is used to

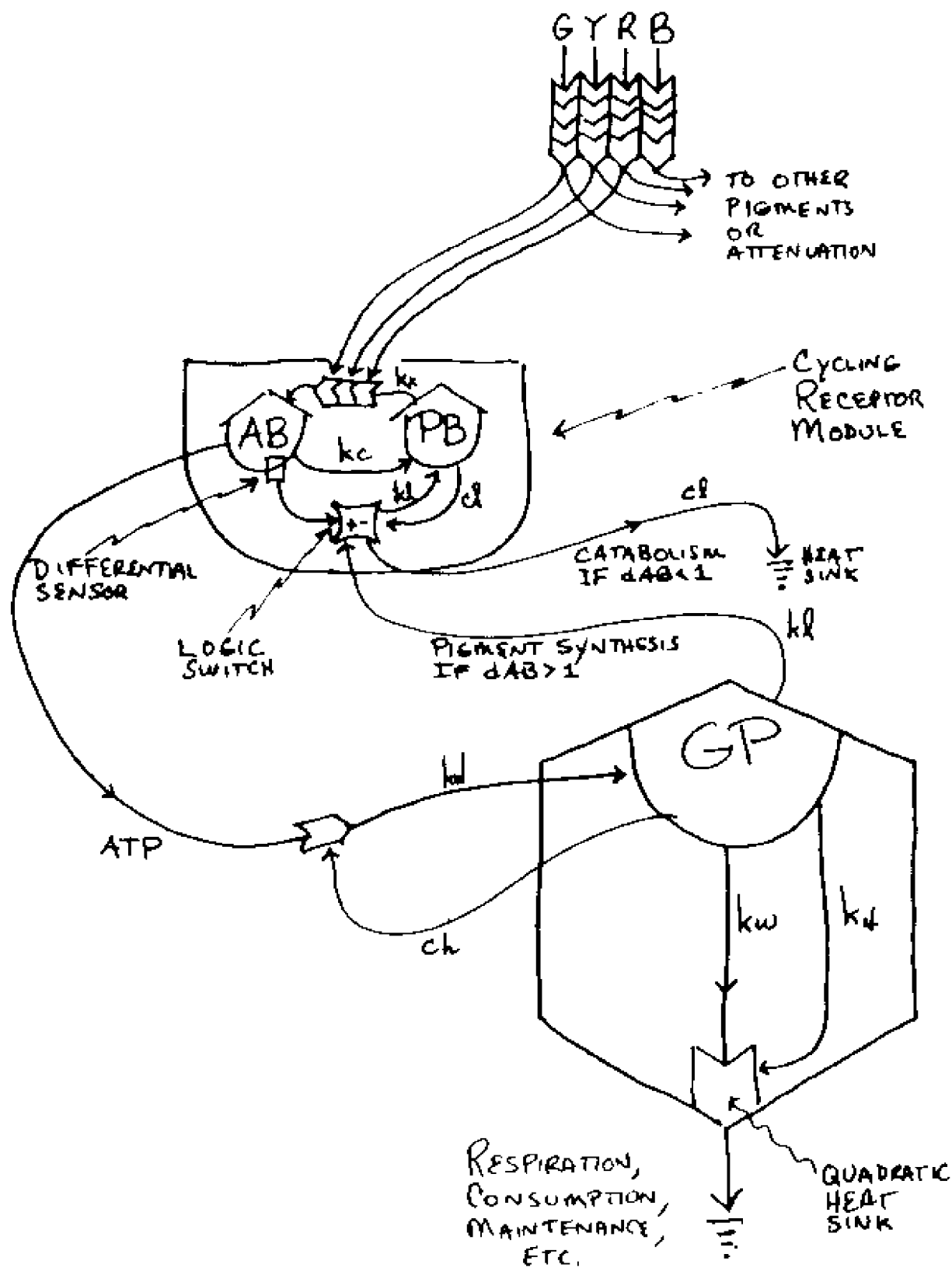


Figure 46. Cycling Receptor (Michaelis-Menten) module for a single photosystem

synthesize organic material accumulated as GP (gross productivity). The amount of activated pigment actually converted into GP depends upon the amount of GP already present in addition to the size of AB. GP is reduced by respiration, animal consumption, maintenance, etc. If AB has grown since the previous iteration then PB is allowed to grow via pigment synthesis based also on the size of GP. If, however, the amount of activated blue pigments has declined since the last iteration then PB is reduced by an amount related to that negative differential (catabolism). Thus, when there is an increasing supply of light which can be absorbed by blue pigments, blue pigment synthesis occurs. But, if the light quality is such that there is a declining supply of light of the proper colors for absorption by blue pigments, then the amount of blue pigment is reduced. The other three photosystems operate in the same fashion, all four dumping their photosynthetic ATP into a common GP which represents the entire production of the ecosystem.

Since the spectral quantum yield of photosynthesis is inconsistent with spectral absorption, coefficients k_d (Blue), k_l (Green), k_i (Yellow), and k_t (Red) were derived from data of Emerson and Lewis (1943) as reported in Kirk (1983). This modification was introduced in model version 4PIG17.5. Quantum yield is lowest for the short wavelengths and best for the long wavelength photons. The coefficients were normalized to yellow light ($k_i=1.0$). The coefficient for Red light, k_t , was set to 0.95 and those for both Blue (k_d) and Green (k_l) were set to 0.85.

Computation

The model was coded in Basic 4.0 on a Commodore 64 with a single VIC-1541 disk drive. The program was set up to dump the output of model runs to disk. It was quickly learned that the disk capacity was insufficient for holding the output of even a three month run, so the program was altered to sample the output based on the length of the run so it would fit on a disk. The first runs of 1 year took about 3 days. A compiler was employed subsequently (Basic-64, Abacus Software, Grand Rapids, MI.). Compiled versions of a 3 year run took only about 24 hours to run and then another 3 hours for a graphics program to read the output from the disk and plot it to the screen in Commodore 1702 High Resolution (64,000 pixels). The graphics program employed a basic extension called Video Basic-64, also from Abacus Software. The screen graphics were dumped to either a Mannesmann Tally MT-160L or an Okimate 10 printer. The challenges of simulating a complex model on a small computer were manifold. The model was run hundreds of times until adjustments of various coefficients resulted in reasonable output of a stable nature. Iteration intervals from .005 day to 0.5 day were tried. It was found that an interval of 0.1 day resulted in stable output and reasonably estimated results obtained using much shorter intervals.

Model Output

Some of the output of the 4PIG Models is presented in Figures 47 through 52. The jaggedness of the curves is due to aliasing caused by the limited resolution of my computer monitor, not the model output which is an

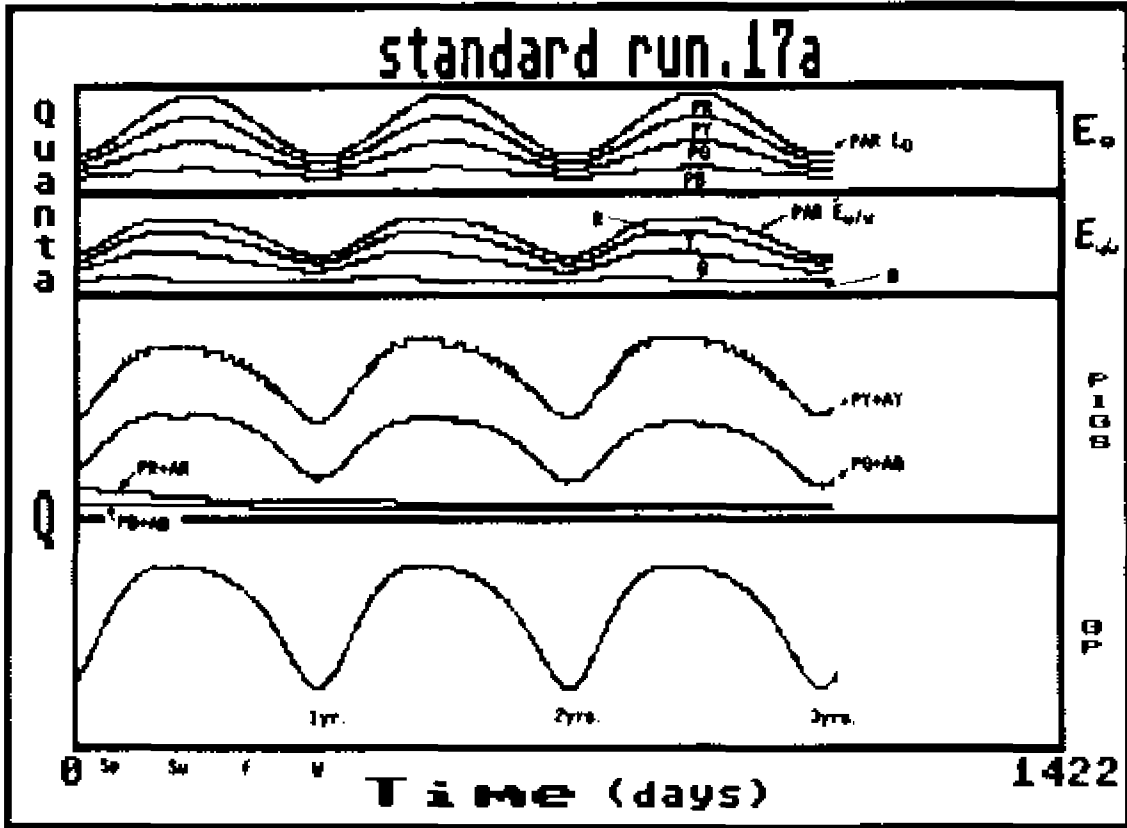


Figure 47. Output of Standard Run of community photosystem simulation model (4PIG.17A).

order of magnitude more detailed than could be shown by the graphic means available. The upper group of curves (E_0) plotted in each graph represent, from top to bottom, JR, JY, JG and JB. They are presented added on top of one another so that the curve for JR is also PAR - taken by itself. The next group of curves ($E_{U/W}$) are from top to bottom R, Y, G, B - also plotted cumulatively so that once again the top curve, R, also represents underwater PAR irradiance. The ($E_{U/W}$) curves were plotted at different scales, there is actually an order of magnitude difference between surface irradiance and underwater irradiance. Below the underwater irradiance are plotted curves (labelled PIGS) representing the combined values of the activated and inactive pigments for each photosystem - for example, AB+PB. In all of the output presented the top PIG curve represents Yellow (AY+PY), the PIG curve below that is Green (AG+PG) and the curves for Red (AR+PR) and Blue (AB+PB) taper off from start up conditions to extremely low values by the end of each run. The bottom curve presented in each Figure represents GP, community photosystem gross productivity.

The output of a four year nominal Standard Run for 4PIG.17a is shown as Fig. 47. The Standard Run forced SS to peak in Spring and DOM to peak in late Summer - early Fall. The relative light quality above and below water has been changed as a result of the differential attenuation of particular wavelengths of light by particles, the seawater itself, pigment absorption, and dissolved organic materials - all time varying themselves. The most obvious differences are that the relative amount of green light is

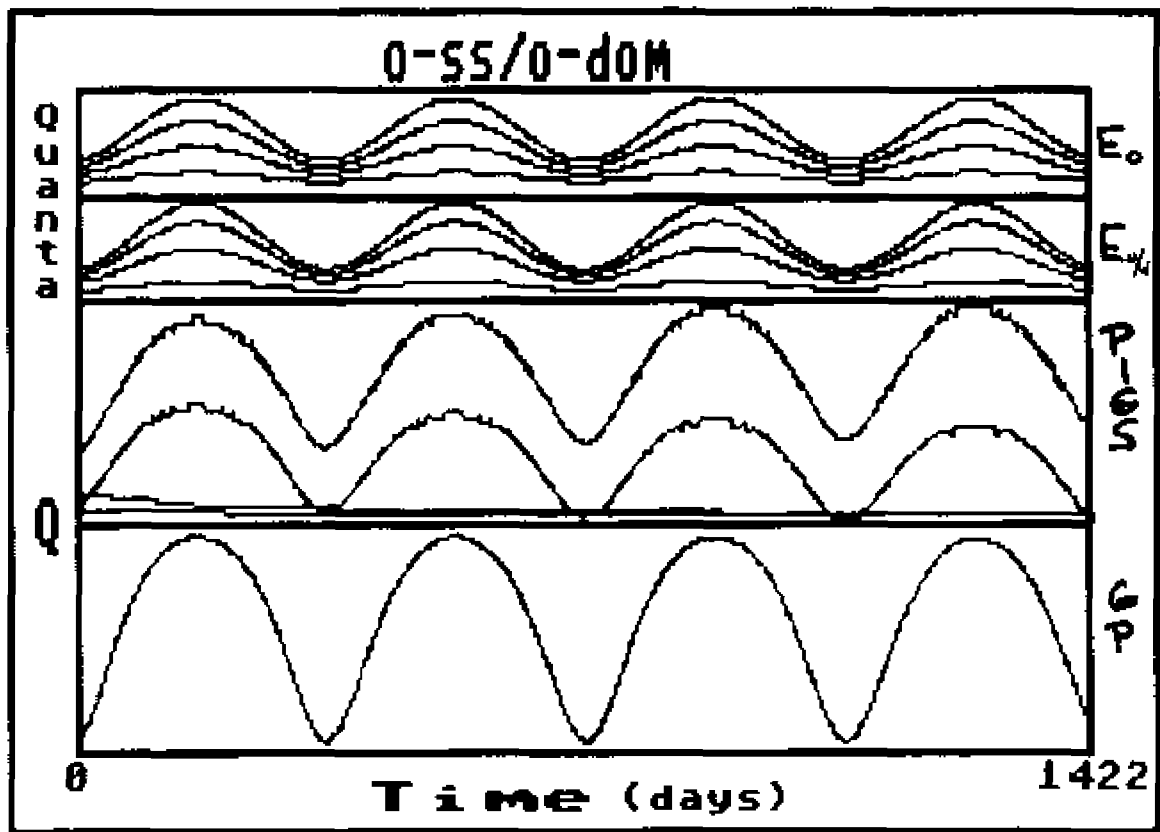


Figure 48. Output of community photosystem model with SS=0 and DOM=0.

much greater in the submarine light field, and the underwater blue light is greatly attenuated, especially in the fall when the model forces the highest concentrations of DOM, which selectively attenuates short wavelengths. Comparing Figures 47 and 48 brings out some of the changes caused by the DOM and SS functions. Figure 48 is the plotted output 4FIG.17a without DOM or SS. The underwater light, pigments and production are all symmetrical about the summer irradiance peaks. In the Standard Run, with its nominal DOM and SS loads, the underwater light, pigments and production are both truncated at the peaks and skewed, by comparison. The Yellow photosystem predominates in all runs of version 17a, closely tracked by the Green photosystem. Output from version 17.5, not shown in these Figures, reverses this - Green pigments become dominant, followed by Yellow pigments. This is probably due to the inclusion of quantum yield coefficients in version 17.5 which favor the conversion of longer wavelength light energy into ATP over that of the shorter wavelengths.

The results of running the model with approximately triple the DOM is plotted in Figure 49. Late Summer and Fall values of PIGS and GP are drastically effected, since that is when the DOM function peaks. In Figure 50 just the opposite situation is simulated: tripled SS and Standard DOM. The simulated water is so turbid that the peak Summer incident surface irradiance is severely attenuated causing the underwater irradiance to be lower during summertime than during winter. This results in Spring and Fall "blooms" of the dominant pigment systems, and GP.

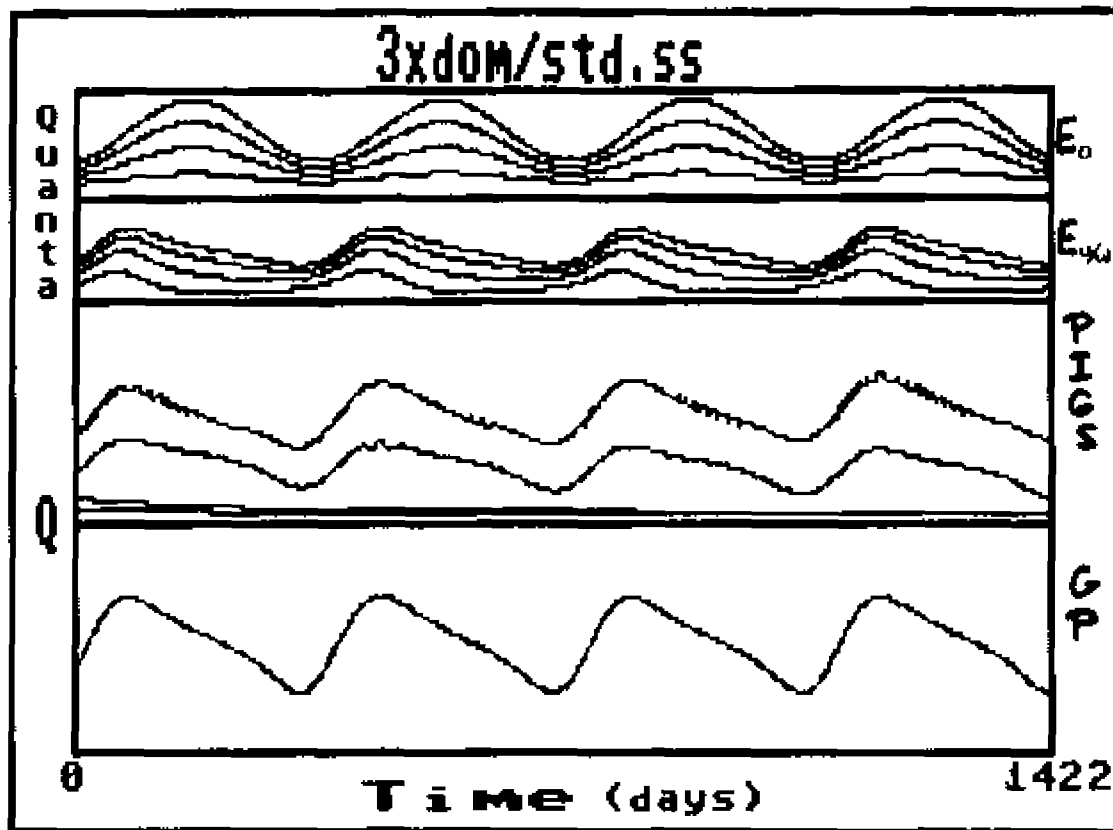


Figure 49. Output of community photosystem model with Standard SS and 3xDOM.

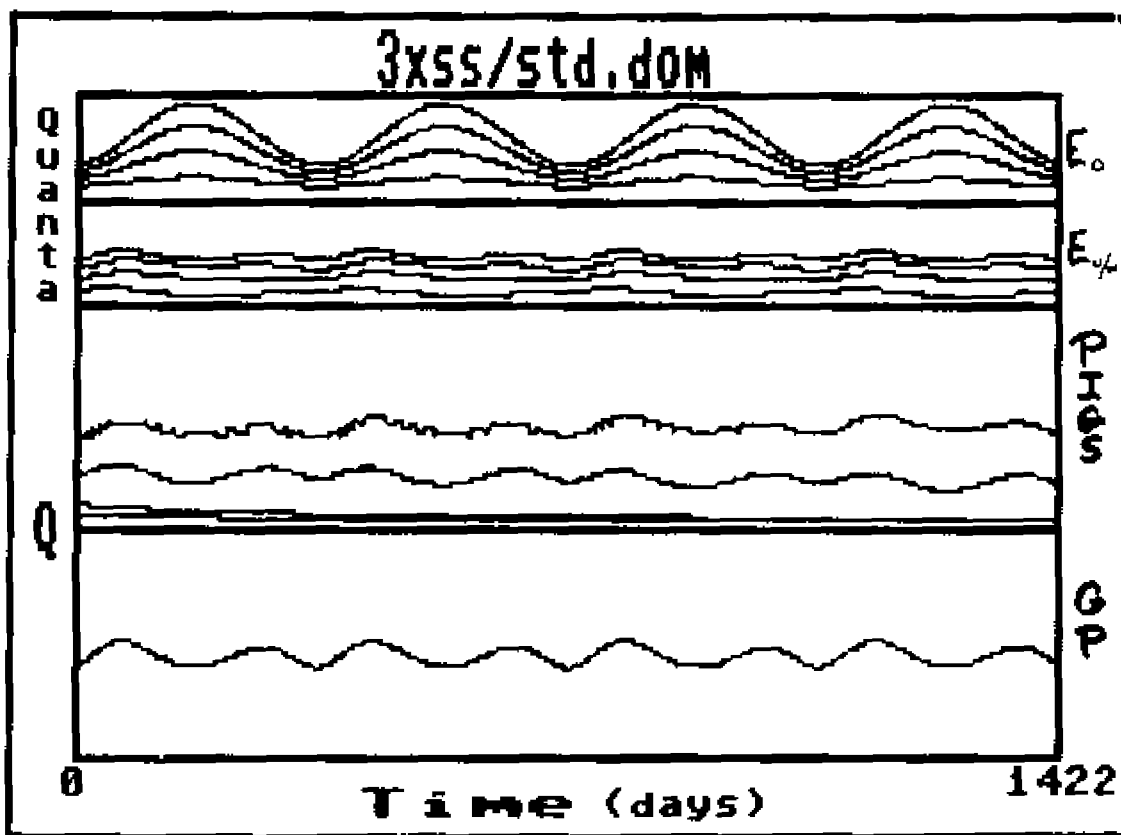


Figure 50. Output of community photosystem model with Standard DOM and 3xSS.

Tripling both DOM and SS during the model run resulted in severe reduction of all photosystems from Spring until Fall, as indicated in Figure 51.

Surface irradiance was held constant at maximum insolation during a run of version 4PIG17.5 (fig. 52) as part of the procedure for stabilizing the output. As has been true for all versions of the model, at high levels (or when the coefficients limiting growth were too low) a series of "blooms" of different photosystems resulted. When one particular pigment complex was able to take advantage of the light environment and grow rapidly, it would change the light quality of the water to such an extent that the very wavelength it needed would no longer be available in sufficient quantity to sustain exponential growth, but the changes that it had caused to submarine light quality would induce another combination of pigment complexes to grow exponentially - and so on - until it stabilized. These changes in the underwater spectral irradiance caused by pigment absorption and the subsequent effect on PIGS and GP can be clearly seen in this Figure (52). It is not unlike the sequential algal blooms sometimes observed in estuaries.

Discussion of Model

The community photosystem response model output has flaws. The red and blue pigments decline to extremely unrealistic levels. The model also assumes that all other conditions (nutrients and temperature, for example) in the estuarine environment which effect photosynthesis do not exist or have no effect on differential pigment production or photosynthesis. The

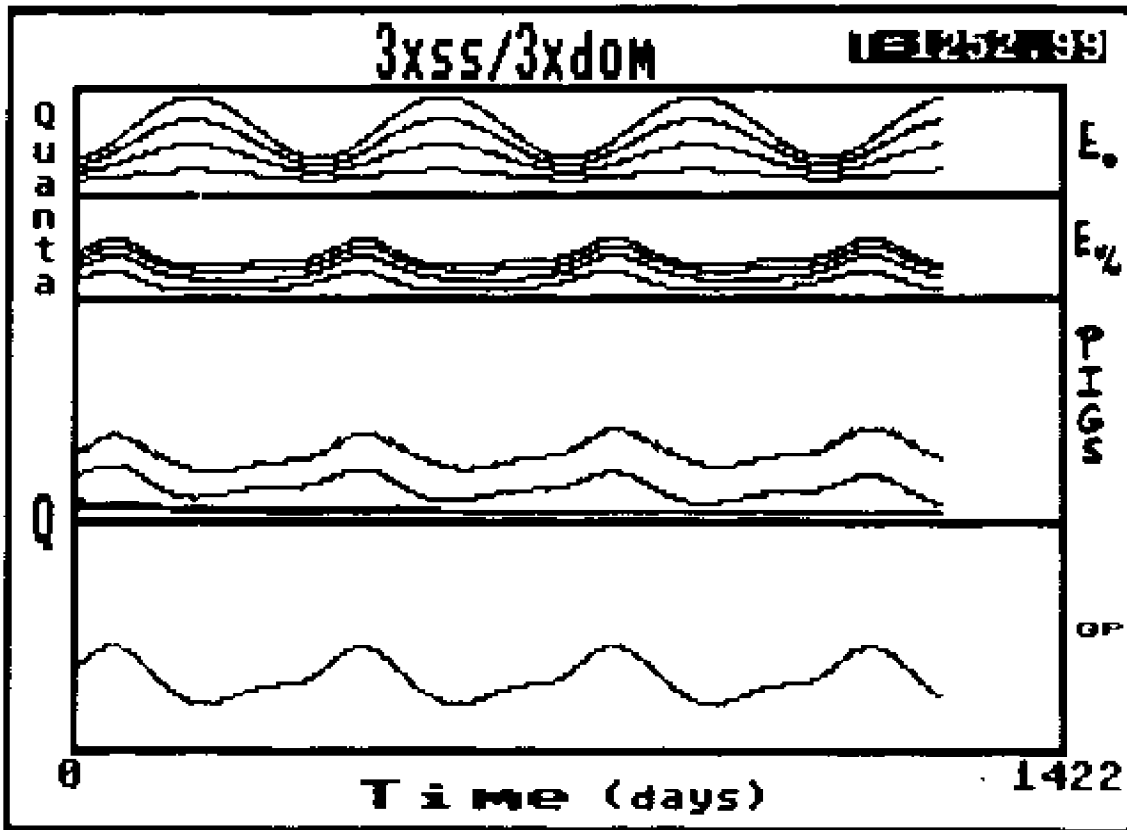


Figure 51. Output of community photosystem model with 3xSS and 3xDOM.

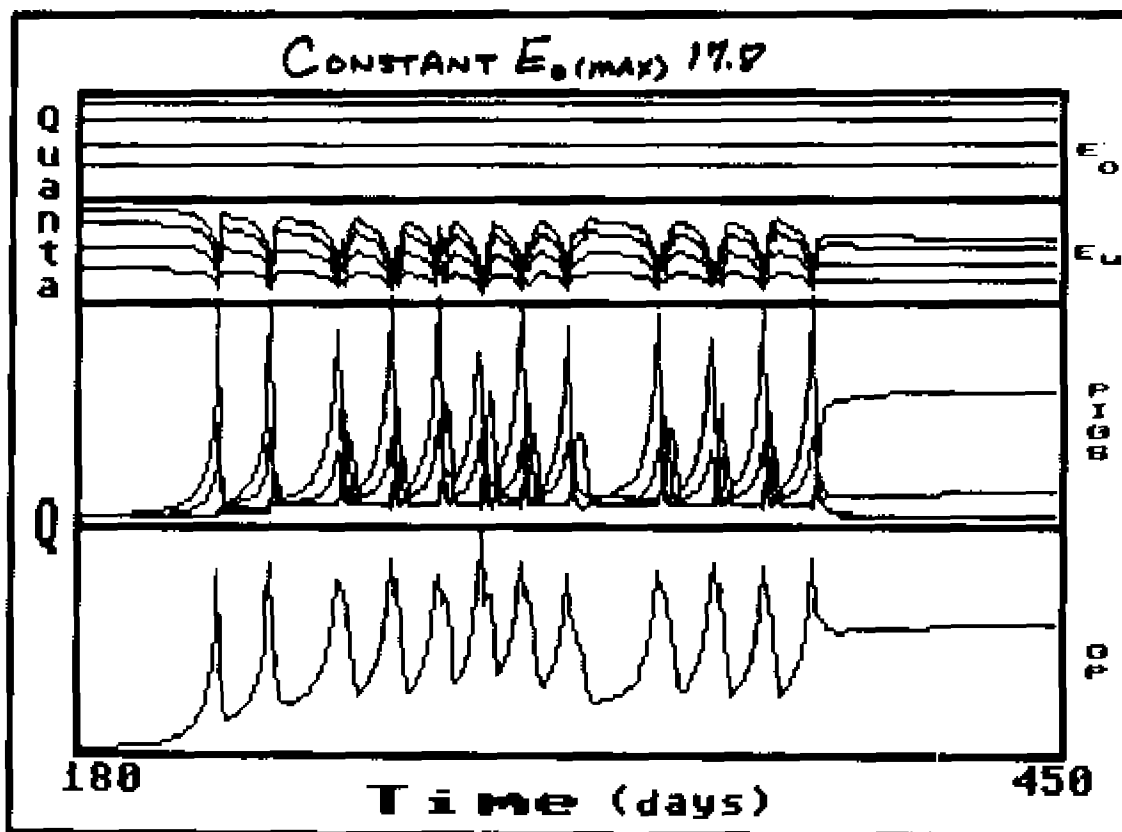


Figure 52. Sequential blooms and crashes of specific photosystems in model run with constant maximum irradiance.

model also has not been calibrated or formally validated against field conditions. However, the initial purposes for which the model was conceptualized were met, i.e., to get a better understanding of the complex interactions between various photons and the living and non-living components of the estuarine environment. The model additionally serves as a starting point for the development of further models which can more adequately address the validity of the concept of a community of cooperating photosystems which coadapt in such a way as to maximize the ecosystem's utilization of available energy - the maximum power principle (Lotka, 1922; Odum & Pinkerton, 1955, Odum 1971b, 1982; Nicolis & Prigogine, 1977).

Despite this model's flaws, it serves to illustrate dramatically the possible effects of changes in dissolved and suspended materials on pigment synthesis and productivity. The many physiological coefficient adjustments that were necessary to stabilize the output also demonstrated the delicate homeostatic mechanisms which must exist within ecosystems in order for them to function successfully within constantly varying environmental constraints. The process of conceptualizing and fine tuning an ecosystem simulation model serves to remind one of the great complexity and flexibility of natural systems and of the mutually interdependent relationships existing between their biotic and abiotic parts. The individual components effect each other and the whole - and the whole effects the individual components.

Future Modifications to the Model

I have begun simulating conceptual model 4PIG.18 which incorporates several changes which may make the model conform more closely to my original conception of an aquatic photosynthetic ecosystem that modifies itself in response to the underwater light quality in such a way as to optimize capture and conversion of quanta into ATP. The changes include: (1) separate GP for each photosystem to allow individual reward loops (feedback) to photosystems successful in capturing photons. All the GP's dump into a community NP; (2) Incorporation of the "Z-scheme" which allows transfer of excited electrons from one photosystem to another; (3) Inclusion of photochemically reversible photochromic pigments. (If Red is stimulated by photons, Blue pigments are synthesized and vice-versa [Bjorn, 1979; Voskresenskaya, 1979] . Also, there is evidence of the existence of a similar Yellow-Green complimentary system Thomas, & O'Kelley, 1973); (4) More realistic absorption spectra for photosystem pigment complexes; (5) Simulation of photoinhibition.

CONCLUSIONS

General Conclusions

The physics of the propagation of light underwater is extremely complex, involving the interaction of myriad living and non-living entities. One way to gain an understanding of the ecology of underwater light is to attempt to conceptualize and simulate ecosystem models of the submarine light environment. Computer ecosystem models were conceptualized and simulated which attempted to describe the interactions between light and the estuarine environment with special reference to pigment systems. The feasibility of determining spectral irradiance and attenuation in shallow estuarine waters was proven. The underwater light environment of an estuary was described. The seasonal dynamics of spectral attenuation in the lower Chesapeake Bay was described. A correlation between the occurrence of seagrasses and spectral attenuation was found. Parameters of the estuarine environment possibly responsible for the specific attenuation were identified: suspended particulate matter, phytoplankton, dissolved organic material. Differences in potential photosynthetically storable radiation were found in vegetated and unvegetated regions of the lower Chesapeake Bay.

Light Quality and Seagrasses in the lower Chesapeake Bay

(1) A seasonal pattern of spectral attenuation occurred in the shallow waters of the lower Chesapeake Bay. Summer showed the highest attenuation, spring and fall were intermediate and winter the lowest.

(2) Over a 15 month period, the date of onset of high attenuation differed from year to year.

(3) The seasonal pattern of attenuation differed between vegetated and unvegetated sites. Attenuation across the entire spectrum at unvegetated sites began earlier in the year and increased at a more rapid rate than at the vegetated sites. The transition from low winter attenuation to high summer attenuation was more abrupt at unvegetated sites. There was a shorter high attenuation season at vegetated sites.

(4) A much greater attenuation of violet light occurred in unvegetated sites during spring, especially during May 1981 and March 1982. During May, 63% less violet light was able to pass through a meter of water at the average unvegetated site compared to the average vegetated site; 88% less through 2.0 meters. (A difference of 1.0 m^{-1} at 441 nm).

(5) The variability of violet attenuation was greater at unvegetated sites during the high turbidity seasons.

(6) The pattern and magnitude of spectral attenuation differed on opposite sides of the Bay.

(7) There was a reduction of potential light energy available for photosynthesis by benthic green plants at the unvegetated sites. Less light was available at those wavelengths most efficiently used by green marine plants.

(8) A critical feedback between the biological and physical components of the seagrass/water column ecosystem must be established if the system is to maintain homeostasis. Increased levels of particulates and phytoplankton blooms may degrade the water clarity and shift its attenuation to the point that sufficient light of the proper quality is unavailable to the re-colonizing seedlings of seagrasses.

APPENDIX I

(Commodore Basic Listing of 4PIG.17.5 Model)

```

1 REM 0GR4PI017.5 12/07/06
2 POKE53200,11;POKE53201,0:PRINT"@"
6 POKE30501,11;POKE30502,0;POKE30540,5
520 INPUT"*****SEQUENTIAL OUTPUT FILENAME";FS
530 INPUT"*****DUMP STATE VARIABLES
  TO PRINTER <R>=N";PS
1650 INPUT"*****NO. OF DAYS FOR SIMULATION (TMAX)
  ";TMAX
1800 I=.1
1850 PRINT"CURRENT ITERATION INTERVAL IS" I
1860 INPUT"NEW INTERVAL <R>=N";I
2700 KB=.03 :KG=.05 :KY=.25 :KR=.4
2705 CC=1 :CD=.5 :CE=.75 :CF=1.25 :C3=.1
2715 C8=1 :C9=.2 :CA=.05 :CB=.01 :CG=.2
2725 K8=.01 :K9=.01 :C1=.01 :C2=.01 :C4=.00001:
  C5=.00001,C6=.00001,C7=.00001
2750 KC=1 :KH=1 :KZ=1 :KS=1
2775 KX=1 :K5=1 :K6=1 :K7=1
2800 KE=.075 :KJ=.075 :K2=.075 :KU=.075
2850 KD=.05 :KI=.05 :K1=1 :K1=.95 :CH=.13
2900 KF=0 :KK=0 :K3=0 :KV=0 :KP=.5
2975 KL=.005 :KM=.005 :K0=.1 :KN=.095 :CL=.75
  :CM=.75 :CO=.75 :CN=.75
3000 KW=.1 :K4=.3
3850 B=2.72;Y=2.77;G=2.57;R=1.66
3900 PB=3.3;PY=3.3;PG=3.3;PR=3.3
4000 AB=7.5;AG=7.5;AY=7.5;AR=7.5
4500 GP=125
4510 T1=0;S1=165;G1=225;S2=2.5;G2=3;G3=2;S3=2
4520 JK$="N";INPUT"*****HOLD IRRADIANCE CONSTANT[<
  R>=NO]";JK$
4530 ZS$="N";INPUT"*****HOLD RUNOFF CONSTANT[<R>=NO]";ZS$
4540 ZD$="N";INPUT"*****HOLD DOM CONSTANT[<R>=NO]";ZD$
4550 DO$="N";INPUT"*****CHANGE COEFFICIENTS";DO$
  :IFDO$="Y"THENGOSUB11000
4560 ID$="N";INPUT"*****CHANGE INITIAL CONDITIONS";I
  D$;IFID$="Y"THENGOSUB14010
4570 SS$="N";INPUT"*****CHANGE RUNOFF/SS";SS$;IFSS$="Y"THENGO
  SUB14700
4572 YS$="N";INPUT"*****CHANGE DOM";YS$;IFYSS$="Y"THENGOSUB140
  00
4575 PRINT"*****TO VIEW SCREEN; PUSH 'V' *****"
4576 PRINT"*****TO STOP ITERATIONS PUSH 'X' *****"
4578 PRINT"*****TO PRINT ITERATION PUSH 'P' *****"
4600 ITIME1=0;XS$=" ";PI=(.1*TMAX)/(115+I);LC=0
4821 OPEN15,0,15;OPEN2,0,2,"0: "+FS+", S,W":PRINT#2,FS
  :PRINT#2,T1:PRINT#2,TH:PRINT#2,I
4622 INPUT#15,SX,IFSX<>0THENPRINT"DISK ERROR NO. ";SX
4623 IFSX=63THENPRINT"FILE EXISTS";STOP
4624 IFSX=72THENPRINT"DISK FULL";STOP
4625 IFSX=74THENPRINT"DRIVE NOT READY";STOP
4626 IFSX<>0THENSTOP
4700 OPEN6,0;PRINT#6,"P";OPEN4,4,2;PRINT#4,CMD4:REM
  (1) MAKES BUFFER PAUSE (2) OPENS PRINTER
4701 PRINT"*****
  *****"
  *****"FS"*****

```

```

4702 PRINT "-----INITIAL
CONDITIONS-----"
4703 PRINT "T1=" T1
4704 PRINT "S1=" S1, "S2=" S2, "S3=" S3, "G1=" G1, "G2=" G2, "G3="
"G3
4705 PRINT "TMAX=" TM, "I=" I
4706 JB=88.1-48.3*COS(2*PI*(T1+10)/365); PRINT "JB=" JB,
4707 JG=84.7-46.5*COS(2*PI*(T1+10)/365); PRINT "JG=" JG,
4708 JY=94.9-52*COS(2*PI*(T1+10)/365); PRINT "JY=" JY,
4709 JR=71.1-39*COS(2*PI*(T1+10)/365); PRINT "JR=" JR
4710 PRINT "B=" B, "G=" G, "Y=" Y, "R=" R
4715 PRINT "PB=" PB, "PG=" PG, "PY=" PY, "PR=" PR
4720 PRINT "AB=" AB, "AG=" AG, "AY=" AY, "AR=" AR
4725 PRINT "GP=" GP
4809 PRINT "-----COEFFICIENTS-----"
4810 PRINT "KB=" KB, "KG=" KG, "KY=" KY, "KR=" KR
4820 PRINT "CC=" CC, "CD=" CD, "CE=" CE, "CF=" CF, "C3=" C3
4830 PRINT "C8=" C8, "C9=" C9, "CA=" CA, "CB=" CB, "CG=" CG
4840 PRINT "K8=" K8, "K9=" K9, "C1=" C1, "C2=" C2
4850 PRINT "C4=" C4, "C5=" C5, "C6=" C6, "C7=" C7
4860 PRINT "KC=" KC, "KH=" KH, "K2=" K2, "KS=" KS
4870 PRINT "KX=" KX, "K5=" K5, "K6=" K6, "K7=" K7
4890 PRINT "KE=" KE, "KJ=" KJ, "K2=" K2, "KU=" KU
4892 PRINT "KL=" KL, "KM=" KM, "KN=" KN, "KO=" KO; PRINT "CL="
"CL, "CM=" CM, "CN=" CN, "CO=" CO
4893 PRINT "KD=" KD, "KI=" KI, "K1=" K1, "KT=" KT, "CH=" CH
4894 PRINT "KQ=" KQ, "KA=" KA, "KW=" KW, "K4=" K4
4895 PRINT "KF=" KF, "KK=" KK, "K3=" K3, "KV=" KV, "KP=" KP
4899 PRINT #4, CLOSE #4, 0
4900 FORT=T1TOTMAXSTEP1; REM*****START
OF MAIN ITERATION LOOP*****
4905 IF JK<>"Y" THEN 5000; JB=88.1-48.3*COS(2*PI*(T1+10)
/365)
4910 JG=84.7-46.5*COS(2*PI*(T1+10)/365)
4950 JY=94.9-52*COS(2*PI*(T1+10)/365)
4975 JR=71.1-39*COS(2*PI*(T1+10)/365); GOTO 5150
5000 JB=88.1-48.3*COS(2*PI*(T+10)/365)
5010 JG=84.7-46.5*COS(2*PI*(T+10)/365)
5050 JY=94.9-52*COS(2*PI*(T+10)/365)
5075 JR=71.1-39*COS(2*PI*(T+10)/365)
5150 IF B<=0 THEN B=1E-38
5160 IF G<=0 THEN G=1E-38
5170 IF Y<=0 THEN Y=1E-38
5180 IF R<=0 THEN R=1E-38
5200 IF PB<=0 THEN PB=1E-38
5250 IF PG<=0 THEN PG=1E-38
5300 IF PY<=0 THEN PY=1E-38
5350 IF PR<=0 THEN PR=1E-38
5500 IF AB<=0 THEN AB=1E-38
5550 IF AG<=0 THEN AG=1E-38
5600 IF AY<=0 THEN AY=1E-38
5650 IF AR<=0 THEN AR=1E-38
5700 IF GP<=0 THEN GP=1E-38
5850 IFLC>PIORIT1=0 THEN GOSUB 20200; REM WRITES ITERATION
FILE TO FIT DISK SIZE
5950 IF P$="Y" OR Z$="P" THEN GOSUB 10600
5951 IF ((TM-.095<T) AND (T<TM+.095)) OR ((TM-46.9>T) AND (T
TM-47.1)) THEN GOSUB 10600
5955 IF ((TM-319.95>T) AND (T>TM-320.05)) OR ((TM-228.95>

```

```

T)AND(T>TM-229.05))THENGOSUB10600
5956 IF((TM-137.95>T)AND(T>TM-138.05))THENGOSUB10600
5957 IF TM>365THENGOSUB15850
5980 GETZZ$:IFZZ$="X"GOTO10400
5981 IFZZ$<>"V"GOTO6500
5990 PRINT"-----"
      -:PRINT":;          @T="T
6000 PRINT"@E(0); @JB,JG:PRINTJY,JR:PRINT"@E(U/W);
      -@B,G:PRINTY,R:PRINT"@INACT.PIGS; @PB;PG:PRINTPY,
      PR
6025 PRINT"@ACT.PIGS; @AB;AG:PRINTAY,AR; @GP="GP
6030 IFLC>PIORT=T1THENPRINT"ITERATION "IT%";WRITE
      N TO DISK FILE:"FS"
6500 ITIME$=ITIME$+1
7627 IFZS$<>"Y"THEN7629:SS=S2+S2*COS(S3*π*(T1-S1)/365)
7629 SS=S2+S2*COS(S3*π*(T-S1)/365)
7650 IFZD$<>"Y"THEN7660:JDOM=G2+G2*COS(G3*π*(T1-G1)
      /365)
7660 JDOM=G2+G2*COS(G3*π*(T-G1)/365);REM DOM
7705 D1=JB*EXP(-KB)-B*((PR^2+PY^2+PG^2)/(PR+PY+PG)+
      C4=K8*B)
7706 D1=D1*EXP(-C8=JD*CG-CC=C3*SS)
7805 D2=JG*EXP(-KG)-G*((PR^2+PY^2+PB^2)/(PR+PY+PB)+
      C5=K9=G)
7806 D2=D2*EXP(-C9=JD*CG-CD=C3*SS)
7905 D3=JY*EXP(-KY)-Y*((PR^2+PB^2+PG^2)/(PR+PB+PG)+
      C6=C1*Y)
7906 D3=D3*EXP(-CA=JD*CG-CE=C3*SS)
8002 D4=JR*EXP(-KR)-R*((PY^2+PG^2+PB^2)/(PY+PG+PB)+
      C7=C2*R)
8003 D4=D4*EXP(-CB=JD*CG-CF=C3*SS);REM DOM ATT. &
      SS AT.
8006 B=D1*I;G=D2*I;Y=D3*I;R=D4*I;REM ###ITERATE U/
      W LIGHT###
8090 REM"
8100 D5=PB^2*KX*((Y/(PB+PR+PG))+G/(PB+PR+PY))+R/(PB+
      PG+PY))-AB*KC
8190 REM"
8200 D6=PG^2*K5*((Y/(PG+PR+PB))+B/(PG+PR+PY))+R/(PG+
      PB+PY))-AG*KH
8290 REM"
8300 D7=PY^2*K6*((B/(PG+PY+PR))+G/(PB+PY+PR))+R/(PB+
      PG+PY))-AY*KZ
8390 REM"
8400 D8=PR^2*K7*((B/(PG+PY+PR))+G/(PB+PY+PR))+Y/(PB+
      PG+PR))-AR*KS
8500 IFD5>0THEND9=AB*KC+(KE=D5=KL=GP):GOTO8520;REM"
      ^PB
8510 D9=AB*(KC+KE=D5=CL);REM D5<0
8520 D9=D9-(KF*KP=TL+PB^2*KX*((Y/(PB+PG+PR))+G/(PB+
      PY+PR))+R/(PB+PG+PR)))
8540 IFD6>0THENE1=AG*KH+(KJ=D6=KM=GP):GOTO8560;REM"
      ^PG
8550 E1=AG*(KH+KJ=D6=CM);REM D6<0
8560 E1=E1-(KK*KP=TL+PG^2*K5*((Y/(PB+PG+PR))+B/(PG+
      PY+PR))+R/(PB+PG+PY)))
8580 IFD7>0THENE2=AY*KZ+(K2=D7=KO=GP):GOTO8590;REM"
      ^PY
8585 E2=AY*(KZ+K2=D7=CO);REM D7<0
8590 E2=E2-(K3=KP=TL+PY^2*K6*((B/(PY+PG+PR))+G/(PB+

```

```

      PY+PR))+(R/(PB+PG+PY)))
8600 IFD8>0THENE3=AR*KS+(KU=DB*KN=GP);GOTO8620:REM^
      ^PR
8610 E3=AR*(KS+KU=DB*CN):REM D8<0
8620 E3=E3-(KV*KP*TL+PR^2*K7=((Y/(PB+PG+PR))+G/(PB+
      PY+PR))+(Y/(PB+PG+PR))))
8720 E4=GP*CH=(KO=AB*KI=AG+K1*AY+KT=AR)-GP*(KW*K4*GP)
      :REM^
      ^GP
8732 IFD5>0THENE4=E4-D5=KE=GP*KL
8736 IFD6>0THENE4=E4-D6=KJ=GP*KM
8740 IFD7>0THENE4=E4-D7=K2=GP*KN
8744 IFD8>0THENE4=E4-D8=KU=GP*KO
8900 AB=AB+(D5=I);AG=AG+(D6=I)
8920 AY=AY+(D7=I);AR=AR+(D8=I);PB=PB+(D9=I);PG=PG+(E1=
      I);PY=PY+(E2=I)
8930 PR=PR+(E3=I);GP=GP+(E4=I)
9000 IFLC<(PI+1)THENLC=LC+1
9050 IFLC>=(PI+1)THENLC=1
9999 NEXTI:REM<-----END+MAIN+LOOP+----->
10400 OPEN4,4,0:PRINT#4:CMD4:PRINT"IT1="IT1:PRINT#4:
      CLOSE4,4,0
10402 IFST<0THEN10499
10404 GOSUB10600
10408 IFSX=63THENPRINT"FILE EXISTS"
10409 IFSX=72THENPRINT"DISK FULL"
10410 IFSX=74THENPRINT"DRIVE NOT READY"
10499 IFST<0THENPRINT"DEVICE NOT PRESENT ERROR"ST
10500 CLOSE2,6,2:PRINT#6,"U":PRINT#6:CLOSE6,6:PRINT"
      *SETUP PRINTER"
10501 END
10600 OPEN1,4,2:PRINT#1:CMD1:IFST<0THEN10499
10601 PRINT"-----
      -----":PRINT"
      @T=@T
10602 IF(TM-319.95>T)AND(T>TM-320.05)THENPRINT"
      STATE VARIABLES DURING MID-WINTER: "
10603 IF(TM-46.95>T)AND(T>TM-47.05)THENPRINT"
      STATE VARIABLES DURING MID-FALL: "
10604 IF(TM-228.95>T)AND(T>TM-229.05)THENPRINT"
      STATE VARIABLES DURING MID-SPRING: "
10605 IF(TM-.095<T)AND(T<TM+.095)THENPRINT" STATE
      VARIABLES AT TMAX: "
10606 IF(TM-137.95>T)AND(T>TM-138.05)THENPRINT"
      STATE VARIABLES DURING MID-SUMMER: "
10607 IFZZ$="X"THENPRINT" STATE VARIABLES WHEN
      EXECUTION TERMINATED:
10610 PRINT"X0=",JB;JG;JY;JR:PRINT"E(U/W)=",B;G;Y;R:
      PRINT"INACTIVE PIGS=",PB;PG;PY;PR
10620 PRINT"ACT. PIGS=",AB;AG;AY;AR:PRINT"GP="GP
10630 IFLC>=PIORIT$>0THENPRINT"ITERATION"IT$*
      EN TO DISK FILE:"F$"
10640 PRINT#1:CLOSE1:RETURN
11000 DA$="N":INPUT"CHANGE ATTENUATION COEFFICIENTS";DA$
      :IFDA$="Y"THENGOSUB12000
11010 DB$="N":INPUT"CHANGE BIOLOGICAL COEFFICIENTS";DB$
      :IFDB$="Y"THENGOSUB13000
11100 RETURN
12000 WA$="N":INPUT"CHANGE PURE SEA WATER ATTENUATION
      ";WA$:IFWA$="Y"THENGOSUB12500
12010 SA$="N":INPUT"CHANGE SS ATTENUATION VALUES";SA$

```

```

: IFSA$="Y" THEN GOSUB 12600
12020 GA$="N": INPUT "CHANGE DOM ATTENUATION VALUES"; GA$
: IF GA$="Y" THEN GOSUB 12700
12025 HS$="N": INPUT "CHANGE QUADRATIC HEAT SINK"; HS$
: IF HS$="Y" THEN GOSUB 12800
12030 RETURN
12500 REM CHANGE SW K
12510 PRINT "K8="K8, "K9="K9, "K1="K1, "K2="K2: INPUT "NEW
K8, K9, K1, K2"; K8, K9, K1, K2
12520 PRINT "VALUES STORED AS: *****"K8; K9; K1
; K2
12599 RETURN
12600 REM CHANGE SS K
12610 PRINT "CC="CC, "CD="CD, "CE="CE, "CF="CF, "C3="C3
12612 INPUT "NEW CC, CD, CE, CF, C3"; CC, CD, CE, CF, C3
12620 PRINT "VALUES STORED AS: *****"CC; CD; CE
; CF; C3
12699 RETURN
12700 REM CHANGE DOM K
12710 PRINT "C8="C8, "C9="C9, "CA="CA, "CB="CB, "CG="CG
12712 INPUT "NEW C8, C9, CA, CB, CG"; C8, C9, CA, CB, CG
12720 PRINT "VALUES STORED AS: *****"C8; C9; CA
; CB; CG
12799 RETURN
12800 REM CHANGE QUAD HEAT SINK
12810 PRINT "K8="K8, "K9="K9, "C1="C1, "C2="C2
12812 PRINT "C4="C4, "C5="C5, "C6="C6, "C7="C7
12813 INPUT "NEW K8, K9, C1, C2, C4, C5, C6, C7"; K8, K9, C1,
C2, C4, C5, C6, C7
12820 PRINT "VALUES STORED AS: *****"K8; K9; C1
; C2; C4; C5; C6; C7
12899 RETURN
13000 AB$="N": INPUT "CHANGE PIG ABSORPTION COEFFICIENTS"; A
B$: IF AB$="Y" THEN GOSUB 13500
13010 PS$="N": INPUT "CHANGE PIG SYNTHESIS COEFFICIENTS"; PS
$: IF PS$="Y" THEN GOSUB 13600
13015 GP$="N": INPUT "CHANGE GROSS PROD. COEFFICIENTS"; GP$
: IF GP$="Y" THEN GOSUB 13750
13020 RS$="N": INPUT "CHANGE RESPIRATION COEFFICIENTS"; RS$
: IF RS$="Y" THEN GOSUB 13700
13030 PH$="N": INPUT "CHANGE PHOTOINHIBITION VALUES"; PH$
: IF PH$="Y" THEN GOSUB 13800
13031 RETURN
13500 REM CHANGE PIG ABSORPTION K
13510 PRINT "KC="KC, "KH="KH, "KZ="KZ, "KS="KS
13512 PRINT "KX="KX, "K5="K5, "K6="K6, "K7="K7
13513 INPUT "NEW KC, KH, KZ, KS, KX, K5, K6, K7"; KC, KH, KZ,
KS, KX, K5, K6, K7
13520 PRINT "VALUES STORED AS: *****"KC; KH; KZ
; KS; KX; K5; K6; K7
13599 RETURN
13600 REM CHANGE PIG SYNTHESIS K
13610 PRINT "KE="KE, "KJ="KJ, "K2="K2, "KU="KU
13612 PRINT "KL="KL, "KM="KM, "KO="KO, "KN="KN: PRINT "CL=
"CL, "CM="CM, "CO="CO, "CN="CN
13613 INPUT "NEW KE, KJ, K2, KU, KL, KM, KO, KN"; KE, KJ, K2,
KU, KL, KM, KO, KN
13620 PRINT "VALUES STORED AS: *****"KE; KJ; K2
; KU; KL; KM; KO; KN
13622 INPUT "NEW CL, CM, CO, CN"; CL, CM, CO, CN

```



```

13624 PRINT"VALUES STORED AS: *****"CL; CM; CO
; CN
13699 RETURN
13700 REM CHANGE RESPIRATION K
13712 PRINT"KW="KW, "K4="K4
13713 INPUT"NEW KW, K4"; KW, K4
13720 PRINT"VALUES STORED AS: *****"KW; K4
13749 RETURN
13750 REM CHANGE GP K
13760 PRINT"KD="KD, "KI="KI, "K1="K1, "KT="KT, "CH="CH
13773 INPUT"NEW KD, KI, K1, KT, CH"; KD, KI, K1, KT, CH
13780 PRINT"VALUES STORED AS: *****"KD; KI; K1
; KT; CH
13799 RETURN
13800 REM CHANGE PHOTOINHIBITION K
13810 PRINT"KF="KF, "KK="KK, "K3="K3, "KV="KV, "KP="KP
13813 INPUT"NEW KF, KK, K3, KV, KP"; KF, KK, K3, KV, KP
13820 PRINT"VALUES STORED AS: *****"KF; KK; K3
; KV; KP
13899 RETURN
14010 T1$="N"; INPUT"CHANGE INITIAL DAY (T1) (Y/<R>
=N)"; T1$; IFT1$="Y"THEN GOSUB14600
14020 IR$="N"; INPUT"CHANGE INITIAL IRRADIANCE"; IR$
; IFIR$="Y"THEN GOSUB14100
14025 PAS="N"; INPUT"CHANGE INITIAL ACTIVE PIGS"; PAS
; IFPAS="Y"THEN GOSUB14300
14030 PGS="N"; INPUT"CHANGE INITIAL INACTIVE PIGS"; PGS
; IFPG$="Y"THEN GOSUB14400
14040 UWS="N"; INPUT"CHANGE INITIAL U/W IRRADIANCE"; UWS
; IFUWS="Y"THEN GOSUB14200
14050 PPS="N"; INPUT"CHANGE INITIAL PRODUCTION"; PPS
; IFPPS="Y"THEN GOSUB14500
14099 RETURN
14100 REM CHANGE INITIAL IRRADIANCE
14110 PRINT"JB="JB, "JG="JG, "JY="JY, "JR="JR
14120 INPUT"NEW JB, JG, JY, JR"; JB, JG, JY, JR
14130 PRINT"VALUES STORED AS: *****"JB; JG; JY
; JR
14199 RETURN
14200 REM CHANGE INITIAL U/W IRRADIANCE
14210 PRINT"B="B, "G="G, "Y="Y, "R="R
14220 INPUT"NEW B, G, Y, R"; B, G, Y, R
14230 PRINT"VALUES STORED AS: *****"B; G; Y; R
14299 RETURN
14300 REM CHANGE INITIAL ACTIVE PIGMENTS
14310 PRINT"AB="AB, "AG="AG, "AY="AY, "AR="AR
14320 INPUT"NEW AB, AG, AY, AR"; AB, AG, AY, AR
14330 PRINT"VALUES STORED AS: *****"AB; AG; AY
; AR
14399 RETURN
14400 REM CHANGE INITIAL INACTIVE PIGMENTS
14410 PRINT"PB="PB, "PG="PG, "PY="PY, "PR="PR
14420 INPUT"NEW PB, PG, PY, PR"; PB, PG, PY, PR
14430 PRINT"VALUES STORED AS: *****"PB; PG; PY
; PR
14499 RETURN
14500 REM CHANGE INITIAL PRODUCTION
14510 PRINT"GP="GP
14520 INPUT"NEW GP"; GP
14530 PRINT"VALUES STORED AS: *****"GP; NP

```

```

14599 RETURN
14600 REM CHANGE INITIAL DAY
14610 PRINT"WINTER: 1-91", "SPRING: 92-182", "SUMMER: 183-
274", "FALL: 275-365"
14620 PRINT"T1="T1
14630 INPUT"NEW T1";T1
14640 PRINT"VALUES STORED AS: *****"T1
14699 RETURN
14700 REM CHANGE RUNOFF/SS
14710 PRINT"G1="G1, "G2="G2, "G3="G3
14720 INPUT"NEW G1, G2, G3";G1, G2, G3
14730 PRINT"VALUES STORED AS: *****"G1; G2; G3
14799 RETURN
14800 REM CHANGE DOM/GILVIN
14810 PRINT"S1="S1, "S2="S2, "S3="S3
14820 INPUT"NEW S1, S2, S3";S1, S2, S3
14830 PRINT"VALUES STORED AS: *****"S1; S2; S3
14899 RETURN
15850 REM PRINT MID-SEASON VALUES
15860 ON-((44.95<T)AND(T<45.05))-((135.95<T)AND(T<136.05))
)GOSUB10600
15865 ON-((226.95<T)AND(T<227.05))GOSUB10600
15870 ON-((317.95<T)AND(T<318.05))GOSUB10600
15875 IFM<731GOTO15892
15878 ON-((409.95<T)AND(T<410.05))GOSUB10600
15880 ON-((500.95<T)AND(T<501.05))-((591.95<T)AND(T<592.05))
)GOSUB10600
15890 ON-((682.95<T)AND(T<683.05))GOSUB10600
15892 IFM<1096THENRETURN
15895 ON-((774.95<T)AND(T<775.05))GOSUB10600
15900 ON-((865.95<T)AND(T<866.05))-((956.95<T)AND(T<957.05))
)GOSUB10600
15911 ON-((1047.95<T)AND(T<1048.05))GOSUB10600
15999 RETURN
20200 T$=STR$(T); JB$=STR$(JB); JG$=STR$(JG); JY$=STR$(
JY); JR$=STR$(JR)
20201 B$=STR$(B); G$=STR$(G); Y$=STR$(Y); R$=STR$(R); PB$
=STR$(PB); PG$=STR$(PG)
20202 PY$=STR$(PY); PR$=STR$(PR); GP$=STR$(GP)
20203 AB$=STR$(AB); AG$=STR$(AG)
20204 AY$=STR$(AY); AR$=STR$(AR)
20206 SS$=STR$(SS); JD$=STR$(JD)
20210 PRINT#2, T$ XX$;
20220 INPUT#15, SX, IFSX<>0THENPRINT"DISK ERROR NO. "; SX
"AT T="; T; GOTO10408
20221 IFST<0THEN10499
20223 IFVAL(JB$)<.01THENPRINT#2, JB$ XX$; GOTO20230
20225 PRINT#2, LEFT$(JB$, 5) XX$;
20230 IFVAL(JG$)<.01THENPRINT#2, JG$ XX$; GOTO20240
20235 PRINT#2, LEFT$(JG$, 5) XX$;
20240 IFVAL(JY$)<.01THENPRINT#2, JY$ XX$; GOTO20250
20245 PRINT#2, LEFT$(JY$, 5) XX$;
20250 IFVAL(JR$)<.01THENPRINT#2, JR$; GOTO20266
20255 PRINT#2, LEFT$(JR$, 5)
20266 IFVAL(B$)<.01THENPRINT#2, B$ XX$; GOTO20276

```

```

20250 IFVAL(JR$)<.01THENPRINT#2,JR$:GOTO20266
20255 PRINT#2,LEFT$(JR$,5)
20266 IFVAL(B$)<.01THENPRINT#2,B$ XX$,:GOTO20276
20270 PRINT#2,LEFT$(B$,5) XX$;
20276 IFVAL(G$)<.01THENPRINT#2,G$ XX$,:GOTO20286
20280 PRINT#2,LEFT$(G$,5) XX$;
20286 IFVAL(Y$)<.01THENPRINT#2,Y$ XX$,:GOTO20296
20290 PRINT#2,LEFT$(Y$,5) XX$;
20296 IFVAL(R$)<.01THENPRINT#2,R$:GOTO20320
20306 PRINT#2,LEFT$(R$,5)
20320 GOSUB20600,REM ==NEW LINE NUMBERS NEEDED TO
MOVE SUBR HERE==
20359 IFVAL(PB$)<.01THENPRINT#2,PB$ XX$,:GOTO20369
20360 PRINT#2,LEFT$(PB$,5) XX$;
20369 IFVAL(PG$)<.01THENPRINT#2,PG$ XX$,:GOTO20379
20370 PRINT#2,LEFT$(PG$,5) XX$;
20379 IFVAL(PY$)<.01THENPRINT#2,PY$ XX$,:GOTO20389
20380 PRINT#2,LEFT$(PY$,5) XX$;
20389 IFVAL(PR$)<.01THENPRINT#2,PR$:GOTO20450
20409 PRINT#2,LEFT$(PR$,5)
20450 IFVAL(GP$)<.01THENPRINT#2,GP$ XX$,:GOTO20510
20455 PRINT#2,LEFT$(GP$,5) XX$;
20510 PRINT#2,SS$:REM ADD DOM$ AND CONVERT "GR0GR"
FOR READ/PLOT
20599 RETURN
20600 REM WRITE ACTIVATED PIGS TO DISK
20659 IFVAL(AB$)<.01THENPRINT#2,AB$ XX$,:GOTO20669
20660 PRINT#2,LEFT$(AB$,5) XX$;
20669 IFVAL(AG$)<.01THENPRINT#2,AG$ XX$,:GOTO20679
20670 PRINT#2,LEFT$(AG$,5) XX$;
20679 IFVAL(AY$)<.01THENPRINT#2,AY$ XX$,:GOTO20689
20680 PRINT#2,LEFT$(AY$,5) XX$;
20689 IFVAL(AR$)<.01THENPRINT#2,AR$:RETURN
20695 PRINT#2,LEFT$(AR$,5)
20699 RETURN

```

APPENDIX II

(Commodore Basic listing of Graphic Routine used for reading and plotting sequential disk files of 4PIG.17 output. Written using Abacus Software's "Video Basic 64".)

```

1 REM  GR0GR.Q 11/24/86
3 POKE30581,11:POKE53280,11
4 POKE30582,0:POKE53281,0
5 POKE30548,5
100 INPUT"VB-64 IS VB-64 IMPLIMENTED <R>=YES";SG$
110 IFSG$="N"THENPRINT"VBDEV":END
400 F$="*":INPUT"FILE FILE TO READ [<R>=*]";F$
530 INPUT"DUMP DUMP STATE VARIABLES
    TO PRINTER <R>=N";P$
532 IFP$="Y"THENPP$="P":OPEN6,6:PRINT#6,"P"
540 REM: (NEEDS WORK) INPUT"IDENTIFY IDENTIFY
    POINTS WITH MARKS <R>=N";C$
546 INPUT"SUPPRESS SUPPRESS CONNECTING LINES <R>=NO";L$
1600 REM: +++GRAPHIC PROPORTIONS++++ ++++++
+++++
1700 MF=1:QMAX=10:YQ=54/QM:ZQ=.04:FM=1:UZ=1.2:MB=0:
    MG=0:MY=0:MR=0:FB=1:FG=1:FY=1
1701 FR=1:MP=0
1702 ZQ$="":INPUT"CHANGE CHANGE INCIDENT LIGHT SCALING FACTOR";Z
    Q$:IFZQ$<>"Y"THEN1706
1704 PRINT"ZQ="ZQ:INPUT"NEW NEW ZQ";ZQ:PRINT"STORED STORED AS:
    "ZQ
1706 UZ$="":INPUT"CHANGE CHANGE U/M LIGHT SCALING FACTOR";UZ$
    :IFUZ$<>"Y"THEN1710
1708 PRINT"UZ="UZ:INPUT"NEW NEW UZ";UZ:PRINT"STORED STORED AS:
    "UZ
1710 MF$="":INPUT"CHANGE CHANGE PIGMENT SCALING FACTORS";MF$
    :IFMF$<>"Y"THEN1800
1712 PRINT"MF="MF:INPUT"NEW NEW MF";MF:PRINT"STORED STORED AS:
    "MF
1714 PRINT"MB="MB;" MG="MG;" MY="MY;" MR="MR:PRINT"FB=
    "FB;" FG="FG;" FY="FY;" FR="FR
1716 INPUT"NEW NEW MINIMUMS: MB, MG, MY, MR";MB, MG, MY, MR:
    PRINT"STORED STORED AS: MB, MG, MY, MR
1718 INPUT"NEW NEW MULT. FACTORS: FB, FG, FY, FR";FB, FG, FY,
    FR:PRINT"STORED STORED AS: FB, FG, FY, FR
1800 FM$="":INPUT"CHANGE CHANGE PRODUCTION SCALING FACTORS";FM$
    :IFFM$<>"Y"THEN1900
1820 PRINT"FM="FM;"MP="MP:INPUT"NEW NEW FM, MP";FM, MP:PRINT"ST
    ORED AS: FM, MP
1830 FORI=1TO500:NEXT
1900 REM++++++AXES++++++
+++++
1950 HIRES 1,12 :TIC 1,1,14
1960 DRAW20,120,299,120,14
1961 DRAW20,129,299,129,14
1962 DRAW20,153,299,153,14
1963 DRAW20,154,299,154,14
1964 DRAW20,74,299,74,14
1965 DRAW20,75,299,75,14
1967 BOX19,19,300,100,14
1968 BOX20,20,299,179,14

```



```

5600 GETPP$: IFPP$="P"ORP$="Y"THENGOSUB30000
5790 PRINT "----- @T=";T;"@-----
--
5800 PRINTJB,JG,JY,JR:PRINT":PRINTB,G,Y,R:PRINT":
PRINTAB,AG,AY,AR:PRINT"
5810 PRINTPB,PG,PY,PR:PRINT":PRINTGP
5850 IFT=T1THENOK$="Y":INPUT"OK (<R>=YES)";OK$:IFOK$
<>"Y"THENCLOSE2:CLOSE15:GOTO400
5900 TP$=LEFT$(T$,7)
5904 MODE1:CHAR2,240,193,14,"T=":CHAR2,240,193,14,"@
",MODE0
5905 GRAPH:MODE1:CHAR2,240,193,14,"@ "":MODE0:
CHAR2,240,193,14,"T="+TP$
5910 IFC$="Y"THENGOSUB62000
5920 IFL$<>"Y"THENGOSUB60000
6150 IFT=T1THEN6250
6100 DRAW(T-T1)*XT+20,JB=ZQ+157,(U-T1)*XT+20,IB=ZQ+
157,15
6190 DRAW(T-T1)*XT+20,ZQ*(JB+JG)+157,(U-T1)*XT+20,ZQ*
(IB+IG)+157,14
6198 DRAW(T-T1)*XT+20,ZQ*(JB+JG+JY)+157,(U-T1)*XT+20,
ZQ*(IB+IG+IY)+157,8
6220 DRAW(T-T1)*XT+20,ZQ*(JB+JG+JY+JR)+157,(U-T1)*XT+
20,ZQ*(IB+IG+IY+IR)+157,11
6222 DRAW(T-T1)*XT+20,131+B*UZ,(U-T1)*XT+20,131+C*UZ,
15
6224 DRAW(T-T1)*XT+20,131+(B+G)*UZ,(U-T1)*XT+20,131+
(C+H)*UZ,14
6226 DRAW(T-T1)*XT+20,131+(B+G+Y)*UZ,(U-T1)*XT+20,131+
(C+H+Z)*UZ,8
6228 DRAW(T-T1)*XT+20,131+(B+G+Y+R)*UZ,(U-T1)*XT+20,
131+(C+H+Z+S)*UZ,11
6250 REM IF(PB+AB)*YQ>54 THEN6305
6300 DOT(T-T1)*XT+20,MF=(PB+AB-MB)*YQ*FB+77,7
6305 REM IF(PG+AG)*YQ>54 THEN6311
6310 DOT(T-T1)*XT+20,MF=(PG+AG-MG)*YQ*FG+77,6
6311 REM IF(PY+AY)*YQ>54 THEN6313
6312 DOT(T-T1)*XT+20,MF=(PY+AY-MY)*YQ*FY+77,8
6313 REM IF(PR+AR)*YQ>54 THEN6325
6314 DOT(T-T1)*XT+20,MF=(PR+AR-MR)*YQ*FR+77,3
6325 REM IF GP*YQ>53 THEN6400
6330 DOT(T-T1)*XT+20,(GP-MP)*YQ*FM+22,5
6400 QB=PB:QG=PG:MP=GP:U=T:C=B:H=G:Z=Y:S=R:QY=PY:QR=
PR:IB=JB:IG=JG:IY=JY
6410 IR=JR:OB=AB:BG=AG:BY=AY:BR=AR
9998 GOTO3250:REM *****
*****END OF LOOP*****
9999 CLOSE2:CLOSE15:PRINT#6,"U":CLOSE6,6
10410 FORW=1TO4000:NEXT
10420 NORM
10430 PRINT"*****PUSH ;RETURN TO CONTINUE":PRINT">CON
T";":::";STOP
10432 PLS="N":INPUT"PROGRAM LISTING TO SCREEN<R>
=N";PL$
10433 IFPL$="Y"THENFORLZ=1TO1500:NEXT:LIST
10440 INPUT"*****DUMP GRAPHIC OUTPUT TO DISK";G$
:POKE53200,11:POKE53201,0
10450 IFG$="Y"THENGOSUB35000
10460 POKE53200,11:POKE53201,0:INPUT"*****HARD COPY OF
GRAPH<R>=N";H$

```



```

40063 GETX$: IFX$<>"Y" THEN 40063
40100 IF0$="Y" GOTO 40110
40105 IF0$<>"Y" GOTO 40100
40100 HARD4, 0
40109 RETURN
40110 HARD4, 1
40120 RETURN
50000 PRINT "P. 1; CLOSE 1, 4; RETURN": OPEN 1, 4: PRINT #1, CMD1:
LIST
60000 REM CONNECTS POINTS
60005 IF T=T1 THEN RETURN
60100 TB=PB+AB-MB, TG=PG+AG-MG, TY=PY+AY-MY, TR=PR+AR-
MR
60101 DRAW (T-T1)*XT+20, MF=FB+TB*YQ+77, (U-T1)*XT+20,
MF=(QB+BB-MB)*FB*YQ+77, 7
60150 DRAW (T-T1)*XT+20, MF=FG+TG*YQ+77, (U-T1)*XT+20,
MF=(QG+BG-MG)*FG*YQ+77, 6
60200 DRAW (T-T1)*XT+20, MF=FY+TY*YQ+77, (U-T1)*XT+20,
MF=(QY+BY-MY)*FY*YQ+77, 0
60250 DRAW (T-T1)*XT+20, MF=FR+TR*YQ+77, (U-T1)*XT+20,
MF=(QR+BR-MR)*FR*YQ+77, 3
60350 DRAW ((T-T1)*XT+20), ((GP-MP)*YQ+FM+22), ((U-T1)
=XT+20), ((HP-MP)*YQ+FM+22), 5
60500 REM IFACT$<>"Y" THEN RETURN
60600 REM DRAW ((T-T1)*XT+20), (MF+AB*YQ+77), ((U-T1)
*XT+20), (MF+BB*YQ+77), 7
60650 REM DRAW ((T-T1)*XT+20), (MF+AG*YQ+77), ((U-T1)
=XT+20), (MF+BG*YQ+77), 6
60700 REM DRAW ((T-T1)*XT+20), (MF+AY*YQ+77), ((U-T1)
=XT+20), (MF+BY*YQ+77), 8
60750 REM DRAW ((T-T1)*XT+20), (MF+AR*YQ+77), ((U-T1)
*XT+20), (MF+BR*YQ+77), 3
60999 RETURN
61000 GOSUB 61050
61040 IF MW=1 THEN GOTO 010497
61050 INPUT "NAME OF VERSION"; NZ$
61100 SAVE NZ$, 0
61998 MW=1
61999 RETURN
62999 STOP: REM END OF BASIC PRGM AREA

```

LITERATURE CITED

- Baker, K.S. and R.C. Smith. 1980. Quasi-inherent characteristics of the diffuse attenuation coefficient for irradiance. In, S.Q. Duntley, (ed.), *Ocean Optics VI, Proc. Soc. Photo-optical Instrumentation Engineers* 208:60-63.
- Björn, L.O. 1979. Photoreversibly photochromic pigments in organisms: properties and role in biological light perception. *Quart. Rev. Biophys.* 12(1):1-23.
- Boqorad, L. 1975. Phycobiliproteins and complementary chromatic adaptation. *Ann. Rev. Plant Physiol.* 26:369-401.
- Booth, C.R. and P. Dunstan. 1979. Diver-operable multiwavelength radiometer. In, *Measurements of Optical Radiations. Soc. Photo-optical Instrumentation Engineers* 196:33-39.
- Boynton, W.R. and K.L. Heck, Jr 1982. Ecological role and value of submerged macrophyte communities: A scientific summary. In, E.G. Macalaster, D.A. Barker and M. Kasper, (eds.), *Chesapeake Bay Program Technical Studies: A Synthesis*, U.S. Environmental Protection Agency, Washington, D.C., pp. 428-502.
- Burt, W.V. 1955. Distribution of suspended materials in Chesapeake Bay. *J. Mar. Res.* 14:47-62.
- Burt, W.V. 1958. Selective transmission of light in tropical Pacific waters. *Deep-sea Res.* 5:51-61.
- Champ, M.A., G.A. Gould, III, W.E. Bozzo, S.G. Ackleson and K.C. Vierra. 1980. Characterization of light extinction and attenuation in Chesapeake Bay, August, 1977. In, V.S. Kennedy, (ed.), *Estuarine Perspectives*, Academic Press, Inc., N.Y., pp. 263-277.
- Clarke, G.L. and H.R. James. 1939. Laboratory analysis of the selective absorption of light by seawater. *J. Optical Soc. Am.* 29:43-55.
- Clarke, G.L. and G.C. Ewing. 1974. Remote spectroscopy of the sea for biological production studies. In, N.G. Jerlov and E. Steeman Nielsen (eds.), *Optical Aspects of Oceanography*, Academic Press, N.Y., pp. 389-413.

- Corré, W.J. 1983. Growth and morphogenesis of sun and shade plants II. The influence of light quality. *Acta Bot. Neerl.* 32(3):185-202.
- Day, J.W., Jr. and A. Yañez-Arancibia. 1980. Coupling of physical and biological processes in the Laguna de Términos, Campeche, Mexico. (unpub. man.)
- Oring, M.J. 1981. Photosynthesis and development of marine macrophytes in natural light spectra. In, H. Smith (ed.), *Plants and the Daylight Spectrum*, pp. 297-314. Academic Press, N.Y.
- Dubinsky, Z. and T. Berman. 1979. Seasonal changes in the spectral composition of downwelling irradiance in Lake Kinneret (Israel). *Limnol. & Oceanogr.* 24(4):652-663.
- Emerson, R.C. and C.M. Lewis. 1943. The dependence of the quantum yield of *Chlorella* photosynthesis on wavelength of light. *Amer. J. Bot.* 30:165-178.
- French, C.S. and D.C. Fork. 1961. Computer solutions for photosynthesis rates from a two pigment model. *Biophys. J.* 1:669-681.
- Gates, D.M. 1971. The flow of energy in the biosphere. *Sci. American* 224(3):88-103.
- Gierloff-Enden, H.G. 1977. Laguna de Términos and Campeche Bay, Gulf of Mexico: Water mass interaction and lagoonal-oceanic visibility due to sediment laden waters. In, *Orbital Remote Sensing of Coastal and Offshore Environments, A Manual of Interpretation*, Walter de Geruyter, Berlin, pp. 77-89.
- Ginsburg, R.N. and H.A. Lowenstam. 1958. The influence of marine bottom communities on the depositional environment of sediments. *J. Geol.* 66:310-318.
- Govindjee and Govindjee. 1975. *Bioenergetics of Photosynthesis*. Academic Press, N.Y.
- Halldal, P. 1974. Light and photosynthesis of different marine algal groups. In, N.G. Jerlov and E. Steeman Nielsen, (eds.), *Optical Aspects of Oceanography*, pp. 343-360, Academic Press, N.Y.
- Haxo, F.T. and L.R. Blinks. 1950. Photosynthetic action spectra of marine algae. *J. Gen. Physiol.* 33(3):389-422.

- Heinle, D.R., C.F. D'Elia, J.L. Taft, J.S. Wilson, M. Cole-Jones, A.B. Caplins and L.E. Cronin. 1980. Historical review of water quality and climatic data from Chesapeake Bay with emphasis on effects on enrichment. Report to U.S. Environmental Protection Agency, Chesapeake Bay Program. Chesapeake Research Consortium, Inc. Pub. No. 84. Univ. Maryland Center for Environmental and Estuarine Studies No. 80-15 CBL.
- Hess, K. and F. White. 1974. A numerical tidal model of Narragansett Bay. Sea Grant Mar.Tech. Rept. 20, Univ. Rhode Island, Kingston, R.I.
- Humphrey, G.F. 1983. The effect of the spectral composition of light on the growth, pigments, and photosynthetic rate of unicellular marine algae. *J. Exp. Mar. Biol.* 66:49-67.
- Hurlburt, E.A. 1945. Optics of distilled and natural water. *J. Optical Soc. Amer.* 35:689-705.
- Inada, K. 1976. Action spectra for photosynthesis in higher plants. *Plant Cell Physiol.* 17:355-365.
- James, H.R. and E.A. Birge. 1938. A laboratory study of the absorption of light by lake waters. *Trans. Wisc. Acad. Sci.* 31, 154pp.
- Jerlov, N.G. 1976. *Marine Optics*. Elsevier Oceanography Series, Vol. 14, Elsevier Scientific Pub. Co., N.Y., 231pp.
- Jerlov, N.G. and M. Fukuda. 1960. Radiance distribution in the upper layers of the sea. *Tellus* 12:348-355.
- Kalle, K. 1966. The problem of the Gelbstoff in the sea. *Oceanogr. Mar. Biol. Annu. Rev.* 4:91-104.
- Kiefer, D.A. and R.W. Austin. 1974. The effect of varying phytoplankton concentration on submerged light transmission in the Gulf of California. *Limnol. Oceanogr.* 19:55-64.
- Kirk, J.T.O. 1976. Yellow substance (Gelbstoff) and its contribution to the attenuation of photosynthetically active radiation in some inland and coastal south-eastern Australian waters. *Aust. J. Mar. Freshwater Res.* 27:61-71.
- Kirk, J.T.O. 1983. *Light and Photosynthesis in Aquatic Ecosystems*. Cambridge Univ. Press, N.Y. 401pp.
- Kranck, K. 1980. Variability of particulate matter in a small coastal inlet. *Can. J. Fish. Aquat. Sci.* 37:1209-1215.
- Kremer, J.N. and S.W. Nixon. 1978. *A Coastal Marine Ecosystem: Simulation and Analysis*. Springer-Verlag. N.Y., 217pp.

- Levring, T. 1947. Submarine daylight and the photosynthesis of marine algae. Göteborgs Vetensk. Samh. Handl., IV Ser., B 5/6:1-89.
- Levring, T. 1966. Submarine light and algal shore zonation. In, R. Bainbridge, G.C. Evans, and O. Rackham (eds.), Light as an Ecological Factor, pp. 305-318. British Ecol. Soc. Symp. Vol. No. 6, Blackwell Sci. Pub. Ltd., Oxford, U.K.
- Lindeman, R.L. 1942. The trophic-dynamic aspect of ecology. Ecology 23:399-418.
- Lotka, A.J. 1925. Elements of Mathematical Biology. Dover, N.Y.
- Morel, A. 1978. Available, useable and stored radiant energy in relation to marine photosynthesis. Deep-sea Research 25:673-688.
- Morrison, R.E. 1970. Experimental studies on the optical properties of sea water. J. Geophys. Res. 75:612-628.
- Murray, L. 1983. Metabolic and structural studies of several temperate seagrass communities, with emphasis on microalgal components. Doctoral dissertation, College of William and Mary, Williamsburg, Va. 91pp.
- Murray, L. and R.L. Wetzel. 1982. Compartmental studies of community oxygen metabolism. In, R.L. Wetzel (ed.), Structural and functional aspects of the ecology of submerged aquatic macrophyte communities in the lower Chesapeake Bay. Final report, Grant Nos. R805974 and X003245-01, U.S. Environmental Protection Agency, Washington, D.C.
- Murray, L. and R.L. Wetzel. 1987. Oxygen production and consumption associated with the major autotrophic components in two temperate seagrass communities. Mar. Ecol. Prog. Ser. In Press.
- Nicolis, G. and I. Prigogine. 1977. Self-organization in Non-equilibrium Systems. Wiley, N.Y.
- Odum, H.T. 1960. Ecological potential and analogue circuits for the ecosystem. Am. Sci. 48:1-8.
- Odum, H.T. 1967. Biological circuits and the marine systems of Texas. In, T.A. Olson and F.J. Burgess, (eds.), Pollution and Marine Ecology, pp. 99-157. Interscience, N.Y.

- Odum, H.T. 1971a. An energy circuit language for ecological and social systems: Its physical basis. In, B.C. Patten (ed.), *Systems Analysis and Simulations in Ecology*, Vol. II, pp. 139-211. Academic Press, N.Y.
- Odum, H.T. 1971b. *Environment, Power, and Society*. Wiley-Interscience, N.Y., 336pp.
- Odum, H.T. 1975a. Combining energy laws and corollaries of the maximum power principle with visual systems mathematics. In, *Ecosystem Analysis and Prediction*, pp. 239-263. Proc. of the Conference on Ecosystems, SIAM Institute for Mathematics and Society.
- Odum, H.T. 1975b. Marine ecosystems with energy circuit diagrams. In, J.C.J. Nihoul, (ed.) *Modelling of Marine Systems*, pp. 127-151. American Elsevier, N.Y.
- Odum, H.T. 1982. Pulsing, power, and hierarchy. In, W.J. Mitsch, R.K. Ragade, R.W. Bosserman, & J.A. Dillon, Jr. (eds.), *Energetics and Systems*. Ann Arbor Science, Ann Arbor, Mich., pp. 33-59.
- Odum, H.T. 1983. *Systems Ecology: An Introduction*. John Wiley & Sons, N.Y., 644pp.
- Odum, H.T. and R. C. Pinkerton. 1955. Time's speed regulator: The optimum efficiency for maximum power output in physical and biological systems. *Am. Sci.* 43:321-343.
- Orth, R.J., K.A. Moore, and H.H. Gordon. 1979. Distribution and abundance of submerged aquatic vegetation in the lower Chesapeake Bay. Final report, Grant No. 600/B-79-029/SAV1, U.S. Environmental Protection Agency, Washington, D.C.
- Orth, R.J. and K.A. Moore. 1983. Chesapeake Bay: An unprecedented decline in submerged aquatic vegetation. *Science* 222:51-53.
- Pickard, G.L. and L.F. Giovando. 1960. Some observations of turbidity in British Columbia Inlets. *Limnol. Oceanogr.* 5:162-170.
- Pierce, J.W., D.L. Cornell, M.A. Faust, W.H. Klein and B. Goldberg. 1981. Spectral quality of underwater light in a turbid estuary, Rhode River, Maryland, U.S.A. Unpub. man.
- Prieur, L. and S. Sathyendranath. 1981. An optical classification of coastal and oceanic waters based on the specific absorption curves of phytoplankton pigments, dissolved organic matter, and other particulate materials. *Limnol. Oceanogr.* 26:671-689.

- Raghavendra, A.S. and V.S.R. Das. 1977. Effects of light quality on photosynthetic carbon metabolism in C₄ and C₃ plants: Rapid movements of photosynthetic intermediates between mesophyll and bundle sheath cells. *J. Exp. Bot.* 28(106):1169-1179.
- Scott, B.D. 1978. Phytoplankton distribution and light attenuation in Port Hacking Estuary. *Aust. J. Mar. Freshwater Res.* 29:31-44.
- Scoffin, T.P. 1970. The trapping and binding of subtidal carbonate sediments by marine vegetation in Bimini Lagoon, Bahamas. *J. Sed. Petrol.* 40:249-273.
- Sellger, H.H. and M.E. Loftus. 1974. Growth and dissipation of phytoplankton in Chesapeake Bay. II. A statistical analysis of phytoplankton standing crops in the Rhode and West Rivers and adjacent section of the Chesapeake Bay. *Chesapeake Sci.* 15:185-204.
- Smith, H. 1982. Light quality, photoperception, and plant strategy. *Ann. Rev. Plant Physiol.* 33:481-518.
- Smith, R.C. 1979. Bio-Optics. In, S.Q. Duntley (ed.), *Ocean Optics VI*, pp. 47-53, *Proc. Soc. Photo-optical Instrumentation Engineers*, Vol. 208.
- Smullen, J.T., J.L. Taft and J. Mackinis. 1982. Nutrient and sediment loads to the tidal Chesapeake Bay system. In, E.G. Macalaster, D.A. Barker and M. Casper, (eds.), *Chesapeake Bay Program Technical Studies: A Synthesis*, pp. 147-258. U.S. Environmental Protection Agency, Washington, D.C.
- Spence, D.H.N. 1975. Light and plant response in freshwater. In, G.C. Evans (ed.), *Light as an Ecological Factor II*, pp. 93-133.
- Spence, D.H.N. 1981. Light quality and plant responses underwater. In, H. Smith (ed.), *Plants and the Daylight Spectrum*, pp. 245-275. Academic Press, N.Y.
- Stoutjesdijk, Ph. 1972. Spectral transmission curves of some types of leaf canopies with a note on seed germination. *Acta Bot. Neerl.* 21(3):185-191.
- Stross, R.G. 1981. Photomorphogenesis in underwater environments. In, H. Smith (ed.), *Plants and the Daylight Spectrum*, pp. 277-296. Academic Press, N.Y.
- Thomas, J.P. and J.C. O'Kelley. 1973. The photoreversible nature of a pigment system in the green alga *Protosiphon botryoides* Klebs. *Photochem. & Photobiol.* 17:469-472.

- Thompson, M.J., L.E. Gilliland and L.F. Rosenfeld. 1979. Light scattering and extinction in a highly turbid coastal inlet. *Estuaries* 2:29-50.
- Tyler, J.E. and R.C. Smith. 1970. *Measurements of Spectral Irradiance Underwater*. Gordon & Breach, N.Y.
- van Tine, R.F. 1977. An ecological comparison of the benthic macroflora of a power plant impacted estuary and an adjacent estuary. Masters Thesis, Univ. of Florida, Gainesville, Fla.
- van Tine, R.F. 1981. Ecology of seaweeds and seagrasses in a thermally impacted estuary in the Eastern Gulf of Mexico. In, G.E. Fogg and W.E. Jones, (eds.), *Proc. VIIIth Intl. Seaweed Symposium*, Marine Science Labs, Menai Bridge, University College of North Wales, U.K., pp. 499-506.
- van Tine, R.F. 1982. The underwater light environment of shallow regions of the lower Chesapeake Bay, its relationship to seagrasses and its potential for benthic primary productivity. In, R.F. van Tine and R.L. Wetzel (eds.), *Submarine Light Quantity and Quality in the Lower Chesapeake Bay and Its Potential Role in the Ecology of Submerged Seagrass Communities*. Final Report, Grant Nos. R805974 and X003245-01, Environmental Protection Agency, Washington, D.C., 156pp. [Special Report No. 267 in Applied Marine Science and Ocean Engineering (SRAMSOE No. 267) Virginia Institute of Marine Science, Gloucester Point, Va.].
- van Tine, R.F. and R.L. Wetzel. 1982. Spectral distribution and attenuation of underwater light in a tropical mangrove creek and seagrass bed, Laguna de Terminos, Campeche, Mexico: A preliminary analysis. In, R.F. van Tine and R.L. Wetzel (eds.), *Submarine Light Quantity and Quality in the Lower Chesapeake Bay and Its Potential Role in the Ecology of Submerged Seagrass Communities*. Final Report, Grant Nos. R805974 and X003245-01, Environmental Protection Agency, Washington, D.C., pp. 144-156. [Special Report No. 267 in Applied Marine Science and Ocean Engineering (SRAMSOE No. 267) Virginia Institute of Marine Science, Gloucester Point, Va.].
- Vázquez-Yanes, C. 1980. Light quality and seed germination in Cecropia obtusifolia and Piper auritum from a tropical rain forest in Mexico. *Byton* 38(1):33-35.
- Voskresenskaya, N.P. 1979. Effect of light quality on carbon metabolism. In, M. Gibbs, and E. Latzko (eds.), *Photosynthesis II*, pp. 174-180.
- Wanless, H.R. 1981. Fining - upwards sedimentary sequences generated in seagrass beds. *J. Sed. Petrol.* 51(2):445-454.

- Wetzel, R.L., R.F. van Tine and P.A. Penhale. 1981. Light and submerged macrophyte communities in the Chesapeake Bay: A scientific summary. In, E.G. Macalaster, D.A. Barker and M. Kasper, (eds.), Chesapeake Bay Program Technical Studies: A Synthesis, U.S. Environmental Protection Agency, Washington, D.C., pp. 568-630. [Special Report No. 260 in Applied Marine Science and Ocean Engineering (SRAMSOE No. 260), Virginia Institute of Marine Science, Gloucester Point, Va.].
- Wetzel, R.L., L. Murray, R.F. van Tine and P.A. Penhale. 1982. Photosynthesis, light response and metabolism of submerged macrophyte communities in the lower Chesapeake Bay. In, R.L. Wetzel, (ed.) Structural and Functional Aspects of the Ecology of Submerged Aquatic Macrophyte Communities in the lower Chesapeake Bay. Final Report, Grant Nos. R805974 and X003245-01, U.S. Environmental Protection Agency, Washington, D.C.
- Wetzel, R.L. and H.A. Neckles. 1986. A model of Zostera marina L. photosynthesis and growth: simulated effects of selected physical-chemical variables and biological interactions. Aquatic Botany 26: 307-323.
- Wetzel, R.L. and P.A. Penhale. 1983. Production ecology of seagrass communities in the lower Chesapeake Bay. Mar. Tech. Soc. J. 17(2):22-31.
- Williams, J. 1970. Optical Properties of the Sea. U.S. Naval Institute, Annapolis, MD., 123pp.
- Yentsch, C.S. 1960. The influence of phytoplankton pigments on the colour of the sea water. Deep-Sea Res. 7:1-9.
- Zepp, R.G. and P.F. Scholtzhauer. Comparison of photochemical behavior of various humic substances in water: III. Spectroscopic properties of humic substances. Chemosphere 10(5): 479-486.
- Zscheile, F.P. and C.L. Comar. 1941. Influence of preparative procedure on the purity of chlorophyll components as shown by absorption spectra. Botan. Gazette 102:463-481.
- Zscheile, F.P., J.W. White, Jr., B.W. Beadle and J.R. Roach. 1942. The preparation and absorption spectra of five pure carotenoid pigments. Plant Physiol. 17:331-346.

YJIA

Born Jan. 1, 1947 in New York City, the only child of poet Evelyn Sylvia Van Tine and artist Francis Van Tine. Graduated from Cocoa High School, Florida in 1965. Received a B.S. in Zoology from the University of Florida in 1970, after a career as a classical pianist and church organist which had begun as a young child and included two years as a music major. While a zoology undergraduate was student assistant in the Biological Ultrastructure Lab of the Division of Biological Sciences and also Lab Assistant in the Anesthesiology Research Lab of the School of Medicine. Taught biology during 1970-1971 at rural West Nassua County High School, north of Jacksonville, Florida.

In 1971, received a teaching assistantship in the Department of Botany at the University of Florida and began graduate studies. Became Research Assistant for the Aquatic Sciences Center in 1972. Accepted position as Marine Biologist for the Resource Management Systems Program of the State of Florida's Institute of Forestry and Agricultural Sciences at the University of Florida in 1972 to analyze the ecological effects of power generation on an estuary. Program was discontinued in 1974.

In 1974, moved with wife to Louisville, Ky., where she had obtained a position as an editor. It was her turn for a career break. Became

Research Associate in the Neuropsychopharmacology Dept. of the School of Medicine of the University of Louisville in 1974. Was Chairman of Science Department of the Louisville Collegiate School from 1976-1978. Received M.S. in Botany from University of Florida in 1977 with a thesis concerning the ecology of macrophytes impacted by a power plant in the Gulf of Mexico. Was Adjunct Instructor of Biology at the University of Kentucky 1977-1978.

In 1978 was accepted into the School of Marine Science doctoral program of the College of William and Mary at Virginia Institute of Marine Science. Received a research assistantship to help develop a simulation model of Kepone in the James River. Taught Marine Botany at the School of Marine Science during the summers of 1979-1981. In 1980 became involved with the E.P.A. Chesapeake Bay Program research into the disappearance of submerged aquatic vegetation in the Chesapeake Bay.

Took a leave of absence from graduate school during 1982-1986 to become a full-time father to my son, Tristan. Became adjunct Professor of Biology and Oceanography for St. Leo College, Tidewater Center's evening program in 1982. In 1987, turned 40, became a single parent, completed requirements for Ph.D., and accepted position as Associate Professor of Biology and Oceanography in the Science and Mathematics Department of St. Leo College, Tidewater Center, Virginia.